ACTIVATION OF SREBP-2 BY ER STRESS

ACTIVATION OF STEROL REGULATORY ELEMENT BINDING PROTEIN-2 BY ENDOPLASMIC RETICULUM STRESS

By

STEPHEN MATTHEW COLGAN, B.Sc. (Hons.)

A Thesis

Submitted to the School of Graduate Studies

in Partial Fulfilment of the Requirements

for the Degree

Doctor of Philosophy

McMaster University

DOCTOR OF PHILOSOPHY (2009) McMaster University

(Medical Science) Hamilton, Ontario

TITLE: Activation of Sterol Regulatory Element Binding Protein-2 by Endoplasmic Reticulum Stress

AUTHOR: Stephen Matthew Colgan, B.Sc. (Hons.) (York)

SUPERVISOR: Richard C. Austin, Ph.D.

NUMBER OF PAGES: xvi, 184

ABSTRACT

Cellular cholesterol homeostasis is a fundamental and highly regulated process. Transcription factors known as sterol regulatory element binding proteins (SREBP) are responsible for the expression of many genes involved in the uptake and biosynthesis of cholesterol. SREBP activation and lipid dysregulation has been associated with cellular endoplasmic reticulum (ER) stress and the activation of the unfolded protein response (UPR). Our lab has previously reported a relationship between ER stress and SREBP activation causing lipid dysregulation and hepatic steatosis. This project was designed to elucidate the mechanism of ER stress-induced SREBP activation and determine its relationship with cellular pathologies associated with ER stress and lipid accumulation. My research has examined the mechanism by which ER stress activates SREBP-2 in various cell lines, including epithelial and macrophage cells. This research revealed that (1) ER stress-induced SREBP-2 activation is not dependent on caspases and occurs through the conventional sterol-mediated proteolytic pathway; (2) the mechanism of ER stress-induced SREBP-2 activation is sensitive to changes in ER calcium; (3) ER stress is associated with SREBP-2 activation and lipid dysregulation in a model of renal injury; and (4) ER stress-induced SREBP activation *in vitro* is not associated with lipid accumulation in macrophage foam cells.

This project has also offered me the opportunity to further enhance our understanding of the mechanism by which ER stress causes SREBP activation in a sterol-independent manner.

ACKNOWLEDGEMENTS

I am grateful for the many people that assisted me over the 6 years I have spent in research at McMaster University. I am thankful to the Heart and Stroke Foundation of Ontario for providing funding for this project (to Dr. Richard Austin) and to the Canadian Liver Foundation for awarding me a Doctoral Research Award. I would like to thank Dr. Damu Tang (McMaster University) for providing me with the MCF7/cas3 cells, Dr. Yiannis Ioannou (Mount Sinai School of Medicine) for providing me with the pSRE-GFP reporter construct, Dr. Sarka Lhotak for her experiments on the in vivo characterization of the mouse atherosclerotic lesion and renal tubules, and Dr. Jeffrey Dickhout for his experiments on ER calcium homeostasis.

I would like to thank my supervisor Dr. Richard Austin for his guidance, knowledge and support. I greatly appreciate Rick for his leadership, friendship, and contagious enthusiasm for research. I am privileged to have had such an outstanding supervisor for my graduate studies and will always value his friendship and advice. I would also like to thank my committee members, Dr. Geoff Werstuck and Dr. Damu Tang for their support throughout this project. I am grateful to them both for their numerous discussions, encouragement, and guidance over the years. I would like to thank Dr. Geoff Werstuck for his stimulating scientific discussions, support, sense of humour and friendship. Together, my supervisory committee significantly contributed to my success in completing the Ph.D. degree.

I am grateful to all members of the Henderson Research Centre and the Austin Laboratory particularly Sarka Lhotak, Sudesh Sood, Lindsay Pozza, Showkat Hossain, Jeffrey Dickhout, Sana Bassari, Ji Zhou, Linda May, Anna Bowes, Peter Shi, Mohamed Khan, Anthony Bruce and Jennifer Caldwell for their technical expertise, friendship and support during my time in the laboratory. I would like to thank my fellow graduate student Dr. Lindsay Pozza for her friendship, support, and source of knowledge for my endless barrage of questions. I feel very honoured to have found such good mentors and friends during my time at McMaster University and the Henderson Research Centre.

I would like to thank my friends, Darren and Colleen Hartigan, for their continuous support, interest, and encouragement in my research. I would also like to thank my friends Anthony and Jacqui Niejadlik, Mark and Rachael Paterson, and Erik and Jen Abayof for their support throughout my studies.

I will always be grateful to my family. My mother and father, Marcus and Linda Colgan, my brother James and sister-in-law Leigh, and sisters Laura and Lisa, for their love and support and for teaching me the importance of asking the question "why"? I am grateful to my mother and father-in-law, Richard and Kathryn Pearl for their love and support throughout my graduate studies. They have been a great source of guidance, mentorship and friendship throughout this difficult process. I would also like to thank my sister and brother-in-law Colleen and Luke. Their constant support and friendship has greatly contributed to my success.

Finally, I would like to thank my biggest supporter, my wife, Andrea. I will always be grateful to her for encouraging me to pursue graduate studies and giving me

the confidence to succeed. Throughout this difficult process, Andrea has always taken an interest in my research, listening and critiquing presentations, and being a constant motivating force that has guided me through graduate school. Without Andrea's enduring encouragement, patience, love and support, I would not have succeeded in completing this Ph.D. Thank you Andrea, I love you.

TABLE OF CONTENTS

LIST OF FIGURES

LIST OF ABBREVIATIONS

ABCA1	ATP binding cassette transporter A1
ABCG1	ATP binding cassette transporter G1
ACAT1	acyl-coenzyme A:cholesterol acyltransferase 1
ATF6	activating transcription factor 6
ATP	adenosine triphosphate
BAP	Bip-associated protein
BAPTA	1,2-bis(2-aminophenoxy)ethane-N,N,N',N'-tetraacetic acid
bHLH	basic helix-loop-helix
Ca^{2+}	calcium
CHO	chinese hamster ovary
CoA	coenzyme A
COPII	coatomer protein II
DAPI	4',6-diamidino-2-phenylindole
DMSO	dimethyl sulfoxide
DNA	deoxyribonucleic acid
DTT	dithiothreitol
eIF2α	eukaryotic translation initiation factor 2(α subunit)

ELISA	enzyme linked immuno-sorbent assay
ER	endoplasmic reticulum
GADD153	growth arrest and DNA damage gene 153
GFP	green fluorescent protein
GLS	golgi localization signals
GRP78	78 kDa glucose-regulated protein
GRP94	94 kDa glucose-regulated protein
HDL	high-density lipoprotein
HMGR	3-hydroxy-3-methyl-glutaryl-CoA reductase
HRP	horseradish peroxidase
ICAD	inhibitory subunit of caspase-activated DNase
INSIG-1	insulin-induced gene-1
IRE-1	inositol-requiring kinase 1
KDEL	lysine-aspartate-glutamate-leucine
LCAT	lecithin:cholesterol acyltransferase
LDL	low-density lipoprotein
LDLR	low-density lipoprotein receptor
M-CSF	macrophage colony stimulating factor
mRNA	messenger ribonucleic acid
NADPH	nicotinamide adenine dinucleotide phosphate-oxidase
NPC1	Niemann-Pick type C1

NPC2	Niemann-Pick type C2
oxLDL	oxidized low-density lipoprotein
PAGE	polyacrylamide gel electrophoresis
PBMC	peripheral blood mononuclear cells
PARP	polyADP-ribose polymerase
PBS	phosphate-buffered saline
PDI	protein disulfide isomerase
PEPCK	phosphoenolpyruvate carboxykinase
PERK	PKR-like ER kinase
RCT	reverse cholesterol transport
S1P	site-1 protease
S2P	site-2 protease
SCA	SREBP cleavage activity
SCAP	SREBP cleavage activating protein
SDS	sodium dodecyl sulfate
SERCA	sarco/endoplasmic reticulum calcium ATPase
SRE	sterol regulatory element
SREBP	sterol regulatory element binding protein
UPR	unfolded protein response
VEGF	vascular endothelial growth factor
XBP-1	x-box binding protein 1

1 INTRODUCTION

1.1 CELLULAR CHOLESTEROL HOMEOSTASIS

1.1.1 Cholesterol Uptake

Through the characterization of human gallstones in 1769, Poulletier de la Salle, became the first scientist to isolate cholesterol (Olson, 1998). The French chemist, Chevreul, rediscovered cholesterol from human gallstones in 1815 and named it cholesterine (*chole* for bile and *stereos* for solid) (Vance and Van den Bosch, 2000). Although cholesterol had been isolated and the empirical formula ($C_{27}H_{46}O$) determined, little was known about its structure at the start of the 20th century.

The structure of cholesterol and its steroidal ring system was published by Heinrich Wieland and Elizabeth Dane in 1932 (Bloch, 1982). Once the structure of cholesterol was determined, research into its biosynthesis began. In 1942, Konrad Bloch and colleagues determined that all 27 carbons in cholesterol originated from acetate and by 1956 the general layout for the biosynthesis of cholesterol was established (Vance and Van den Bosch, 2000). The biosynthesis of cholesterol from acetyl-CoA through the four key intermediates mevalonate, farnesyl pyrophosphate, squalene, and lanosterol is accomplished by at least 20 enzymes all of which are regulated by a family of transcription factors termed the sterol regulatory element binding proteins (SREBP) (Goldstein *et al*, 2006). The 20th century proved to be an exciting time for biochemists as they determined the structure of cholesterol and its biosynthetic pathway, as well as

uncovering the mechanisms that regulate cholesterol metabolism (Vance and Van den Bosch, 2000).

Mammalian cell membranes provide a permeability barrier to establish concentration gradients and act as a scaffold for supporting membrane proteins. Membranes must also be sufficiently fluid to allow for rapid movement of membrane proteins and for the budding of vesicles during intracellular trafficking (Maxfield and Tabas, 2005). In addition to being a precursor of steroid hormones, cholesterol is essential for the fluidity and the proper functioning of mammalian cellular membranes (Maxfield and Wustner, 2002). However, in excess it is toxic and its proper membrane distribution is essential for many biologic functions (Maxfield and Tabas, 2005). As a result, cellular cholesterol homeostasis is tightly regulated through a complex array of pathways regulating its cellular uptake, biosynthesis, trafficking, storage, and export.

Exogenously derived cholesterol is delivered to the cell plasma membrane through transport in low-density lipoprotein (LDL) particles. LDL particles enter mammalian cells through an endocytic pathway regulated by the expression of the LDL receptor (LDLR). Upon binding of the LDL particles, the LDLR is internalized through clathrin-coated vesicles. The fate of LDL bound to the LDLR within the endocytic pathway includes dissociation of LDL from its receptor in early endosomes and transport to late endosomes and lysosomes where it is degraded into its primary components. Following dissociation in early endosomes, LDLR is recycled to the plasma membrane where it participates in subsequent rounds of LDL binding and internalization (Chang *et al.*, 2006).

Cholesterol esters from LDL undergo hydrolysis in late endosomal compartments enriched in acid lipase (Sugii, 2003). LDL-derived cholesterol exits the endocytic compartment and is transported, depending on requirement, to various other cellular membranes throughout the cell. The removal of cholesterol from late endosomes relies on Niemann-Pick types C1 and C2 (NPC1, NPC2) proteins. These proteins are named after Niemann-Pick type C disease characterized by excessive accumulation of unesterified cholesterol within the endocytic compartments (Chang *et al.*, 2005).

A kinetic difference exists in the arrival of LDL-derived cholesterol to various cell membranes. Time course studies show that LDL-derived cholesterol appears at the plasma membrane within approximately 30 minutes compared with 60 to 90 minutes at the ER (Sugii, 2003). LDL-derived cholesterol may either be transported to the plasma membrane before transport to the ER or LDL-derived cholesterol may be transported to the plasma and ER membranes by two distinct mechanisms (Chang *et al*, 2006).

1.1.2 Cholesterol Trafficking

Cholesterol metabolism requires its proper transport from and delivery to multiple intracellular compartments. Sources of cholesterol consist of (1) the late endocytic compartment, where uptake of LDL-derived cholesterol occurs; (2) the ER, where cholesterol biosynthesis takes place; and (3) cytosolic lipid droplets, where cholesterol esters are stored. Cholesterol is removed from these distinct compartments and distributed throughout the cell by both vesicular and nonvesicular transport mechanisms (Soccio and Breslow, 2004).

Cholesterol can be incorporated into transport vesicles that move between organelles. Vesicular transport follows the cytoskeleton and requires energy in the form of ATP (Soccio and Breslow, 2004). Another route for cholesterol to distribute throughout the cell is through nonvesicular transport. Nonvesicular transport includes the binding of cholesterol to cytosolic carrier proteins. These cholesterol carriers could be a large number of cytosolic proteins that have a low affinity and specificity for cholesterol or could be specific cholesterol transport proteins (Maxfield and Wustner, 2002). Sterol-binding proteins provide a rapid mechanism for shuttling cholesterol among membranes. Another form of nonvesicular cholesterol transport is the direct movement of cholesterol between two membranes in close contact to each other. Since the ER is in close association with the plasma membrane in many cell types, this could facilitate the rapid exchange of cholesterol between these two membranes (Maxfield and Wustner, 2002).

1.1.3 Cholesterol Biosynthesis

In addition to the uptake of cholesterol through binding and internalization of lipoproteins, cells have the enzymatic capacity to endogenously synthesize cholesterol. The rate-limiting enzyme in the cholesterol biosynthetic pathway is HMG-CoA reductase (HMGR). HMGR is localized to the ER membrane where it utilizes two NADPH molecules to convert one molecule of HMG-CoA to mevalonate. The production of mevalonate is the first step in the mevalonate pathway leading to cholesterol synthesis (Espenshade and Hughes, 2007). Many genes are involved in the synthesis of cholesterol and their expression is tightly controlled by SREBP.

1.1.4 Cholesterol Storage

In circumstances where increases in cellular cholesterol are required, cells respond by increasing cholesterol uptake and/or biosynthesis. When cells accumulate excess unesterified cholesterol, membrane fluidity and dysfunction of membrane proteins can occur leading to cholesterol-induced cellular toxicity (Maxfield and Tabas, 2005). Cells have various mechanisms to deal with excess unesterified cholesterol. Firstly, the homeostatic imbalance of increased membrane associated cholesterol inhibits the expression of the LDLR and the enzymes responsible for cholesterol biosynthesis (described in detail below). Secondly, excess cholesterol from various cellular compartments is transported to the ER where it is available to the ER resident enzyme acyl-coenzyme A:cholesterol acyltransferase 1 (ACAT1) (Sakashita *et al.*, 2000; Chang *et al.*, 1995). ACAT1 is an ER membrane-bound protein that is responsible for the esterification of free cholesterol and its subsequent use in lipoprotein assembly (hepatocytes) or cytoplasmic lipid droplet storage (macrophages) (Chang *et al.*, 2006). ACAT1 upregulation is important for the handling of the large quantities of exogenously derived lipoprotein cholesterol that is internalized by macrophages during the development of atherosclerosis. ACAT1-induced cholesterol esterification leads to an accumulation of cytoplasmic lipid droplets that give the macrophage its characteristic "foam cell" appearance.

1.1.5 Reverse Cholesterol Transport

Excess intracellular cholesterol can be stored in cytoplasmic lipid droplets for later hydrolysis and use or it can be transported from peripheral tissues to the liver. The removal of extrahepatic cellular cholesterol to the liver is known as reverse cholesterol transport (RCT) (Chang *et al.*, 2006). The major components of RCT are the plasma membrane associated ATP-binding cassette transporters A1 and G1 (ABCA1 and ABCG1). ABCA1 mediates the transport of cholesterol from the plasma membrane to apoAI to form nascent HDL particles. The plasma enzyme lecithin:cholesterol acyltransferase (LCAT) then uses phospholipids and cholesterol in the nascent HDL to esterify cholesterol and produce mature HDL. Mature HDL can mediate the transfer of cholesterol from plasma membrane associated ABCG1 molecules. Although ABCA1 is expressed in various tissues, ABCG1 is highly expressed in macrophages (Chang *et al.*, 2006). A rare genetic disorder known as Tangier Disease is caused by mutations in the *Abca1* gene, thereby leading to HDL deficiency and premature cardiovascular disease (Oram, 2002).

Mature HDL particles transport cholesterol esters to the liver or steroidogenic tissues. At the liver, HDL binds to and is internalized by the scavenger receptor type B class I (SR-BI). HDL-derived cholesterol is an important precursor for bile acid synthesis where it can enter the bile duct and be excreted from the body (Chang *et al.*, 2006).

1.2 STEROL REGULATORY ELEMENT BINDING PROTEINS (SREBP)

1.2.1 Role of SREBP in Cholesterol Homeostasis

Intracellular cholesterol content is regulated by the action of multiple proteins that act as membrane receptors, transporters, and enzymes important in maintaining control over the concentration of membrane cholesterol in various intracellular compartments. The experiments conducted over the past three decades by Drs. Michael S. Brown and Joseph L. Goldstein have generated the foundation for better understanding the regulation of cellular cholesterol metabolism (Goldstein and Brown, 2008).

Brown and Goldstein's early work to identify the molecular pathology associated with Familial Hypercholesterolemia initiated an explosion of reports examining cellular lipid metabolism. The findings that mutations in the LDLR were responsible for Familial Hypercholesterolemia (Goldstein *et al.,* 1975; Goldstein *et al.,* 1974; Brown and Goldstein, 1974) led to a decade of research describing the mechanism and regulation of LDLR-mediated lipoprotein internalization. Following the identification of a sterol regulatory element in which a transcription factor that is negatively regulated by cholesterol binds to the promoter of the LDLR gene (Sudhof *et al.,* 1987a; Sudhof *et al.,* 1987b), Brown and Goldstein identified SREBP as the transcription factor responsible for transcriptional regulation of the LDLR (Briggs *et al.,* 1993; Wang *et al.,* 1993; Hua *et al.,* 1993; Yokoyama *et al.,* 1993; Horton *et al.*, 2002; Rawson, 2003). Subsequent experiments revealed that SREBP was not only associated with cholesterol uptake through the LDLR, but it was additionally responsible for LDLR expression through the upregulation of proprotein convertase subtilisin/kexin type 9 (PCSK9) which promotes the degradation of the LDLR from the cell surface (Seidah *et al.*, 2006; Jeong *et al.*, 2008). In addition SREBP has been determined to be the transcriptional regulator of

genes required for cholesterol biosynthesis (through multiple enzymes involved in the conversion of acetyl-CoA to cholesterol) (Goldstein and Brown, 1990) such as HMG-CoA reductase (Vallett *et al.,* 1996). Further studies revealed the complex nature of the regulation of SREBP activation leading to its transcriptional control over cholesterol homeostasis (Sheng *et al.,* 1995; Wang *et al.,* 1994).

1.2.2 SREBP structure and genetic regulation

While searching for adipocyte specific transcription factors, Tontonoz *et al.* (1993) isolated adipocyte determination and differentiation dependent factor 1 (ADD1) that was expressed predominantly in adipose tissue and was active during adipocyte differentiation (Tontonoz *et al.,* 1993; Kim *et al.,* 1995) Independent experiments from the Brown and Goldstein lab isolated and cloned the human homolog of ADD1, SREBP-1, through purification of hepatocyte nuclear lysates (Briggs *et al.,* 1993; Wang *et al.,* 1993; Yokoyama *et al.,* 1993) and its ability to bind a 10 base pair sterol regulatory element 1 (SRE-1; 5'-ATCACCCCAC-3') from the promoter of the LDLR gene (Smith *et al.,* 1990). The mammalian genome encodes three SREBP isoforms, SREBP-1a, SREBP-1c, and SREBP-2 (Hua *et al.,* 1995). Hua *et al.* (1995) used somatic cell hybrids and *in situ* localization to determine that SREBP-1a, SREBP-1c and SREBP-2 are transcribed from two genes (SREBF-1 and SREBF-2) which reside on chromosome 17 (17p11.2) and 22 (22q13), respectively (Hua *et al.,* 1995).

The SREBP-1 gene (SREBF-1) is 26 kilobases in length and consists of 22 exons and 20 introns (Hua *et al.,* 1995). *SREBF-1* encodes an 1147 amino acid bHLH-ZIP

transcription factor that is bound to the ER membrane and nuclear envelope (Hua *et al.*, 1993; Yokoyama *et al.*, 1993). The bHLH-ZIP proteins form homodimers and heterodimers that bind to a consensus sequence on the target DNA. The purification and cloning of human SREBP-1 identified cDNA clones with two alternative 5' and 3' sequences that were designated "a" and "c" (Yokoyama *et al.*, 1993). Subsequent experimentation revealed that the different 5' and 3' ends in the SREBP-1a and SREBP-1c genes arise from alternative splicing (Hua *et al.*, 1995). Although exons 2 to 17 are found in all SREBP-1 cDNAs, SREBP-1a and SREBP-1c differ in exon 1, 18, and 19. The different 5' exons (1a and 1c) are alternatively spliced to a common exon 2 and at the 3' end, exon 17 is alternatively spliced to either exon 18 and 19 "a" or "c" (Hua *et al.*, 1995). Although it would be expected that the alternatively spliced forms of SREBP-1 have the same DNA binding affinity due to their identical bHLH-Zip domains, there are differences in both expression and activity of SREBP-1a versus SREBP-1c (Shimomura *et al.*, 1997; Shimano *et al.*, 1997). The first exon of SREBP-1a encodes a long acidic sequence of 29 amino acids that includes 8 negatively charged amino acids. The 8 negatively charged amino acids from exon 1 in combination with 4 negatively charged amino acids from exon 2, form a transcriptional activation domain of 42 amino acids (Yokoyama *et al.*, 1993). In contrast, the first exon of SREBP-1c encodes only a short sequence of five amino acids, in which only one is negatively charged (Yokoyama *et al.*, 1993). The different length of the acidic region produced by exon 1a and 1c may result in varying transcriptional activity.

SREBP-2 is not generated by alternative splicing, as in the case of SREBP-1a and 1c, but rather is transcribed from a different gene located on chromosome 22q13 (Hua *et al.*, 1995). The original screen for SREBPs produced 5 cDNA clones in which 4 were SREBP-1 and the remaining clone was identified as SREBP-2. The SREBP-2 gene (SREBF-2) spans 72 kilobases and is composed of 19 exons and 18 introns (Miserez *et al.*, 1997). The 5'-flanking regions of *SREBF-2* and *SREBF-1* were sequenced and the transcriptional start sites determined. Interestingly, an SRE binding sequence was identified in the promoter of *SREBF-2* but not *SREBF-1* (Miserez *et al.*, 1997). Human *SREBF-2* encodes an 1141 amino acid protein that is 47% identical to human SREBP-1a and shares its bHLH-ZIP transcriptional activation domain, the acidic NH_2, and COOH-terminal domains (Hua *et al.*, 1993).

1.2.3 SREBP tissue distribution, cellular localization and expression

When overexpressed in cultured cells, both SREBP-1a and SREBP-1c activate transcription of cholesterol and fatty acid biosynthetic genes (Yokoyama *et al.*, 1993). Shimano *et al.* (1996) examined the effect of overexpressing the truncated (active) form of SREBP-1a in murine liver. The animals developed fatty liver that was associated with increased transcription of genes involved in cholesterol and fatty acid biosynthesis and uptake (LDL receptor) (Shimano *et al.*, 1996). Shimano *et al.* (1997) examined whether there was a difference between the activity of SREBP-1a and SREBP-1c on lipid biosynthesis in livers from transgenic mice and in cell culture (Shimano *et al.*, 1997). Transgenic mice were generated that overexpressed SREBP-1c predominantly in the liver

and compared to mice that similarly overexpressed SREBP-1a used in a previous study (Shimano *et al.,* 1996). As previously reported (Shimano *et al.,* 1996), the livers of the SREBP-1a transgenic mice were engorged with cholesterol and triglycerides, whereas the SREBP-1c transgenic mice had only a small increase in triglycerides and not cholesterol (Shimano *et al.,* 1997). In correlation with this finding, the mRNA for genes involved in both cholesterol and fatty acid biosynthesis were elevated in the SREBP-1a transgenic animals compared to genes for only fatty acid biosynthesis in the SREBP-1c transgenic mice (Shimano *et al.,* 1997). Human cell culture experiments confirmed the *in vivo* findings that SREBP-1a is a stronger activator of transcription than SREBP-1c (Shimano *et al.,* 1997). Along with the difference between SREBP-1a and SREBP-1c activity, the endogenous expression of the two transcripts varies between organs and cell lines (Shimomura *et al.* 1997). Shimomura *et al.* (1997) found that SREBP-1c is predominantly expressed in the liver, adrenal gland and adipose tissue of adult mice, whereas SREBP-1a was found to be more abundant than 1c in the spleen and numerous cultured cell lines (Shimomura *et al.* 1997).

The mRNA for SREBP-2 was found to be expressed in a wide variety of human fetal and adult tissues. Similar to the transcriptional activation experiments performed with SREBP-1 (Yokoyama *et al.,* 1993), SREBP-2 was found to efficiently induce transcription of a reporter plasmid driven by the SRE-1 element from the promoter of the LDL receptor gene (Hua *et al.,* 1993). In an effort to characterize potential differences between SREBP-1 and SREBP-2, Horton and colleagues (Horton *et al.,* 1998) produced transgenic mice that express a truncated, active form of SREBP-2 in liver and adipose

tissue similar to that used in the previous experiments comparing SREBP-1a and SREBP-1c (Shimano *et al.*, 1996; Shimano *et al.*, 1997). The mRNA levels of multiple genes in the cholesterol biosynthesis pathway were upregulated in livers from the transgenic SREBP-2 mice. Increased gene transcription resulted in a 28-fold increase in cholesterol synthesis compared to a 4-fold increase in fatty acid synthesis (Horton *et al.*, 1998). These results are in contrast to those found with SREBP-1 transgenic mice in which truncated SREBP-1a increased fatty acid synthesis, 25-fold, and cholesterol synthesis, 5-fold (Shimano *et al.*, 1996). Horton and colleagues (1998) make the conclusion that SREBP-2 is a more selective activator of the cholesterol biosynthetic pathway (Horton *et al.*, 1998). Taken together, the above results suggest that SREBP-1a and –2 are the predominant isoforms of SREBP in most cultured cell lines, whereas SREBP-1c and SREBP-2 are found in most tissues (Shimomura *et al.*, 1997).

1.2.4 Regulation of SREBP Activation

1.2.4.1 SREBP-cleavage activating protein

Much of the SREBP regulatory pathway has been determined (Figure 1) by the characterization of mutant Chinese hamster ovary (CHO) cell lines that have defects in sterol feedback regulation (Hua *et al.*, 1996a). Two types of mutant CHO cells have been characterized. Sterol auxotrophs are one type of mutant cell that cannot respond to decreased intracellular cholesterol through the normal synthesis of new cholesterol. The second type is sterol resistant. These cells do not respond to increased levels of intracellular cholesterol by turning off cholesterol synthesis and uptake. Sterol resistant

cells are divided into two classes. Class 1 sterol resistant cells produce a truncated, unregulated SREBP protein that contains the transcriptionally active NH_2-terminal segment of SREBP. Class 1 sterol resistant cells continue to internalize cholesterol without any feedback regulation. In contrast, class 2 sterol resistant cells produce full-length SREBP but cannot mediate their proteolytic activation. These cells express SREBP normally, but the protein(s) responsible for the regulation of SREBP proteolytic activation is functionally impaired.

The study of class 2 sterol resistant cells led researchers to the identification of the SREBP-cleavage activating protein (SCAP) (Hua *et al.*, 1996a). Hua and colleagues isolated a cDNA that encodes SCAP from a mutant Chinese hamster ovary (CHO) cell line that was resistant to sterol-regulated suppression of cholesterol biosynthesis and uptake. These cells have a single mutation in SCAP at codon 443, thereby replacing aspartic acid with asparagine (D443N) (Hua *et al.*, 1996a; Nohturfft *et al.*, 1996). This mutation was found to enhance the ability of SCAP to induce SREBP cleavage even in the presence of sterols (Hua *et al.*, 1996a). Analysis of the amino acid sequence of SCAP suggested that it is a membrane protein of 1,276 amino acids with an NH_2-terminal domain of approximately 730 amino acids having multiple membrane spanning segments and a COOH-terminal domain of approximately 550 amino acids (Hua *et al.*, 1996a).

Additional evidence for the importance of SCAP in regulating SREBP activation came from the characterization of another mutant CHO cell line that required the addition of exogenous cholesterol for survival (Rawson *et al.*, 1999). The CHO cell line, designated SRD-13A, was unable to cleave SREBPs due to mutations in the gene

Figure 1. Model of the SREBP regulatory pathway

SREBP is anchored to the ER membrane through SCAP and insulin-induced gene-1 protein (INSIG-1). During low levels of intracellular cholesterol, INSIG-1 dissociates from SCAP and allows the SCAP-SREBP complex to travel to the Golgi apparatus. The S1P in the Golgi cleaves SREBP within its luminal loop allowing it to disassociate from SCAP. The zinc metalloproteinase, S2P, cleaves SREBP within its transmembrane domain, releasing the bHLH transcription factor from the membrane. Nuclear SREBP binds to the SRE element of various genes to increase their expression. (Modified from Horton *et al*. 2002)

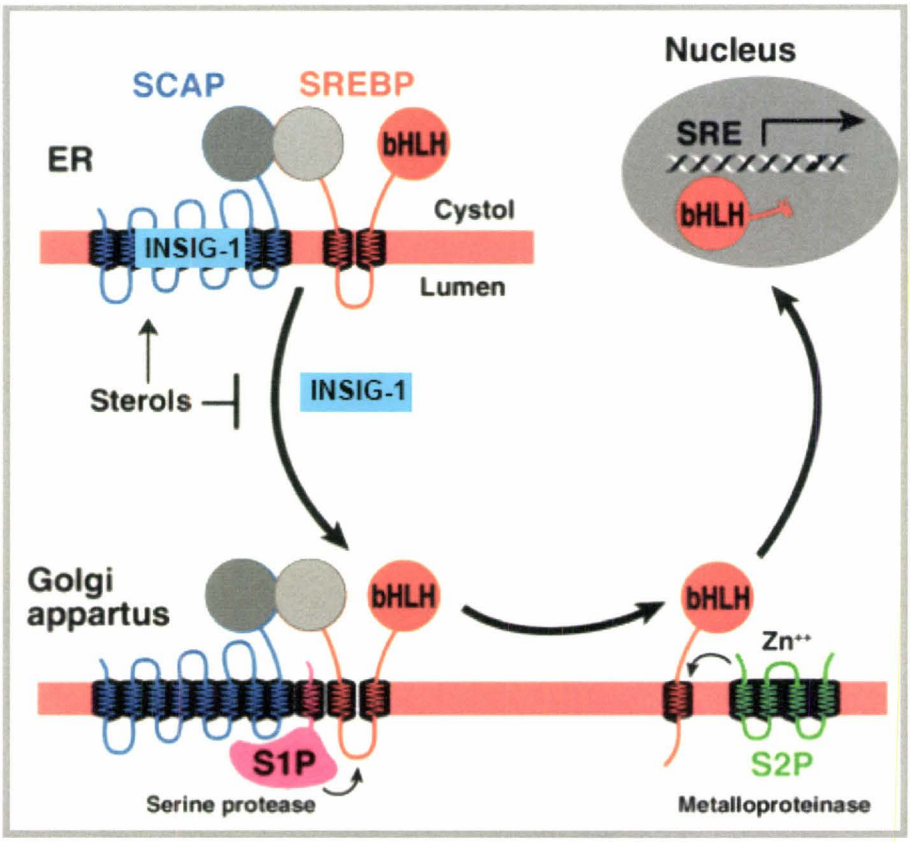
Nucleus
SCAP
SREBP
SRE
ER
bHLH
bHLH
Cystol
INSIG-1
Lumen
Sterols
INSIG-1
Golgi
appartus
bHLH
bHLH
Zn++
S1P
S2P
Serine protease
Metalloproteinase

encoding SCAP which led to the production of a non-functional protein. SRD-13A cells transfected with a cDNA for SCAP restored SREBP cleavage as well as cholesterol biosynthesis and uptake. These findings revealed the importance of SCAP for sterol-regulated cleavage of SREBP.

Nohturfft and colleagues used a protease protection and N-linked glycosylation mapping strategy to determine the topology of SCAP (Nohturfft *et al.*, 1998a). It was found that the NH_2- and COOH-terminus of SCAP face the cytosol while its 8 membrane spanning segments, with sequence homology to the sterol sensing domain of HMG-CoA reductase, are separated by glycosylated segments that extend into the lumen of the ER (Nohturfft *et al.*, 1998a). The NH_2-terminal domain, with its membrane spanning segments, anchors SCAP to the ER membrane while the COOH-terminal domain projects into the cytosol. The COOH-terminal domain contains multiple WD-repeats (tryptophan-aspartate motif) that are commonly found in many intracellular proteins where they mediate protein-protein interactions (Brown and Goldstein, 1999; Neer *et al.*, 1994).

Co-immunoprecipitation experiments by Sakai and colleagues (Sakai *et al.*, 1998; Sakai *et al.*, 1997) demonstrated that the COOH-terminal domains of SCAP and SREBP form a complex that is required for the proteolytic cleavage of SREBP. Immunoprecipitation of the complex occurs even when cells express only the COOH-terminals of SCAP and SREBP, although immunoprecipitation does not occur when the COOH-terminal of SREBP is truncated (Sakai *et al.*, 1997). Overexpression of a truncated COOH-terminal of either SREBP or SCAP competitively disrupted the endogenous SREBP-SCAP complex and inhibited SREBP proteolytic cleavage and

reporter gene expression. Overexpression of full-length SCAP or SREBP restored SREBP activation (Sakai *et al.*, 1998).

In sterol-depleted cells, the SCAP-SREBP complex is transported from the ER to the Golgi where SREBP proteolysis takes place (Nohturfft *et al.*, 2000). Nohturfft and colleagues demonstrated the movement of GFP-SCAP from the ER to the Golgi in sterol depleted cells (Nohturfft *et al.*, 2000). With the use of an *in vitro* system to measure SCAP incorporation into ER membrane vesicles, Nohturfft and colleagues (2000), found that depletion of intracellular cholesterol causes SCAP to integrate into ER membrane-associated vesicles that are transported to the Golgi (Nohturfft *et al.*, 2000). The specific mechanism of SCAP incorporation into membrane vesicles was determined by the work of Espenshade *et al.* (2002). The SCAP-SREBP complex is included into membrane vesicles through the binding of coatomer protein II (COPII) to SCAP. Sar1, Sec23 and Sec24 are the COPII proteins that are responsible for incorporation into membrane vesicles and transport to the Golgi. Cholesterol inhibits Sar-1 dependent binding Sec23 and Sec24 to SCAP and therefore blocks its integration into vesicles and movement from the ER to the Golgi (Espenshade *et al.*, 2002). The mechanism by which cholesterol blocks SCAP binding of Sec23/24 and vesicular formation was determined by experiments by Brown and colleagues (2002) using a trypsin cleavage assay (Brown *et al.*, 2002). Following isolation of SCAP containing membrane vesicles, trypsin was used to digest the cytoplasmic portion of proteins incorporated into the membrane of the vesicles. This technique removes the cytoplasmic amino acids but conserves the transmembrane and luminal domains of the membrane incorporated proteins. An anti-

SCAP antibody directed against an ER luminal segment of SCAP was used to show that the addition of cholesterol generated a smaller fragment following electrophoresis compared to that seen in the absence of cholesterol. This experiment provides evidence that SCAP undergoes a conformational change following the addition of cholesterol which allows a larger portion of the molecule to be in contact with the trypsin, thereby resulting in a smaller fragment when examined by immunoblotting (Brown *et al.*, 2002). To confirm these results, sterol resistant SCAP mutants did not undergo an *in vitro* conformational change when sterols were added. Together, these experiments suggest that ER membrane cholesterol regulates SREBP activation by maintaining the conformation of SCAP in a state in which Sec23/24 can not bind and SCAP-SREBP is unable to incorporate into membrane vesicles, be transported from the ER to Golgi where activation occurs.

1.2.4.2 Insulin-induced gene-1

Yang *et al.* (2000) determined that sterols cause the SCAP-SREBP complex to bind to an ER retention protein through an interaction involving the sterol-sensing domain (Yang *et al.*, 2000). Cells were transfected with cDNA encoding the transmembrane domain (TM1-6) of SCAP which contains its sterol sensing domain. Overexpression of SCAP(TM1-6) increased SREBP activation even in the presence of increasing amounts of cholesterol. The authors suggest that overexpression of the SCAP(TM1-6) peptide competes for some ER retention factor that normally binds to the

SCAP-SREBP complex in the presence of sterols and retains SREBP in the ER in an inactive state (Yang *et al.*, 2000).

It has previously been described that mutations at two conserved residues within the sterol sensing domain of SCAP (Y298C and D443N) disrupt SCAP's ability to respond to sterols (Nohturfft *et al.*, 1998b; Hua *et al.*, 1996a). In support of these findings, Yang *et al.* (2000) overexpressed a shorter segment of SCAP, designated SCAP(TM1-5), containing an incomplete sterol sensing domain or a cDNA for SCAP(TM1-6) that contains a point mutation in the sterol sensing domain (Y298C), rendering both unresponsive to sterols. Both peptides had no effect on SREBP activation which responded normally to the addition of sterols since presumably their incomplete sterol sensing domain was not capable to bind and compete for the then unknown ER retention factor (Yang *et al.*, 2000). A subsequent publication by Yang *et al.* (2002) determined the identity of the ER retention factor that binds to the sterol sensing domain of SCAP and retains the SCAP-SREBP complex in the ER in the presence of sterols (Yang *et al.*, 2002). In these experiments, two stably transfected cell lines were generated that overexpressed either SCAP(TM1-6) or SCAP(TM1-5), the latter of which does not have an intact sterol sensing domain. Yang and colleagues (2002) used coimmunoprecipitation and mass spectrometry of proteins that bound to SCAP(TM1-6) but not SCAP(TM1-5) to identify insulin-induced gene-1 (INSIG-1) as the ER retention protein that binds to the sterol sensing domain of SCAP in the presence of sterols (Yang *et al.*, 2002). To test the hypothesis that INSIG-1 is the ER retention protein that regulates the movement of SCAP-SREBP, Yang and colleagues (2002) transfected

mutant cells that do not express SCAP with a cDNA for SCAP and SREBP (Yang *et al.*, 2002). In the absence of SCAP overexpression, SREBP was not activated, but expression of SCAP restored SREBP processing. In the presence of overexpressed SCAP and SREBP, overexpression of INSIG-1 blocked SREBP activation. These experiments provide evidence that INSIG-1 can block SREBP processing even in the absence of sterols.

To demonstrate a direct interaction between INSIG-1 and SCAP, Yang *et al.* (2002) used blue native-PAGE (Shagger *et al.*, 1994) to examine native membrane proteins (Yang *et al.*, 2002). In these experiments, cells were transfected with a plasmid containing INSIG-1. Following various experimental conditions including overexpression of SCAP and/or the addition of cholesterol, membrane proteins were isolated and subjected to blue native-PAGE. Antibodies directed against INSIG-1 revealed conditions that resulted in bound or unbound INSIG-1. Overexpression of INSIG-1 alone resulted in unbound protein which was not affected by the addition of cholesterol. Co-expression of INSIG-1 and SCAP resulted in a decrease in the amount of unbound INSIG-1 and the addition of cholesterol caused a complete loss of unbound INSIG-1 (Yang *et al.*, 2002). The addition of an antibody directed against SCAP prior to electrophoresis produced a higher molecular weight complex and in the absence of SCAP co-transfection, the anti-SCAP antibody had no effect on the migration of unbound INSIG-1 (Yang *et al.*, 2002). Yang and colleagues (2002) found that at low INSIG-1 levels, SREBP-2 cleavage was high, and these levels fall as INSIG-1 levels increase, which reflects the sterol-induced inhibition of SREBP-2 cleavage. The relative amount

of unbound INSIG-1 rises inversely to SREBP-2 cleavage. Together, these experiments show that INSIG-1 binds to SCAP and retains SREBP-2 in the ER and SREBP-2 cleavage is blocked by sterols only when there is excess unbound INSIG-1 available to bind to SCAP-SREBP-2.

INSIG is an ER resident anchor that binds SCAP and maintains the ER localization of the SCAP-SREBP complex (Yabe *et al.,* 2002; Yang *et al.,* 2002). Upon cellular sterol depletion, cholesterol dissociates from the sterol-sensing domain of SCAP, releasing INSIG and allowing SCAP-SREBP to exit the ER through COPII vesicle transport (Sun *et al.,* 2005; Sun *et al*., 2007). Adams *et al* (2003) used a trypsin cleavage assay, previously reported to identify cholesterol induced conformational changes in SCAP (Brown *et al.,* 2002), to examine the effect of INSIG proteins on SCAP conformation (Adams *et al.,* 2003). Adams *et al* (2003) found that co-expression of INSIG-1 with SCAP decreases the amount of cholesterol needed to alter the conformation of SCAP and the effect of INSIG-1 was decreased when mutations in the sterol-sensing domain of SCAP was introduced that inhibit the INSIG-SCAP interaction (Adams *et al.,* 2003). Sun and colleagues (Sun *et al*., 2005; Sun *et al*., 2007) used recombinant COPII proteins (Sar1, Sec23/24) to show by immunoprecipitation that in sterol-deprived cells, the Sar1/Sec23/24 complex bound SCAP. Using *in vitro* mutagenesis, Sun *et al.,* (2005) determined that the COPII proteins bind to a six amino acid sezuence of methionine-glutamic acid-leucine-alanine-aspartic acid-leucine (MELADL). Together, these findings suggest a model where sterols alter the conformation of SCAP which blocks the accessibility of the MELADL sequence from

Sar1/Sec23/24 protein binding and promotes the binding of INSIG-1 and retains the SCAP-SREBP complex in the ER.

1.2.4.3 S1P/S2P

The transcriptional segment of SREBP must be released from its membrane localization in order to activate transcription of multiple genes responsible for cholesterol biosynthesis, unsaturated fatty acid biosynthesis, triglyceride biosynthesis, and lipid uptake. A complex two-step proteolytic process has been described in which SREBPs are released from the membrane (Hua *et al.,* 1996b; Sakai *et al.,* 1996). Hua and colleagues (1996) developed a transfection experiment that monitors sterol-regulated proteolytic cleavage of tagged SREBP-2 (Hua *et al.,* 1996b). This transfection experiment was used to identify two important sites for sterol-regulated cleavage of SREBP-2. Using mutational analysis of transfected cells, Hua and colleagues (1996) determined that two sites on either side of the ER membrane are required for sterol-regulated proteolysis (Hua *et al.,* 1996b). An arginine within the luminal loop and a sequence (DRSR) on the cytosolic side of the first transmembrane domain are required for efficient sterol-regulated proteolysis (Hua *et al.,* 1996b). Sakai and colleagues (1996) determined the importance of the two sequences identified by Hua *et al* (1996) (Hua *et al.,* 1996b; Sakai *et al.,* 1996). Sakai and colleagues made the observation that the release of the NH2-terminal SREBP-2 from membranes requires two sequential cleavages to occur. The first cleavage is sterol-regulated and occurs in the luminal loop and the second occurs following the first cleavage and it takes place within the first

transmembrane domain (Sakai *et al.*, 1996). The process begins when a protease cleaves SREBP-2 near Arg-519 in the luminal loop in sterol-depleted cells. The second cleavage site was found to occur in the membrane and requires the D_{478}RSR sequence immediately adjacent to the membrane on the cytosolic domain (Sakai *et al.*, 1996). Duncan and colleagues (1997) identified the site of sterol-regulated cleavage as the Leu^{522}-Ser^{523} bond within the ER luminal loop (Duncan *et al.*, 1997). The cleavage site was identified through the use of a vector encoding an SREBP fusion protein that allowed for immunoprecipitation of the cleaved COOH-terminal fragment (Duncan *et al.*, 1997). Cleavage by S1P separates SREBP into two halves that remain bound to the membrane. This has been determined by immunoprecipitation experiments using an antibody directed against the COOH-terminal domain which does not precipitate the NH2-terminal domain following cleavage by S1P (Sakai *et al.*, 1996). Following cleavage of SREBP into two halves by S1P, a second protease, designated Site-2 protease (S2P), cleaves the NH2-terminal fragment within its membrane-spanning domain. This cleavage occurs between a leucine and cysteine, three residues within the membrane-spanning domain (Duncan *et al.*, 1998). Interestingly the proteolytic action of S2P cannot occur without the prior cleavage of SREBP by S1P (Sakai *et al.*, 1996).

Using complementation cloning of mutant Chinese hamster ovary (CHO) cell lines that are unable to cleave SREBP at either Site-1 or Site-2, the genes responsible for the expression of S1P and S2P were identified (Rawson *et al.*, 1997; Sakai *et al*, 1998). Sakai and colleagues identified S1P as a novel serine protease of the subtilisin family (Sakai *et al.*, 1998), while Rawson and colleagues suggested that the S2P was a zinc

metalloprotease that cleaves proteins within their transmembrane domains (Rawson *et al.*, 1997).

Nohturfft and colleagues provided the first evidence that SREBP cleavage by S1P and S2P occurs in the Golgi and not the ER where previously thought (Nohturfft *et al.*, 1998b; Nohturfft *et al.*, 1999). Nohturfft and colleagues (1998) made the observation that the N-linked carbohydrate chains of SCAP were endoglycosidase H-sensitive in wild-type CHO cell lines but when grown in sterol-depleted medium, these carbohydrate chains became endoglycosidase H-resistant. These results suggest that sterols block the movement of SCAP between the ER and the Golgi (Nohturfft *et al.*, 1998b). Using glycosidase inhibitors and a glycosylation-defective mutant cell line, Nohturfft and colleagues subsequently concluded that sterols regulate the cleavage of SREBPs by modifying the ability of SCAP to transport SREBPs to the Golgi where it interacts with S1P (Nohturfft *et al.*, 1999).

In addition to the classical ER cholesterol-mediated regulation of SREBP-2, SREBP-1 responds to insulin stimultation through its increased expression and activation (Rawson, 2003). SREBP-1c expression is induced by the activation of the nuclear liver X receptor (LXR) (Hegarty *et al., 2005*). In addition, insulin levels reciprocally affect levels of a second INSIG isoform, INSIG-2. Increased insulin signaling decreases INSIG-2 levels and induces SREBP-1c activation (Yellaturu *et al., 2009*). Together, the regulation of SREBP-1c in tissues such as the liver is highly regulated by changes in membrane cholesterol and insulin signaling.

1.3 THE ENDOPLASMIC RETICULUM

1.3.1 ER Function

In addition to the location of SREBP, SCAP, and INSIG-1, the ER is the principal site for folding and maturation of transmembrane, secretory and ER-resident proteins (Lee, 2001). The conditions within the lumen of the ER are similar to the extracellular environment where there is a high concentration of calcium (Ca^{2+}) and the redox environment is more oxidizing compared to the cytosol (Sitia and Braakman, 2003). Several co-translational and post-translational modifications take place in the ER that do not occur in the cytosol. The abundance of ions and molecular chaperones in combination with its oxidizing environment provides the ER with the optimal conditions for various posttranslational modifications to take place. Important modifications that take place in the ER include disulphide-bond formation between cysteine residues, cleavage of the ER signal peptide, N-linked glycosylation and glycophosphatidylinositol (GPI)-anchor addition. These modifications are important for the correct folding of secretory and transmembrane proteins (Ellgaard and Helenius, 2003).

Folding of nascent polypeptide chains occur as they enter the ER lumen through the translocon complex (Johnson and van Waes, 1999). Post-translational folding occurs when the polypeptide chain is released from the ribosome-translocon complex and following individual subunit assembly, oligomerization takes place (Ellgaard and Helenius, 2003). ER protein chaperones are required for the successful completion of each folding step and although most chaperones are ubiquitously expressed there are examples of tissue specific expression (Sitia and Braakman, 2003). Oxidation of cysteine

residues causing the formation of disulphide bonds or the addition of glucose moieties to glycoproteins (N-linked glycosylation) are important for the folding and maturation of secretory and membrane proteins (Sitia and Braakman, 2003).

The chaperone proteins, calnexin and calreticulin, assist in protein folding by binding to N-linked glycans and unfolded regions of glycoproteins (Hebert *et al.*, 1995; Sitia and Braakman, 2003, Ma and Hendershot, 2004). N-linked glycosylation occurs on newly forming glycoproteins entering the ER lumen and the glucose molecules become a substrate for calnexin and calreticulin. As correct folding and maturation of the protein occurs, glucosidase enzymes remove the glucose molecules which inhibit binding of calnexin and calreticulin and allow the protein to be transported to the Golgi where further modification occurs (Ma and Hendershot, 2004). Calnexin and calreticulin form a complex with an ER oxidoreductase, ERp57, which aids in protein folding through oxidation of cysteine residues and disulphide bond formation (Sitia and Braakman, 2003).

Alterations in intracellular Ca^{2+} homeostasis are important for various cellular functions such as protein synthesis, folding, transport, contraction–relaxation, motility, metabolism, gene expression, cell-cycle progression and apoptosis (Corbett and Michalak, 2000). The ER is the principle site of intracellular Ca^{2+} storage and the importance of calreticulin to maintaining ER Ca^{2+} stores was determined when Nakamura and colleagues (2001) reported that calreticulin is capable of binding over 50% of ER luminal Ca^{2+} (Nakamura *et al.*, 2001). Nakamura and colleagues showed that calreticulin null cells have decreased levels of Ca^{2+} storage in the ER lumen even though the levels of

free Ca^{2+} is normal (Nakamura *et al.,* 2001). In response to various stimuli, Ca^{2+} is released from the ER lumen via Ca^{2+} channels and becomes an important signalling molecule in the cytosol. Ca^{2+} released into the cytosol is transported back into the ER lumen via the sarcoplasmic–endoplasmic-reticulum Ca^{2+}-ATPase (SERCA) pump. Conditions that cause the inhibition of the SERCA pump lead to prolonged ER Ca^{2+} depletion causing misfolding of proteins and ER stress (Denmeade and Isaacs, 2005).

The second ER chaperone system requires the presence of unfolded and hydrophobic polypeptide domains that are recognized by the ER chaperones glucose-regulated proteins (GRPs) GRP78 and GRP94 (Flynn *et al.,* 1991; Ron, 2002; Kaufman, 2002). GRPs were identified following viral transformation and glucose depletion (Shiu *et al.,* 1977). The expression of GRPs were determined not to be a consequence of viral transformation but rather the depletion of glucose caused by increased cellular metabolism (Shiu *et al.,* 1977). Munro and Pelham (1986) identified a cDNA clone from rat liver that was identical with GRP78 and proposed that the protein played a specific role in the assembly of secreted and membrane-bound proteins (Munro and Pelham, 1986). GRP78 identifies newly synthesized and unfolded proteins by their exposed hydrophobic domains (Flynn *et al.,* 1991) and assists in their proper folding (Flynn *et al.,* 1991).

GRP78 binds ATP and ADP which regulate its binding and release of unfolded proteins (Gething, 1999; Ma and Hendershot, 2004). Binding of ATP to GRP78 alters its conformation to allow for the binding of unfolded proteins. DnaJ proteins are co-chaperones of GRP78 which interact with unfolded proteins in the ER (Meunier *et al.,*

2002) by binding to GRP78 and catalyzing the hydrolysis of ATP (Liberek *et al*, 1991). The conversion of ATP to ADP causes a conformational change in GRP78 that enhances its affinity with its substrate unfolded protein (Ma and Hendershot, 2004). The nucleotide exchange factor BiP-associated protein (BAP) promotes the release of ADP from GRP78 causing a conformational change that releases the unfolded protein (Chung *et al.,* 2002; Ma and Hendershot, 2004). Together, GRP78, BAP and DnaJ proteins continuously promote folding of unfolded proteins through binding and release, with folding occurring during cycles where proteins are released from GRP78 (Hendershot *et al.,* 1996; Ma and Hendershot, 2004).

1.3.2 ER Stress and the Unfolded Protein Response (UPR)

The accumulation of misfolded proteins within the ER is known as ER stress. Physiological or pharmacological conditions that change the homeostasis of the ER can cause ER stress and induce the unfolded protein response (UPR). From a pharmacological perspective, the most robust way to disrupt ER homeostasis and protein folding is through the depletion of ER Ca^{2+} stores with Ca^{2+} ionophores (A23187) or sarco/endoplasmic reticulum Ca^{2+} ATPase inhibitors (thapsigargin). Although A23187 is not specific to the ER membrane as it enables Ca^{2+} ions to cross membranes in general, thapsigargin specifically targets the SERCA pump in the ER membrane affecting ER Ca^{2+} concentration. *In vitro* depletion of ER Ca^{2+} with thapsigargin (Tg) or A23187 causes a decrease in the activity of Ca^{2+}-dependent chaperones such as GRP78. Reduced ER chaperone function leads to a decrease in the protein folding capacity of the ER and

causes an accumulation of misfolded proteins. Physiologic induction of ER stress can result from alteration in ER Ca^{2+} homeostasis, increased protein synthesis and secretion, an increase in misfolded proteins, glucose deprivation, or changes in protein glycosylation (Ron, 2002; Kaufman, 2002).

Disruption in ER function (ER stress) that interferes with proper folding and maturation of proteins initiates the unfolded protein response (UPR), an intracellular signalling pathway that induces temporary translational inhibition followed by upregulation of ER chaperones (Ron, 2002; Kaufman, 2002) (Figure 2). The UPR is mediated via three ER-resident sensors: a type-I ER transmembrane protein kinase (IRE-1), activating transcription factor 6 (ATF-6) and the PKR like ER kinase (PERK). Under non-ER stress conditions, GRP78 binds to the ER luminal domain of these three sensors, but upon conditions that cause ER stress, dissociation of GRP78 causes activation of IRE-1, ATF-6, and PERK (Lee, 2001; Ron, 2002; Kaufman, 2002; Rutkowski and Kaufman, 2004; Lawrence de Koning *et al.,* 2003). IRE-1 is a transmembrane protein with endoribonuclease activity (Kaufman, 2002; Ron and Hubbard, 2008). IRE-1 is bound to GRP78 under non-ER stress conditions and undergoes dimerization and trans-autophosphorylation in the presence of ER luminal unfolded proteins. Phosphorylated IRE-1 is active as an RNase which splices its target mRNA of XBP-1, removing an intron and enabling XBP-1 to be translated into an active transcription factor that upregulates UPR response genes such as GRP78 (Yoshida *et al.,* 1998; Yoshida *et al.,* 2001; Tirasophon *et al.,* 2000).

Figure 2. ER stress and the unfolded protein response

The UPR is regulated by the proximal sensors IRE-1, ATF-6, and PERK. Activation of these sensors occurs following their dissociation from GRP78 in response to ER stress. Once activated, the UPR functions as an integrated, intracellular signaling pathway to a) attenuate protein translation through eIF2α phosphorylation, b) increase ER chaperone expression, and c) enhance degradation of unfolded proteins via the proteasome (modified from Austin *et al*. 2004).

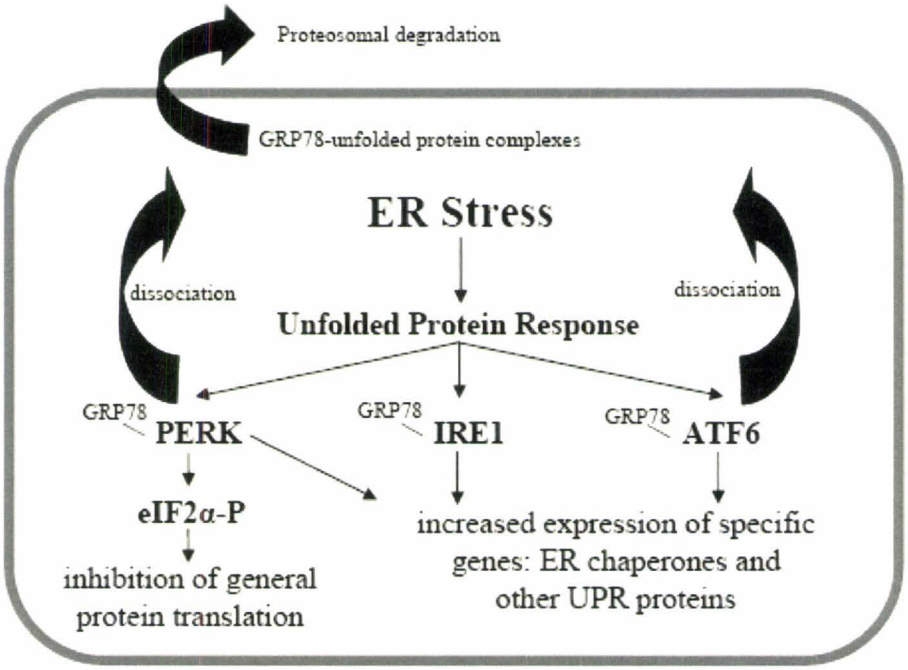
Proteosomal degradation
GRP78-unfolded protein complexes
ER Stress
dissociation
dissociation
Unfolded Protein Response
GRP78
PERK
GRP78
IRE1
GRP78
ATF6
eIF2α-P
inhibition of general protein translation
increased expression of specific genes: ER chaperones and other UPR proteins

Activating transcription factor 6 (ATF6) is an ER transmembrane protein with its luminal domain bound to GRP78 under non-ER stress conditions. In the presence of unfolded proteins, GRP78 dissociates from the luminal domain of ATF6, exposing Golgi localization signals (GLS) that promote the translocation of ATF6 to the Golgi (Chen *et al.,* 2002; Shen *et al.,* 2002). Activation of ATF6 occurs in the Golgi through the proteolytic cleavage of its transmembrane domain by S1P and S2P, the same proteases that process SREBP upon cholesterol depletion (Haze *et al.,* 1999; Ye *et al.,* 2000). Translocation of active ATF6 to the nucleus leads to upregulation of XBP-1 mRNA providing more substrate for IRE-1 (Yoshida *et al.,* 2001; Lee *et al.,* 2002) and creating a positive feedback for UPR activation (Kaufman, 2002).

In parallel with the activation of transcription factors XBP-1 and ATF6 and the subsequent upregulation of UPR response genes, the accumulation of misfolded proteins leads to a decrease in protein translation. The ER kinase PERK is another ER transmembrane sensor that binds GRP78 to its luminal domain. ER stress-induced GRP78 dissociation allows PERK to homodimerize and trans-autophosphorylate causing activation of its cytosolic kinase domain (Ron, 2002). ER stress-induced activation of PERK induces the phosphorylation of the α subunit of eukaryotic translation initiation factor 2 (eIF2α) which blocks general protein translation (Harding *et al.,* 1999). Although eIF2α phosphorylation inhibits general protein translation, certain UPR associated mRNAs such as GRP78 have an internal ribosome entry site that allows translation under conditions of ER stress and eIF2α phosphorylation (Ron, 2002). Together, the ER-resident sensors IRE-1, ATF-6, and PERK respond to ER stress by

upregulating ER chaperones and inhibiting protein translation, thereby enhancing cell survival by ensuring that the adverse effects of ER stress are dealt with in an efficient manner. Initially, the UPR provides a protective advantage for the cell; however prolonged or severe ER stress can activate UPR-dependent pathways that increase caspase activation and apoptosis (Hossain *et al.,* 2003; Morishima *et al.,* 2002; Nakagawa *et al.,* 2000; Feng *et al.,* 2003).

1.3.3 ER Stress and SREBP Activation

We and others have shown that disruption in ER function, leading to ER stress and activation of the UPR, induces lipid dysregulation (Kim *et al.,* 2005; Esfandiari *et al.,* 2005; Ji and Kaplowitz, 2003; Werstuck *et al.,* 2001; Colgan *et al.,* 2007; Kammoun *et al.,* 2009). ER stress-induced lipid dysregulation was observed when Outinen and colleagues, showed by cDNA microarray analysis that elevated homocysteine levels upregulate ER stress response genes and SREBP expression in human umbilical vein endothelial cells (Outinen *et al.,* 1998; Outinen *et al.,* 1999). Homocysteine (Hcy) is an amino acid that is biosynthesized from methionine and can be converted to cysteine. Werstuck *et al* (2001) subsequently found that Hcy-induced ER stress activates SREBP, which in turn increased gene expression essential for biosynthesis and uptake of cholesterol and triglycerides. The Hcy-induced SREBP-1 activation caused the accumulation of cholesterol *in vitro* and led to hepatic steatosis *in vivo* (Werstuck *et al.,* 2001). Since the report by Werstuck *et al* (2001), subsequent publications have confirmed the findings that ER stress is associated with activated SREBP and lipid

accumulation (Esfandiari *et al.,* 2005; Ji and Kaplowitz, 2003; Woo *et al.,* 2005). However, the underlying mechanism of how ER stress induces SREBP activation is yet to be determined. A recent report by Kammoun and colleagues (2009) confirmed previous findings that ER stress promotes SREBP-1 activation and hepatic lipogenesis and overexpression of GRP78 reduced hepatic ER stress and inhibited SREBP-1 activation *in vivo* (Kammoun *et al.,* 2009). Through co-immunoprecipitation experiments, Kammoun and colleagues (2009) suggested that GRP78 binds to the SREBP complex (SREBP, SCAP, or INSIG) and inhibits its movement from the ER to the Golgi (Kammoun *et al.,* 2009).

The current scientific literature points to the possibility of two potential mechanisms of how ER stress induces SREBP activation. Investigations by Brown and Goldstein to identify the cellular proteases that cleave sterol-regulatory element binding proteins (SREBPs), demonstrated that a cysteine protease termed SCA (SREBP cleavage activity), could cleave both SREBP-1 and –2. SCA was purified, sequenced and revealed to be the hamster equivalent of human CPP32 or caspase-3 (Wang *et al.,* 1995). Caspases (cytosolic aspartate-specific proteases) are key enzymes responsible for the disassembly of a cell during apoptosis (Porter and Janicke, 1999). Apoptosis is a fundamental biological process that enables an organism to kill and remove unwanted cells during animal development, normal homeostasis and disease (Thompson, 1995; Jacobson *et al.,* 1997). Caspases are a family of cysteine proteases that are synthesized as inactive zymogens and possess an active-site cysteine that cleaves substrates after aspartic acid residues.

The 'caspase cascade' occurs when one of these caspases is activated, setting in motion the subsequent cleavage of several downstream caspase substrates (Hengartner, 2000). Caspase-3 and –7 are downstream effector caspases with multiple substrates. Two of the most well known substrates of effector caspases during apoptosis are ICAD (inhibitory subunit of caspase-activated DNase) and PARP (polyADP-ribose polymerase). Cleavage of the inhibitory subunit allows CAD to cleave genomic DNA between nucleosomes to generate DNA fragments (Hengartner, 2000). PARP is a 116 kDa nucleosomal protein that functions in the repair of DNA and is cleaved to an 85 kDa non-functional fragment by caspase-3 during apoptosis. Many of the known caspase substrates are specifically cleaved by caspase-3 or a related protease (Porter and Janicke, 1999).

Subsequent to the initial finding demonstrating that caspase-3 had the capacity to cleave SREBP-1 and SREBP-2 (Wang *et al.,* 1995), a study by the same group demonstrated that CPP32 (caspase-3) was activated by staurosporine (STS), a protein kinase inhibitor that induces programmed cell death, and the activation of CPP32 correlated with SREBP cleavage that could not be inhibited by the presence of sterols (Wang *et al.,* 1996). Wang *et al* (1996), used a stably transfected Chinese hamster ovary (CHO) cell line with a mutation of the aspartic acid at the caspase-3 cleavage site to show that apoptosis-induced SREBP cleavage was caused by caspase-3. Immunoblot analysis using anti-SREBP-1 and –2 monoclonal antibodies directed toward either the N- or C-terminus, showed that SREBP cleavage in the presence of STS produced a smaller fragment then that of sterol regulated cleavage of SREBP (Wang *et al.,* 1996). Together,

this evidence reveals that apoptosis-induced SREBP cleavage occurs by caspase-3 at a site different from the S1P.

A following study by Pai *et al* (1996) showed that caspase-7 was also capable of cleaving SREBP at the caspase-3 site in a sterol independent manner (Pai *et al.*, 1996). Although the Brown and Goldstein group found that the N-terminus of SREBP was located in the nucleus after the induction of apoptosis, it was not known whether the transcription factor was functional due to the alternative cleavage by caspase-3/-7. To answer this question, Higgins and Ioannou (2001) developed a reporter plasmid controlled by the SRE element of the human LDL receptor (Higgins and Ioannou, 2001). Binding of active SREBP to the SRE sequence caused increased expression of green fluorescent protein (GFP). They showed that expression of sterol response element (SRE) controlled genes (which increase lipid and cholesterol biosynthesis and uptake) were increased by the induction of apoptosis, and blocked by caspase inhibitors. An important aspect of this finding is that SREBP activation and gene expression occurs early in the apoptotic process while the cells are still viable (Higgins and Ioannou, 2001)). It was reported by Nhan *et al.* (2003) that the active form of caspase-3 (p17) was present in viable macrophages *in vitro*, and was observed in macrophages within atherosclerotic plaques (Nhan *et al.*, 2003). These findings suggest that caspase-3 or other caspases may function independently of apoptotic cell death and may play a role in cellular lipid accumulation.

Since ER stress causes increased SREBP cleavage (Werstuck *et al.*, 2001; Wang *et al.*, 2005) and caspase activation (Feng *et al.*, 2003; Hossain *et al.*, 2003; Nakagawa *et*

al., 2000), and activated caspase-3 or caspase-7 cleaves SREBP, it has been suggested that ER stress causes SREBP activation and subsequent cholesterol accumulation through a caspase-dependent mechanism.

Although ER stress-induced SREBP-2 activation occurs in the presence of sterols, it may not be mediated by caspases during apoptosis but rather could occur through the conventional sterol mediated activation pathway normally reserved for SREBP activation following intracellular cholesterol depletion. It was reported by Lee and Ye (2004) that translational inhibition following Tg-induced eIF2α phosphorylation causes SREBP-2 activation (Lee and Ye, 2004). Lee and Ye (2004) correlated Tg-induced SREBP-2 cleavage with INSIG-1 degradation. The proposed mechanism of ER stress-induced SREBP-2 activation was suggested to involve the degradation of INSIG-1. Since INSIG-1 is the molecular "anchor" that binds and retains the SCAP/SREBP complex in the ER, it was suggested that ER stress-induced inhibition of protein synthesis caused INSIG-1 degradation and subsequent SREBP-2 activation (Lee and Ye, JBC, 2004).

Recent findings by Kammoun *et al.* (2009) have proposed an additional mechanism of ER stress-induced SREBP activation (Kammoun *et al.,* 2009). To determine whether ER stress promotes SREBP-1 and -2 activation, Kammoun and colleagues (2009) overexpressed GRP78 in the livers of mice using an adenoviral vector. Similar to the findings reported by Werstuck and colleagues (2001) who showed that *in vitro* overexpression of GRP78 could attenuate ER stress-induced SREBP activation and lipid accumulation (Werstuck *et al.,* 2001), Kammoun *et al.* (2009) showed that increased *in vivo* expression of GRP78 resulted in decreased ER stress, SREBP-1 and -2 target gene

expression, as well as hepatic lipid content (Kammoun *et al.*, 2009). In addition to the role of GRP78 on reducing ER stress, it may have a direct effect on SREBP activation. Interestingly, coimmunoprecipitation experiments revealed that GRP78 associates with the SREBP-1 precursor complex and was suggested that although it may not directly bind SREBP, it may interact with SCAP to block its COPII binding sequence and retain it in the ER under non-ER stress conditions (Kammoun *et al.*, 2009). Further examination is required to determine the precise mechanism of ER stress-induced SREBP activation under several physiological and pathophysiological conditions.

1.4 SREBP DYSREGULATION

1.4.1 Hepatic Lipid Accumulation

Dysregulation of the SREBP pathway has been implicated in many cellular lipid pathologies associated with intracellular lipid accumulation. Cholesterol and fatty acids are synthesized in the liver and have been shown to be controlled by the SREBP pathway. Hepatic cholesterol synthesis is elevated when mice are fed a cholesterol-free diet and declines when their diet is replete with cholesterol. Hepatic fatty acid biosynthesis responds to dietary carbohydrate and subsequent insulin levels. As discussed above, both of these lipid biosynthetic pathways are regulated by SREBPs. Brown and Goldstein's group designed studies to determine the role of the three SREBP isoforms in the liver and described the potential pathological effect of *in vivo* SREBP dysregulation.

Transgenic mouse models that overexpress truncated dominant-positive SREBPs were created (Shimano *et al.*, 1997; Shimano *et al.*, 1996; Horton *et al.*, 1998). The

encoded SREBPs were terminated before the first transmembrane domain and therefore not regulated by their interaction with SCAP and INSIG or cellular lipid content. Therefore, these active SREBPs were not down-regulated by cholesterol accumulation. *In vivo* expression of the SREBPs was driven using the promoter for phosphoenolpyruvate carboxykinase (PEPCK), which is expressed in liver, adipose tissue, and kidney. High level expression was induced in the liver when mice consumed a low carbohydrate/high protein diet (Shimano *et al.*, 1996; Shimano *et al.*, 1997).

Transgenic mice expressing a constitutive active form of SREBP-1a developed progressive liver enlargement with hepatocyte cholesterol and triglyceride accumulation. The rate of cholesterol and fatty acid synthesis in the liver was enhanced by 5- and 25-fold, respectively (Shimano *et al.*, 1996). Interestingly, the white adipose tissue mass decreased as the liver accumulated lipid. This study indicates that active SREBP-1a can cause enhanced lipid accumulation in the liver leading to hepatic steatosis.

The same model was used to examine the effect of the SREBP-1c isoform on liver lipid content (Shimano *et al.*, 1997). SREBP-1c transgenic mice showed only moderate increases in triglycerides but not cholesterol in the liver. The mRNAs for many of the elevated cholesterol biosynthetic enzymes in the SREBP-1a overexpressing mouse were not significantly elevated in the SREBP-1c model. Although the mRNAs for fatty acid biosynthesis were significantly elevated in SREBP-1a transgenic mice, they were only slightly elevated in SREBP-1c mice. Shimano *et al.* (1997) determined that SREBP-1c is a weaker transcriptional activator than SREBP-1a (Shimano *et al.*, 1997).

Horton *et al* (1998) produced transgenic mice that overexpressed a truncated dominant-positive form of SREBP-2 under the control of the PEPCK promoter (Horton *et al.,* 1998). The livers of the transgenic mice had increased mRNAs for multiple enzymes of cholesterol and fatty acid biosynthesis. The transgenic livers had a 28-fold increase in cholesterol synthesis and a 4-fold increase in fatty acid biosynthesis. Since these results were inversely related to those seen with the SREBP-1a transgenic mice, Horton and colleagues concluded that SREBP-2 is a predominantly selective activator of the cholesterol biosynthetic pathway (Horton *et al.,* 1998).

The *in vivo* overexpression of SREBP-1a in mouse adipose tissue produces adipocyte hypertrophy, increased fatty acid secretion, and hepatic steatosis (Horton *et al.,* 2003). In contrast, the overexpression of the SREBP-1c isoform in mouse adipose tissue inhibits adipocyte differentiation. The resultant transgenic SREBP-1c phenotype includes lipodystrophy or a loss of peripheral white adipose tissue, diabetes, and hepatic steatosis (Shimomura *et al.,* 1998). As described above, our group has demonstrated that diet-induced hyperhomocysteinemia caused ER stress-induced SREBP activation and hepatic steatosis (Werstuck *et al.,* 2001). Importantly, attenuation of ER stress by overexpression of GRP78 attenuated SREBP activation and decreased the expression of genes responsible for cholesterol/triglyceride biosynthesis.

1.4.2 Renal Lipid Accumulation

Renal proximal tubular cells have been shown to be sensitive to ER stress when mice are injected with tunicamycin (Zinszner *et al.,* 1998). Tunicamycin (Tm) blocks the

synthesis of all N-linked glycoproteins and induces ER stress. Recently, Kimura and colleagues (2008) showed the importance of the UPR to protect cells from toxicity-induced renal cell damage (Kimura *et al.*, 2008). A knock-in mouse model of mutant GRP78 was used to inhibit the normal increased GRP78 expression following ER stress. A BSA-overload proteinuria model, which causes protein overload-induced toxicity in renal tubular cells, was used to accelerate chronic tubular-interstitial injury in mice expressing mutant GRP78. Following chronic protein overload-induced nephrotoxicity, mice expressing mutant GRP78 suffered tubular-interstitial lesions and cell apoptosis due to proteinuria induced toxicity (Kimura *et al.*, 2008). This study demonstrates the importance of the UPR in the normal physiological maintenance of renal cells challenged with toxic injury. The benefit from ER chaperone protein upregulation during the UPR to protect renal cells from ER stress-induced cytotoxicity was shown in multiple renal cell lines with various cytotoxic agents (Peyrou and Cribb, 2007). Peyrou and Cribb (2007) demonstrated that preconditioning renal cells with ER stress-inducing agents, including Tm, Tg, or Dithiothreitol (DTT; reducing agent that causes ER stress), protected cells from clinically relevant nephrotoxins (Peyrou and Cribb, 2007). The upregulation of ER chaperones following treatment with ER stress-inducing agents, protected renal cells from subsequent toxic injury. The previously described experiments show the importance of ER chaperone upregulation during the UPR in the protection of renal cells from toxic agents.

The pathology associated with acute renal toxicity is the accumulation of lipid, mainly cholesterol, within the proximal tubules. Zager and colleagues have extensively

studied lipid accumulation in proximal tubules in response to ischemia and cytotoxic compounds both *in vivo* and *in vitro* (Zager and Johnson, 2001; Zager *et al.,* 2001; Zager *et al.,* 2002; Zager *et al.,* 2003; Johnson *et al.,* 2005). Interestingly, a commonality of the studies is the increase in the expression of enzymes and receptors responsible for the uptake and biosynthesis of cholesterol and triglycerides (Zager and Johnson, 2001; Zager *et al.,* 2001; Zager *et al.,* 2003; Johnson *et al.,* 2005; Zager *et al.,* 2005). Although SREBP regulation is an essential component of cell growth and differentiation, these studies have demonstrated that disruption of this tightly controlled lipogenic pathway can lead to various lipid-associated pathologies.

2 RATIONALE, OBJECTIVES AND HYPOTHESIS OF STUDY

2.1 RATIONALE

We and others have shown that SREBP activation and lipid dysregulation is associated with conditions that cause ER stress and the activation of the UPR (Kim *et al.*, 2005; Esfandiari *et al.*, 2005; Ji and Kaplowitz, 2003; Werstuck *et al.*, 2001; Colgan *et al.*, 2007). Werstuck *et al.* (2001) reported that ER stress was able to activate SREBP-1, which in turn increased gene expression essential for the biosynthesis and uptake of cholesterol and triglycerides. Furthermore, ER stress-induced SREBP-1 activation caused the accumulation of cholesterol *in vitro* and led to hepatic steatosis *in vivo* (Werstuck *et al.*, 2001). Since the report by Werstuck *et al* (2001), subsequent publications have confirmed the findings that ER stress is associated with the activation of SREBP and hepatic lipid accumulation (Esfandiari *et al.*, 2005; Ji and Kaplowitz, 2003; Woo *et al.*, 2005; Kammoun *et al.*, 2009).

This project was designed to elucidate the mechanism of ER stress-induced SREBP activation and determine its relationship with cellular pathologies associated with ER stress and lipid dysregulation. Our research has examined the mechanism by which ER stress activates SREBP-2 in various cell lines, including HeLa, MCF7, MDCK epithelial cells and THP-1 macrophage cells. We determined that (1) ER stress activates SREBP-2 by the conventional sterol-mediated proteolytic pathway (Colgan *et al.*, 2007); (2) there exists a strong relationship between changes in ER Ca^{2+} and SREBP-2 activation; (3) ER stress is associated with SREBP-2 activation and lipid dysregulation in

a model of renal injury; and (4) ER stress-induced SREBP activation is not associated with lipid accumulation in macrophage foam cells.

2.2 HYPOTHESIS

ER stress causes SREBP-2 activation and lipid accumulation through the conventional proteolytic pathway and contributes to lipid dysregulation in various cell types.

2.3 OBJECTIVES

2.3.1 Overall Objective

The overall objective of this project is to define the mechanism by which sterol regulatory element binding proteins (SREBP) are activated by endoplasmic reticulum (ER) stress and apoptosis.

2.3.2 Specific Objective

1. To examine whether ER stress activates SREBP-2 and causes lipid dysregulation
2. To determine if ER stress activates SREBP-2 through conventional pathways
3. To investigate the role of eIF2α-phosphorylation on SREBP-2 cleavage
4. To assess the role of ER Ca^{2+} on SREBP-2 cleavage
5. To determine the role of SREBP activation in renal lipid dysregulation
6. To examine the role of SREBP activation in macrophage lipid dysregulation

3 EXPERIMENTAL PROCEDURES

3.1 MATERIALS

Thapsigargin (Tg), Tunicamycin (Tm), homocysteine (Hcy), 25-hydroxycholesterol, dithiothreitol (DTT), A23187, and staurosporine (STS) were obtained from Sigma-Aldrich (Oakville, ON). 4-(2-Aminoethyl)benzenesulfonyl fluoride hydrochloride (AEBSF), Z-VAD-FMK, salubrinal, 3b-(2-Diethylaminoethoxy)androst-5-en-17-one,HCl (U18666A), cyclopiazonic acid (CPA), BAPTA-AM were obtained from Calbiochem (VWR Canlab; Mississauga, ON).

3.2 CELL LINES AND CULTURE CONDITIONS

3.2.1 MCF7

The human breast adenocarcinoma cell line MCF7 was obtained from the American Type Culture Collection (ATCC; Manassas, VA) and cultured in DMEM containing 10% fetal bovine serum (FBS), 100 mg/ml penicillin and 100 mg/ml streptomycin. MCF7 cells stably transfected with pBabe or pBabe-caspase 3 expression plasmids were obtained from Dr. Damu Tang (McMaster University). MCF7 cells were used in the initial experiments to define the contribution of caspase-3 to ER stress-induced SREBP cleavage. MCF7 cells are useful in these studies because they have a mutation in the Cas3 gene and do not express caspase-3.

3.2.2 HELA

The human cervical carcinoma cell line HeLa was obtained from ATCC (Manassas, VA) and cultured in DMEM containing 10% FBS, 100 mg/ml penicillin and 100 mg/ml streptomycin. HeLa cells were used in many of the experiments as they are a widely used cell line for cell biological studies as they are easily manipulated in culture.

3.2.3 MDCK

The canine tubule epithelial cell line, MDCK, was obtained from Dr. Damu Tang (McMaster University) and cultured in DMEM containing 10% FBS, 100 mg/ml penicillin and 100 mg/ml streptomycin. Due to their tubule epithelial cell origin, MDCK cells were used as a proof of principle to confirm the *in vivo* findings *in vitro*.

3.2.4 THP-1

The human monocytic leukemia cell line, THP-1, was obtained from the American Type Culture Collection (ATCC; Manassas, VA) and cultured in RPMI-1640 medium (Sigma) containing 100 μg/ml penicillin, 100 μg/ml streptomycin and 10% fetal bovine serum. To induce macrophage differentiation, THP-1 monocytes were treated with 100 ηM phorbol 12-myristate acetate (PMA) (Sigma) for 24 hours, washed and incubated in complete RPMI-1640 growth medium. THP-1 monocytes were used as a cellular model for macrophage differentiation and lipid metabolism.

3.2.5 PBMC

Human peripheral blood mononuclear cells (PBMCs) were isolated fresh from donors by the adherence of CD14 microbeads (Miltenyi Biotech; Auburn, CA) to a magnetic column. Following CD14+ monocyte isolation, cells were plated at $0.5x10^6$ cells/ml in RPMI-1640 medium (Sigma) containing 100 μg/ml penicillin, 100 μg/ml streptomycin and 1% fetal bovine serum. To induce differentiation, PBMCs were incubated in the presence of 150 ηg/ml macrophage colony stimulating factor (m-CSF) for 7 days. All cell lines were cultured in a humidified incubator at 37 degrees Celsius with 5% CO_2. PBMC were used due to their physiological significance and to confirm the findings from the THP-1 macrophage cell model.

3.3 CELL LYSIS

Cell lysates were prepared by removing the growth medium, washing the cells 3 times with cold phosphate buffer saline (PBS), adding 4X SDS-PAGE buffer (0.1 ml per 33 mm well) containing 25 μg/ml of the proteasome inhibitor, N-acetyl-leucinal-leucinal-norleucinal (ALLN) (Calbiochem) and a protease inhibitor cocktail (Roche). Cell lysates were manually scraped from plates and collected in eppendorf centrifuge tubes. Cell lysates were centrifuged at maximum speed for 10 minutes to remove cellular debris. Following centrifugation, supernatants were collected and the protein concentration of lysates was determined by the Dc Protein Assay (Bio-Rad). Lysates were stored frozen at -20 degrees Celsius.

3.4 IMMUNOBLOT ANALYSIS

The anti-SREBP-2 (IgG-1C6) monoclonal antibody that recognizes a C-terminal epitope of SREBP-2 was purchased from BD Pharmingen (Mississauga, ON). The anti-SREBP-2 (N-19) monoclonal antibody that recognizes an N-terminal epitope of SREBP-2 was purchased from SantaCruz Biotechnologies (Santa Cruz, CA). The anti-SREBP-1 (H160) monoclonal antibody that recognizes an N-terminal epitope of SREBP-1 was purchased from SantaCruz Biotechnologies (Santa Cruz, CA). The anti-Caspase-3 antibody, which recognizes full length, inactive caspase-3 was purchased from BD Pharmingen (Mississauga, ON). The anti-KDEL monoclonal antibody, which recognizes GRP78, GRP94 and HSP47, was purchased from Stressgen Biotechnologies (Victoria, BC). The anti-GFP and anti-phospho-eIF2alpha (Ser51) antibodies were purchased from Cell Signaling (New England Biolabs Ltd., Pickering, ON). The anti-GADD153 (R-20) antibody was purchased from SantaCruz Biotechnologies (Santa Cruz, CA). The anti-β-actin monoclonal antibody used as a loading control for immunoblotting was purchased from Sigma-Aldrich (Oakville, ON). 50 μg of total protein lysates per well were separated on 10% SDS-polyacrylamide gels under reducing conditions and transferred to nitrocellulose membranes. After incubation with the appropriate primary and horseradish peroxidase (HRP)-conjugated secondary antibodies (DakoCytomation Inc., Mississauga ON), the membranes were developed using the Renaissance Chemiluminescence Reagent kit (Perkin-Elmer, Boston, MA).

3.5 TRANSIENT TRANSFECTION

Transient transfection of MCF7 and HeLa cells was performed using Effectene transfection reagent (Qiagen). Wildtype MCF7 and HeLa cells were grown in appropriate medium until 50% confluence. Cells were washed once with 1X PBS and transfected with 0.5–4 μg DNA. Cells were incubated in media containing Effectene for 18 hours. Media was replaced after 18 hours and cells were examined for reporter plasmid expression (fluorescence). Transient transfection of MDCK cells was performed using Polyfect transfection reagent (Qiagen). MDCK cells were grown to 75% confluence in the appropriate media. Cells were washed once with 1X PBS, transfected with 0.5–4 μg DNA and incubated in media containing Polyfect for 18 hours. The pEGFP-C1 expression plasmid was used to determine the transfection efficiency of THP-1 cells. Following the use of various transfection reagents and techniques, we determined that Lipofectamine Plus (Qiagen) produced the most consistent transfection efficiency of approximately 10-15%. Transient transfection of THP-1 cells was performed by seeding 0.5×10^6 cells/well in a 6-well plate. Cells were treated with PMA (100 μM) for 24 hours to undergo differentiation. Cells were washed and allowed to incubate for an additional 48 hours. Differentiated macrophages were then washed with 1X PBS and transiently transfected using Lipofectamine Plus transfection reagent. Cells were incubated in media containing Lipofectamine Plus and plasmid DNA for 18 hours. Media was replaced after 18 hours and cells were incubated for various time points under different experimental conditions. Cells were washed twice with 1X PBS prior to protein lysate preparation, total RNA extraction, Filipin or Oil-Red-O staining.

3.6 FILIPIN STAINING

THP-1 or MDCK cells were cultured on coverslips and incubated under various experimental conditions. Cells were washed with PBS and fixed with 3% paraformaldehyde for 20 minutes on ice. Cells were washed with PBS and incubated with 1 mg/ml Filipin (Sigma-Aldrich; Oakville, ON) for 2 hours at RT. Cells were observed with ultraviolet light for Filipin staining, which indicates intracellular free cholesterol.

3.7 OIL-RED-O STAINING

THP-1, MDCK, and PBMCs cells were cultured on coverslips and incubated under various experimental conditions in 35 mm plates. Cells were washed with PBS and fixed with 3.7% paraformaldehyde for 20 minutes on ice. Cells were washed 3X with PBS and incubated with Oil Red O (ORO) staining solution (Sigma-Aldrich; Oakville, ON) for 2 hours at room temperature (as described by Kuri-Harcuch and Green, 1978). Cells were observed under the light microscope for ORO staining representing intracellular neutral lipid accumulation. Quantification of ORO was performed through the extraction of lipid-bound ORO by the addition of isopropanol to stained cells (as described by Katsuri and Joshi, 1982). Following 1 hour incubation with 60% isopropanol, the dissolved ORO-isopropanol solution was quantified by a spectrophotometer at a wavelength of 510 nM.

3.8 REAL-TIME PCR ANALYSIS

Following incubation under various experimental conditions, cells were lysed and total RNA was extracted with RNeasy RNA Mini Kit (Qiagen; Mississauga, ON). RT-PCR was conducted using 2 μg total RNA that was reverse transcribed to cDNA using the High Capacity cDNA Archive Kit (Applied Biosystems; Foster City, CA) and a PTC-100 Programmable Thermal Controller (MJ Research, Inc., NV). Real-time PCR analysis was performed in an ABI PRISM 7300 (Applied Biosystems) thermocycler using Taqman gene expression assays (Applied Biosystems; Foster City, CA) for sterol regulatory element binding protein-2 (SREBP-2), 3-hydroxy-3-methyl-glutaryl-CoA reductase (HMG-CoA), glucose regulated protein-78 (GRP-78), and interleukin-8 (IL-8). Cycle parameters were as follows: denaturation at 95°C for 15 seconds, followed by annealing and extension for 1 minute at 60°C, for 40 cycles. Results were expressed as a fold increase over the corresponding 18S rRNA control.

3.9 INTRACELLULAR LIPID ANALYSIS

Intracellular total cholesterol, free cholesterol, and total triglycerides were measured using the Cholesterol E, Free Cholesterol E and L-Type TG M enzymatic assays, respectively (Wako Diagnostics; Richmond, VA). THP-1 differentiated macrophages were grown at a density of $2x10^6$ cells per 60 mm plate. Following incubation, cells were washed 3 times with cold PBS and lysed with 1 ml 0.2N NaOH. Lipids were extracted with hexane:isopropanol (3:2) and centrifuged for 5 minutes at 500 X *g*. Supernatents were isolated and dried in a fumehood (24 hours). Lipids were resuspended in 0.3 ml isopropanol and 0.1 ml of each sample was incubated with 1 ml of

the Cholesterol E, Free Cholesterol E or the L-Type TG M reagent. Samples were quantified using a spectrophotometer at wavelength of 500 nm and compared to standard solution containing cholesterol, free cholesterol, or triglycerides.

3.10 LOW DENSITY LIPOPROTEIN UPTAKE ANALYSIS

Binding and internalization of low density lipoprotein (LDL) and acetylated LDL (acLDL) was measured using DiI-LDL (alexa594) and AcLDL (alexa488) (Molecular Probes). THP-1 differentiated macrophages were seeded at a density of $3x10^5$ cells per 35 mm well. Following incubation in growth medium under different experimental conditions, cells were washed and incubated for 1 hour in serum free medium with or without 10 μg/ml DiI-LDL or 10 μg/ml AcLDL. Following 1 hour incubation with the fluorescent labelled LDL, cells were washed 3X with PBS and incubated with 4% paraformaldehyde for 20 minutes. DiI-LDL and AcLDL uptake was examined with fluorescent microscope using 594 and 488 filters.

3.11 INTRACELLULAR FREE CALCIUM ANALYSIS

HeLa cells were seeded in 96-well plates and allowed to adhere for 12 hours. HeLa cells were loaded with 5 μM Fura-2 AM for 30 minutes at room temperature and protected from light. Fura-2 AM fluoresces upon binding with cytosolic free Ca^{2+}. HeLa cells were washed three times and incubated under experimental conditions. Fluorescence was measured using a microplate spectrofluorometer at excitation wavelengths, 340 nm and 380 nm and emission wavelength of 515 nm. The fluorescence

intensity produced at 340 nm compared to 380 nm was used to determine the intracellular free Ca^{2+} concentration.

3.12 STATISTICAL ANALYSIS

All experiments were completed in triplicate. Significant differences for cholesterol, triglycerides, and mRNA levels were determined between the untreated control and experimental conditions by unpaired Student's *t* test. For all analyses, $p<0.05$ was considered significant.

4 RESULTS

4.1 ER STRESS-INDUCED SREBP-2 ACTIVATION

4.1.1 SREBP-2 Activation

We and others have shown that disruption in endoplasmic reticulum (ER) function, leading to ER stress and activation of the unfolded protein response (UPR), induces lipid dysregulation (Kim *et al.,* 2005; Esfandiari *et al.,* 2005; Ji and Kaplowitz, 2003; Werstuck *et al.,* 2001; Colgan *et al.,* 2007). ER stress-induced lipid dysregulation was observed when Outinen and colleagues showed by cDNA microarray analysis that elevated Hcy levels induced the expression of ER stress response genes and the SREBPs in cultured human umbilical vein endothelial cells (Outinen *et al.,* 1998; Outinen *et al.,* 1999). Werstuck *et al.* (2001) subsequently found that agents/conditions known to cause ER stress activated SREBP-1, which in turn increased the expression of genes essential for the biosynthesis and uptake of cholesterol and triglycerides. The ER stress-induced SREBP-1 activation caused the accumulation of cholesterol *in vitro* and led to hepatic steatosis *in vivo* (Werstuck *et al.,* 2001). Since the report by Werstuck *et al.* (2001), subsequent publications have confirmed the findings that ER stress is associated with activated SREBP and hepatic lipid accumulation (Esfandiari *et al.,* 2005; Ji and Kaplowitz, 2003; Woo *et al.,* 2005, Kammoun *et al.,* 2009).

The goal of our initial studies was to determine whether conditions that cause ER stress activate SREBP-2 and increase lipid accumulation *in vitro*. Initially, following treatment of HeLa cells with ER stress-inducing agents, cell lysates were prepared and

examined by immunoblotting for markers of ER stress and SREBP-2 activation. To determine whether various agents known to induce ER stress could activate SREBP-2, HeLa cells were treated with ER stress-inducing agents including Tg, A23187, Tm and Hcy. The lysosomal cholesterol efflux inhibitor U18666A (3-beta-[2-diethyl-amino)ethoxy]androst-5-en-17-one) (Liscum and Faust, 1989) was used as a positive control for SREBP-2 activation. U18666A inhibits cholesterol transport from lysosomes to other cellular compartments such as the ER. U18666A-inhibition of cholesterol transport decreases ER membrane cholesterol content and increases SREBP-2 activation and lipid accumulation. Following treatment of HeLa cells with either U18666A or ER stress inducing agents, cell lysates were examined by immunoblotting for SREBP-2 activation. The intensity of the 70-kDa mature form of SREBP-2 (m, Figure 3A) revealed that the ER stress inducing agents activate SREBP-2 to various levels. However, Tg produced the most robust induction of SREBP-2 cleavage, similar to that of U8666A (Figure 3A). All ER stress agents, to some degree, induced the expression of GRP78, a marker of ER stress/UPR activation. The observation that U18666A treatment causes SREBP-2 activation without inducing ER stress suggests that U18666A activates SREBP-2 by a mechanism independent of UPR activation.

4.1.2 SRE-Controlled Gene Expression

To confirm that ER stress-induced SREBP-2 proteolytic cleavage resulted in a functionally active transcription factor, SREBP-2 activity was assessed by measuring SRE promoter activity. HeLa cells were transfected with a pSRE-GFP reporter plasmid

(Higgins and Ioannou, 2001). The pSRE-GFP reporter plasmid contains the SRE element from the LDLR promoter in which SREBP binds to upon activation. Following HeLa cell transfection with pSRE-GFP, cells were treated with either U18666A or Tg (Figure 3B). Treatment of pSRE-GFP transfected HeLa cells with Tg, caused an increase in GFP expression compared to untreated cells, similar to that induced by U18666A.

4.1.3 Lipid Accumulation

Since intracellular lipid accumulation is a downstream effect of SREBP-2 activation, HeLa cells were treated with Tg and stained with Filipin to assess free cholesterol accumulation (Figure 3C). HeLa cells treated with Tg had increased free cholesterol which appeared to be associated with membranes compared to the characteristic lysosomal accumulation seen with U18666A treatment (Figure 3C). Consistent with the results seen in Figure 3A, these experiments demonstrate that the ER stress-inducing agent, Tg, upregulates SREBP-2 responsive genes via the SRE-element (Figure 3B) and causes intracellular lipid accumulation (Figure 3C). Taken together, these experiments provide evidence that ER stress-induced SREBP-2 activation produces a functional transcription factor that can drive the expression of genes containing an SRE element and increase intracellular lipid content.

4.1.4 Tg-Induced SREBP-2 Cleavage is not Mediated by Caspases

Brown and Goldstein described the sterol-independent activation of SREBP-2 by caspases during apoptosis (Wang *et al.*, 1995; Pai *et al.*, 1996). These studies revealed

Figure 3. ER Stress Agents Activate SREBP-2, Induce SRE Element-Controlled Gene Expression, and Increase Free Cholesterol Accumulation in HeLa Cells

Panel A, Treatment of HeLa cells with ER stress agents cause SREBP-2 cleavage and activation. HeLa cells were treated with various ER stress agents, including thapsigargin (Tg; 0.01 μM), A23187 (1 μM), tunicamycin, (Tm; 5 μg/ml), and homocysteine (Hcy; 5 mM). As a positive control for SREBP-2 activation, cells were treated with U18666A (2 μg/ml). Following incubation for 18 hours, protein lysates were subjected to immunoblot analysis using antibodies against SREBP-2 (to assess SREBP activation) or GRP78 (to assess ER stress). p, ER membrane-bound precursor form of SREBP-2. m, mature cleaved form of SREBP-2. *Panel B*, HeLa cells were transiently transfected with the reporter plasmid pSRE-GFP using Effectene transfection reagent. Transiently transfected HeLa/pSRE-GFP cells were treated with U18666A (2 μg/ml) or Tg (0.01 μM) for 18 hours and examined for SRE-controlled GFP expression. *Panel C*, HeLa cells were treated with U18666A (2 μg/ml) as a positive control for free cholesterol accumulation or the ER stress-inducing agents, Tg (0.01 μM) or Hcy (5 mM), for 24 hours. Following treatment, cells were stained with Filipin to examine intracellular free cholesterol content.

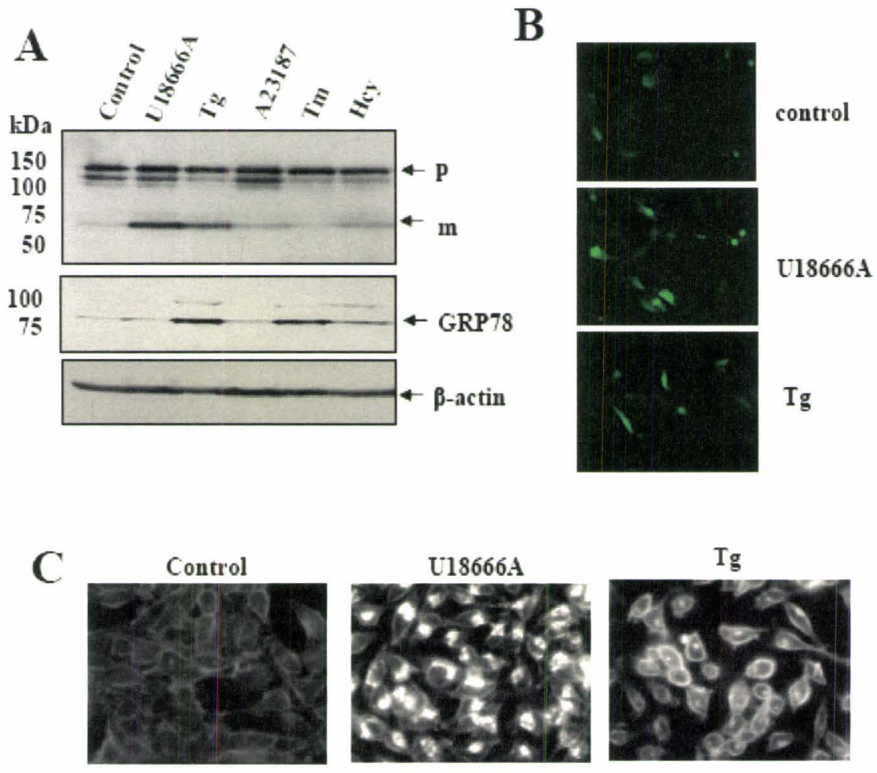
A
Control
U18666A
Tg
A23187
Tm
Hcy
kDa
150
100
75
50
p
m
100
75
GRP78
β-actin
B
control
U18666A
Tg
C
Control
U18666A
Tg

that in the presence of cholesterol, caspase-3 and -7 directly cleave SREBP-2 following apoptotic stimuli. Higgins and Ioannou (2001) revealed that SREBP-2 was not simply a random substrate of caspases during apoptosis, but when cleaved it had the potential to increase gene expression associated with cholesterol accumulation that preceded the apoptotic process. Higgins and Ioannou (2001) suggested that an increase in SREBP-2 activation and subsequent lipid accumulation may be required for the successful completion of the apoptotic program.

Since it has previously been reported that prolonged ER stress can lead to caspase activation and apoptosis (Shiraishi *et al.,* 2006; Rao *et al.,* 2002) it was our goal to determine whether the observed SREBP-2 activation following ER stress was dependant on caspase activation. The human mammary adenocarcinoma cell line (MCF7) contains a mutation in the caspase-3 gene causing complete loss of caspase-3 expression (Janicke, 1998). Since caspase-3 has been shown to induce SREBP-2 cleavage in response to apoptotic stimuli (Higgins and Ioannou, 2001; Wang *et al.,* 1995; Pai *et al.,* 1996), MCF7 cells stably transfected to express functional caspase-3 (Figure 4A) were used to examine the effects of caspase-3 on ER stress-induced SREBP-2 cleavage. MCF7/pbabe (empty vector control) and MCF7/cas3 cells were treated with the apoptotic agent, STS, to induce caspase-3 activation and determine whether this was associated with SREBP-2 cleavage. Although it was found that STS caused SREBP-2 cleavage in MCF7/pbabe cells, it activated caspase-3 (shown by loss of pro-caspase-3) and appeared to induce SREBP-2 cleavage to a greater extent in MCF7/cas3 cells (Figure 4B). To determine whether ER stress-induced SREBP cleavage is dependant on caspase-3,

Figure 4. Thapsigargin and staurosporine increase SREBP cleavage in MCF7 cells. *Panel A*, MCF7 cells that do not express caspase-3 (MCF7/pBabe) were stably transfected to overexpress caspase-3 (MCF7/cas3). *Panel B*, Treatment of MCF7 cells with staurosporine induces SREBP cleavage. MCF7/pBabe or MCF7/cas3, which overexpress active caspase-3, were treated with staurosporine (1 μM) for 4 hours. Total cell lysates were subjected to immunoblot analysis using antibodies against SREBP-2 (IgG-1C6) (to assess SREBP activation) or caspase-3 (to assess caspase-3 activation). p, ER membrane-bound precursor form of SREBP-2. m, mature active form of SREBP-2. *Panel C*, Treatment of MCF7 cells with Tg increases SREBP cleavage. MCF7/pbabe or MCF7/cas3, which overexpress active caspase-3, were treated with U18666A (2 μg/ml) or Tg (0.01 μM) for 18 hours. Protein lysates were subjected to immunoblot analysis using antibodies against SREBP-2 (to assess SREBP activation) or GRP78 (to assess ER stress).

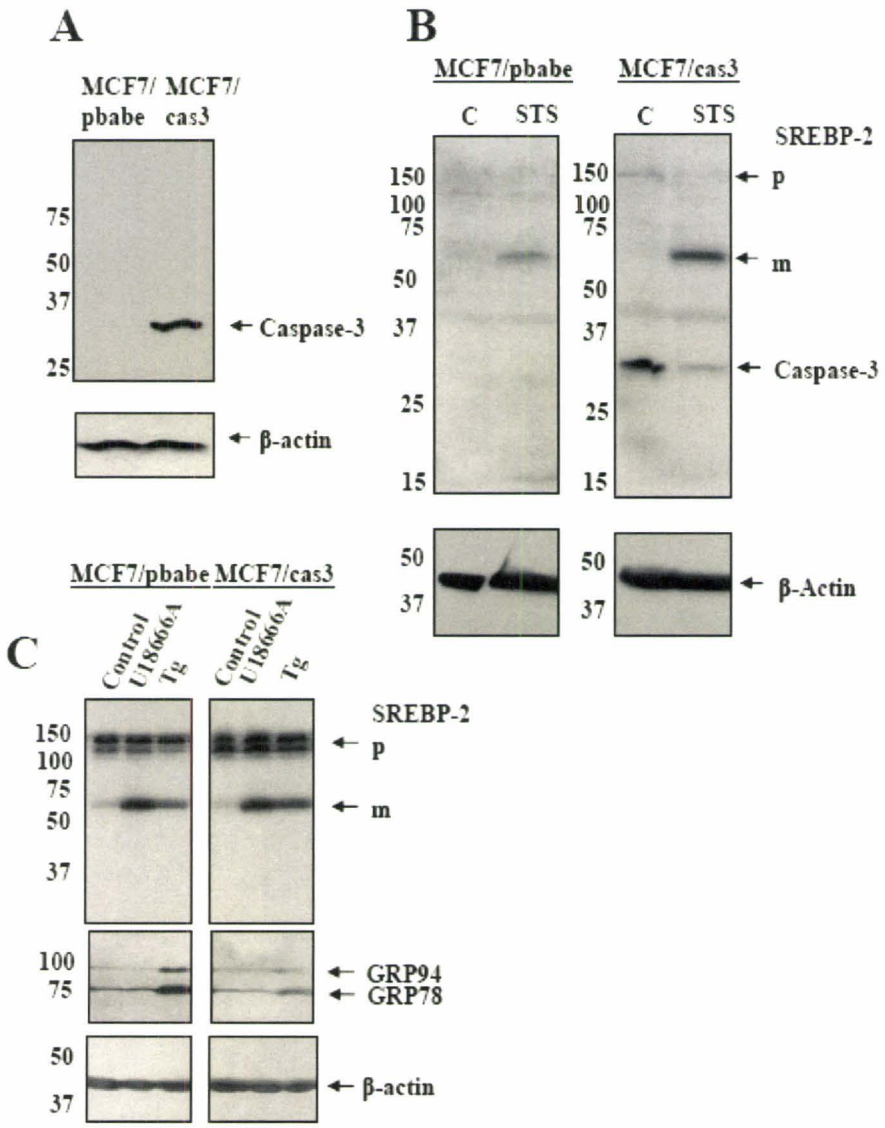
A
MCF7/ pbabe
MCF7/ cas3
75
50
37
25
Caspase-3
β-actin
B
MCF7/pbabe
MCF7/cas3
C
STS
C
STS
SREBP-2
150
100
75
50
37
25
15
p
m
Caspase-3
β-Actin
C
MCF7/pbabe
MCF7/cas3
Control
U18666A
Tg
Control
U18666A
Tg
SREBP-2
p
m
GRP94
GRP78
β-actin

MCF7/pbabe and MCF7/cas3 cells were treated with U18666A or the ER stress-inducing agent Tg and examined for SREBP-2 cleavage. MCF7/pbabe and MCF7/cas3 cells characteristically upregulated GRP78 and GRP94 following treatment with Tg (Figure 4C). Interestingly, the absence of caspase-3 in MCF7/pbabe cells had no effect on Tg-induced SREBP-2 cleavage (Figure 4C).

Although the above experiments determined that caspase-3 is not required for ER stress-induced SREBP-2 activation, caspase-7 is an additional caspase that was identified to cleave SREBP-2 similarly to caspase-3 (Wang *et al.*, 1995; Pai *et al.*, 1996) and could potentially be activated during ER stress and lead to SREBP-2 cleavage. To determine whether other caspases are involved in SREBP-2 activation during ER stress, HeLa cells were pre-treated with the pan-caspase inhibitor ZVAD-fmk and exposed to either STS or Tg to induce caspase activation and ER stress, respectively. Consistent with caspase-induced SREBP activation previously shown by Brown and Goldstein (Wang *et al.*, 1995; Pai *et al.*, 1996), ZVAD-fmk successfully decreased STS-induced caspase-3 activation (shown by loss of pro-caspase-3) and SREBP-2 cleavage. In contrast to the proposed hypothesis that ER stress-induced SREBP-2 activation occurs through the activation of caspases, pre-treatment with ZVAD-fmk had no effect on Tg-induced SREBP-2 cleavage (Figure 5). In addition to ZVAD-fmk, inhibitors of caspase-1, caspase-7 or calpain did not decrease Tg-induced SREBP-2 cleavage (data not shown).

Figure 5. Thapsigargin-Induced SREBP Cleavage is not Mediated by Caspases.

Thapsigargin induces SREBP activation in the presence of a pan-caspase inhibitor, ZVAD-fmk. Although ZVAD decreased STS-induced SREBP and caspase-3 activation, it had no effect on Tg-induced SREBP processing. HeLa cells pretreated for 2 hours with the pan-caspase inhibitor ZVAD-fmk (100 μM) were treated with 1 μM staurosporine (STS) or 0.5 μM Tg for 4 hours to examine SREBP processing. Protein lysates were subjected to immunoblot analysis using antibodies against SREBP-2 (IgG-1C6) (to assess SREBP activation) or caspase-3 (to assess caspase activation). p, ER membrane-bound precursor form of SREBP-2. m, mature active form of SREBP-2.

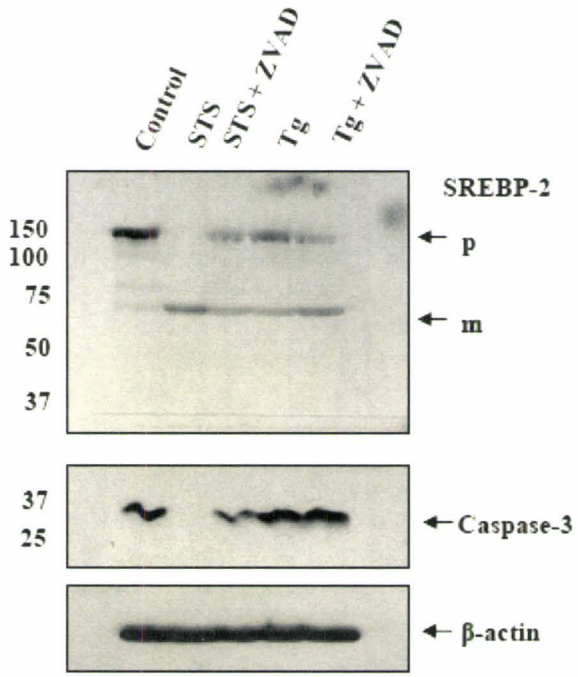
Control
STS
STS + ZVAD
Tg
Tg + ZVAD
SREBP-2
150
100
75
50
37
p
m
37
25
Caspase-3
β-actin

4.1.5 ER Stress-Induced SREBP-2 Cleavage Occurs Through the Conventional Pathway

The above experiments examining the role of caspases in ER stress-induced SREBP-2 activation provided evidence that the effect of ER stress on SREBP-2 cleavage occurs independent of caspase activation. It became apparent that ER stress-induced SREBP-2 cleavage may occur through the conventional sterol-mediated pathway. The serine protease inhibitor Pefabloc (AEBSF), although not specific for S1P it is a known inhibitor of S1P that blocks ER stress-induced ATF6 cleavage (Okada *et al.*, 2003), was used to examine whether ER stress-induced SREBP-2 cleavage occurs through the conventional proteolytic pathway. Following treatment of MCF7 cells with U18666A or Tg, cell lysates were prepared and examine by immunoblotting for SREBP-2 cleavage. MCF7 cells were also treated with U18666A or Tg in the presence of AEBSF to examine whether Tg-induced SREBP-2 cleavage is altered by inhibition of S1P. Consistent with the hypothesis that ER stress-induced SREBP-2 cleavage occurs through the conventional sterol-mediated pathway, pre-treatment with AEBSF inhibited both U18666A and Tg-induced SREBP-2 cleavage (Figure 6A). In contrast, STS-induced (caspase-mediated) SREBP activation in HeLa cells was not inhibited by AEBSF (Figure 6B). Based on these findings, we have hypothesized that ER stress-induced SREBP-2 activation occurs through a mechanism independent of caspase activation and likely involves the expression and/or activity of the proteins that regulate SREBP-2 activation.

To provide further evidence that ER stress causes SREBP-2 activation through the conventional S1P/S2P proteolytic pathway, HeLa cells were treated with the serine

Figure 6. The Serine Protease Inhibitor, AEBSF, Blocks Thapsigargin but not Staurosporine-Induced SREBP-2 Activation

Thapsigargin-induced SREBP-2 activation is inhibited by the site-1, serine protease inhibitor AEBSF. *Panel A*, MCF7 cells were pretreated with or without the serine protease inhibitor AEBSF (0.3 mM) for 2 hours. MCF7 cells were then treated with U18666A (2 μg/ml), or thapsigargin (0.01 μM) for 18 hours. Panel B, HeLa cells were pretreated with or without AEBSF (0.3 mM) for 2 hours. HeLa cells were then treated with staurosporine (STS; 1 μM) for 4 hours. Protein lysates were subjected to immunoblot analysis using antibodies against SREBP-2 (IgG-1C6). p, ER membrane-bound precursor form of SREBP-2. m, mature active form of SREBP-2.

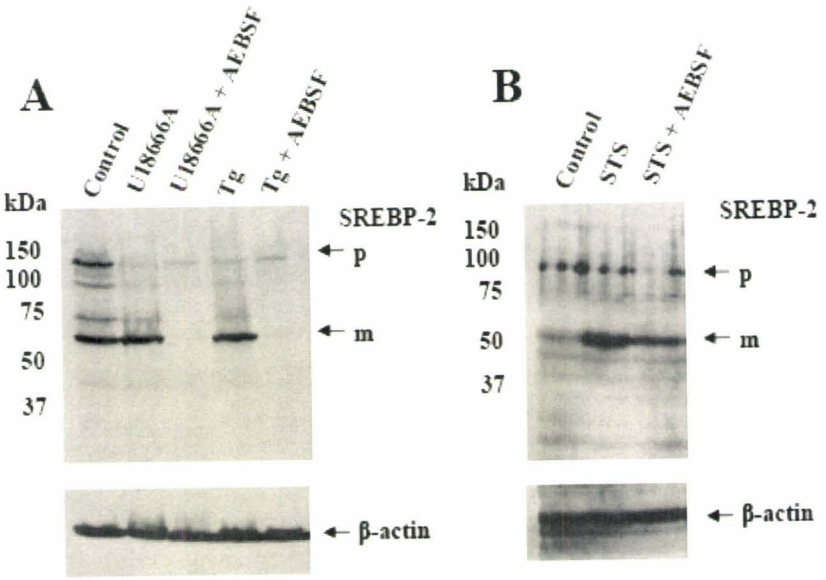
A
Control
U18666A
U18666A + AEBSF
Tg
Tg + AEBSF
kDa
150
100
75
50
37
SREBP-2
p
m
β-actin
B
Control
STS
STS + AEBSF
kDa
150
100
75
50
37
SREBP-2
p
m
β-actin

protease inhibitor, AEBSF, and examined for cholesterol accumulation. When HeLa cells were treated with the lysosomal efflux inhibitor, U18666A, free cholesterol accumulated in a punctate pattern compared to the membrane-like incorporation observed with Tg or Tm (Figure 7). The degree of cholesterol accumulation is consistent with the increase in SREBP cleavage observed in Figure 3. When HeLa cells were incubated in the presence of AEBSF (previously shown to inhibit SREBP-2 cleavage in MCF7 cells), HeLa cells accumulated less free cholesterol as measured by Filipin staining (Figure 7). This experiment provides additional evidence that ER stress-induced SREBP-2 activation and cholesterol accumulation occurs through the conventional S1P/S2P proteolytic pathway.

4.1.6 eIF2α Phosphorylation and SREBP-2 Activation

Our lab has previously demonstrated a relationship between ER stress, SREBP activation and lipid accumulation (Outinen *et al.*, 1998; Outinen *et al.*, 1999; Wersuck *et al.*, 2001; Colgan *et al.*, 2007). These results have shown that the ER stress-inducing agent Tg causes SREBP activation independent of sterol regulation. Since it has been suggested that Tg-induced SREBP cleavage occurs under translation inhibition causing INSIG-1 degradation (Lee and Ye, 2004), we wanted to determine whether Tg-mediated SREBP-2 activation involves eIF2α phosphorylation or provide evidence for an alternative mechanism that would explain the previously reported hypothesis (Lee and Ye, 2004) that Tg-induced SREBP-2 cleavage follows INSIG-1 degradation (Figure 8).

Figure 7. The Serine Protease Inhibitor, AEBSF, Blocks Cholesterol Depleted and ER Stress-Induced Lipid Accumulation

HeLa cells were incubated for 18 hours with U18666A (2 μg/ml), thapsigargin (0.3 μM), or tunicamycin (2 μg/ml) in the presence or absence of AEBSF (0.3 mM). Following treatment, cells were washed, fixed, and stained with Filipin to examine free cholesterol accumulation. Cellular free cholesterol content was measure using Sigma Scan Pro 5 software. Filipin intensity was determined by measuring intensity per number of cells per field. (# $p<0.05$, treatment compared to control, n=3; * $p<0.05$, treatment plus AEBSF compared to treatment alone, n=3)

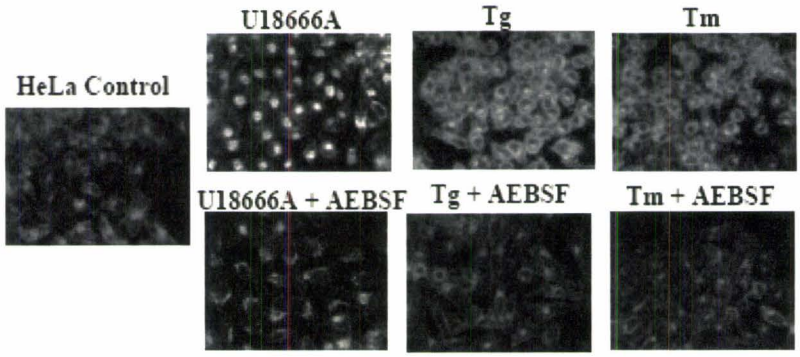
HeLa Control
U18666A
Tg
Tm
U18666A + AEBSF
Tg + AEBSF
Tm + AEBSF

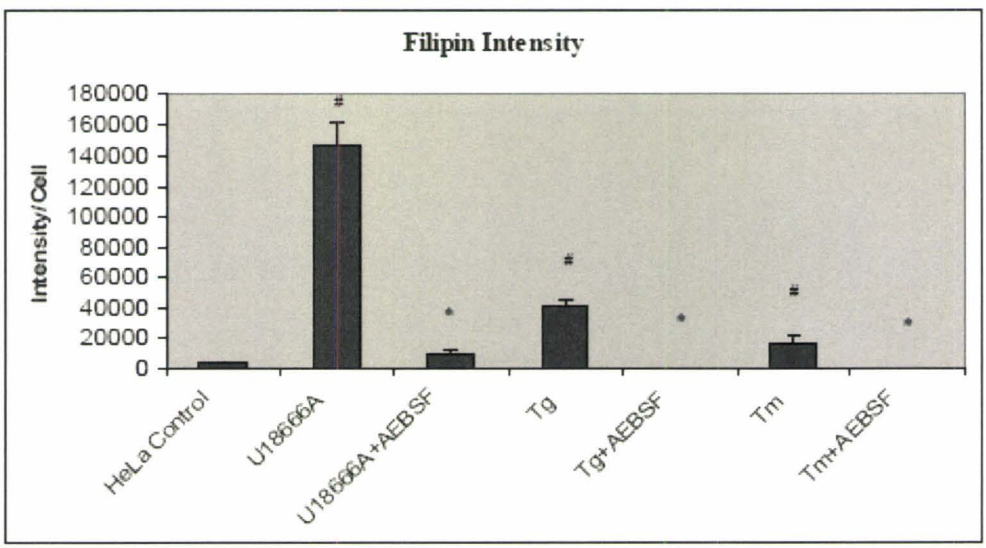
Filipin Intensity
Intensity/Cell
180000
160000
140000
120000
100000
80000
60000
40000
20000
0
HeLa Control
U18666A
U18666A+AEBSF
Tg
Tg+AEBSF
Tm
Tm+AEBSF

Figure 8. ER Stress-Induced INSIG Degradation Causes SREBP Cleavage

Lee and Ye (2004) showed that Tg causes increased SREBP activation due to a loss in INSIG protein. These findings imply that since INSIG-1 has a short half-life, a block in protein translation by conditions/agents that cause ER stress would decrease endogenous INSIG-1 protein levels thereby allowing SCAP/SREBP complex to be escorted to the Golgi where it is cleaved and activated (i.e. anchor-free SREBP activation).

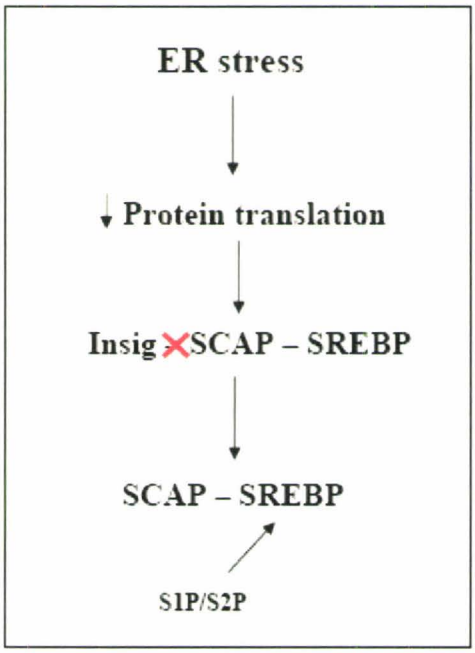
ER stress
Protein translation
Insig SCAP – SREBP
SCAP – SREBP
S1P/S2P

Lee and Ye (2004) and Gong *et al.* (2006), report that INSIG-1 has a short half life when dissociated from SCAP and is rapidly ubiquinated and degraded through the proteasome pathway. In addition to the short half life of INSIG-1, it was suggested that ER stress-induced eIF2α phosphorylation and translation inhibition could decrease the amount of INSIG-1 available to SCAP and may promote SREBP activation (Lee and Ye, 2004). To help assess whether ER stress-induced eIF2α phosphorylation was required for SREBP activation we examined whether Tg-induced SREBP-2 cleavage correlated with eIF2α phosphorylation. Following treatment of HeLa cells with 0.5 μM Tg for 5 to 30 minutes, cells were lysed at the indicated time point and examined for eIF2α phosphorylation and SREBP-2 cleavage by immunoblotting. A time dependant increase in eIF2α phosphorylation (following 10 minutes of Tg treatment) was correlated with the activation of SREBP-2 at 25 minutes (Figure 9). These results provide evidence that Tg-induced eIF2α phosphorylation and translation inhibition leads to SREBP-2 cleavage. This experiment also helped determine the earliest time point for SREBP-2 cleavage and whether it is relevant to a decrease in INSIG protein levels due to inhibition of translation. Our results show that eIF2α phosphorylation occurs very rapidly and is followed by an increase in SREBP-2 cleavage (Figure 9). These results support the hypothesis stated by Lee and Ye (2004) and Gong *et al.* (2006) that ER stress-induced eIF2α phosphorylation and translation inhibition may cause SREBP-2 cleavage by decreasing INSIG-1 protein levels.

To provide further evidence that eIF2α phosphorylation causes SREBP-2 activation, HeLa and 293 cells were transiently transfected with a plasmid that expresses

a mutant form of eIF2α (eIF2α-S51D). The serine at amino acid 51 was mutated to aspartic acid that mimics the phosphorylated form of eIF2α. Cells were transfected using Effectene transfection reagent (Qiagen) and incubated for 48 hours to allow for gene expression. An expression vector for wild type (WT) eIF2α was used as a negative control and 0.5 μM Tg was used as a positive control. Cells were lysed at the indicated time points and examined by immunoblotting for eIF2α expression and SREBP-2 cleavage. Although the eIF2α-S51D mutant caused the loss of the SREBP-2 precursor protein following 48 hours, overexpression of eIF2α-WT also induced SREBP-2 cleavage after 48 hours to the same extent seen with the eIF2α-S51D mutant (Figure 10). This could be explained by the fact that SREBP-2 is being activated or no new protein is being translated due to the translational inhibition. To further examine the role of eIF2α phosphorylation-induced SREBP-2 activation, HeLa cells were treated with the GADD34 inhibitor (Boyce *et al.*, 2005), salubrinal, to examine whether inhibition of eIF2α dephosphorylation causes SREBP-2 cleavage (Figure 11). HeLa cells were treated with either 10 μM salubrinal for 8-36 hours (Figure 11A) or 0.1-100 μM for 8 hours (Figure 11B). Tg (0.5 μM) was used in Figure 11B as a positive control for SREBP-2 cleavage. Although salubrinal induced and maintained eIF2α phosphorylation, there was no observed increase in SREBP-2 cleavage over time (Figure 11A) or over various concentrations (Figure 11B). Since salubrinal-induced eIF2α phosphorylation did not increase SREBP-2 cleavage in HeLa cells, these results provide evidence that eIF2α phosphorylation may not be required for SREBP-2 activation.

Figure 9. Tg-Induced eIF2α Phosphorylation Correlates with SREBP Activation

HeLa cells were treated with 0.5 μM Tg for 5 to 30 minutes. Cells were lysed at the indicated time points and protein lysates were subjected to immunoblot analysis using antibodies against eIF2α phosphorylation (Ser51) and SREBP-2 (IgG-1C6). This experiment helped to determine the earliest time point for SREBP cleavage and whether it is relevant to a decrease in INSIG protein levels due to a loss in translation.

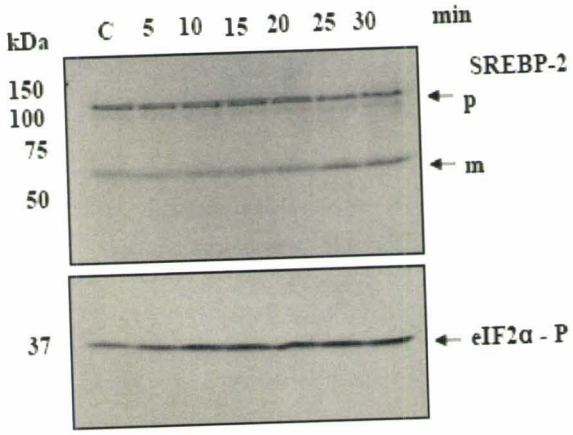
kDa
C 5 10 15 20 25 30
min
SREBP-2
150
100
75
50
p
m
37
eIF2α - P

Figure 10. Overexpression of the eIF2α-S51D mutant induces SREBP cleavage in HeLa cells

Overexpression of the eIF2α-S51D mutant that functionally imitates the phosphorylated form of eIF2α, causes SREBP activation. HeLa cells were transiently transfected with expression plasmids encoding eIF2α-S51D (mutant), eIF2α-WT (functional eIF2α), or pGFP (control) using Effectene transfection reagent and incubated for 24 hours. As a positive control for SREBP activation, HeLa cells were incubated with Tg (0.5 μM) for 4 hours before lysates were prepared. Total cell lysates were subjected to immunoblot analysis using antibodies against SREBP-2 (IgG-1C6) or GRP78 (KDEL). p, ER membrane-bound precursor form of SREBP-2. m, mature active form of SREBP-2.

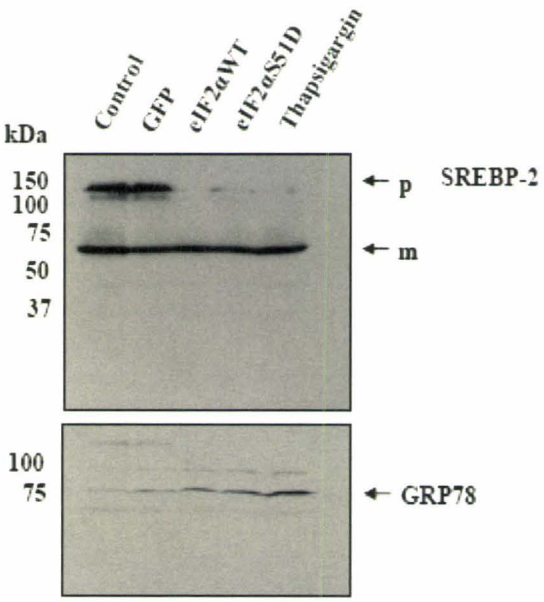
Control
GFP
eIF2αWT
eIF2αS51D
Thapsigargin
kDa
150
100
75
50
37
p
m
SREBP-2
100
75
GRP78

Figure 11. Sustained eIF2α phosphorylation does not induce SREBP-2 cleavage

HeLa cells were treated with the GADD34 inhibitor, salubrinal, to examine whether inhibition of eIF2α dephosphorylation causes SREBP cleavage. HeLa cells were treated with salubrinal (10 μM) for 8-36 hours (A) or 0.1-100 μM salubrinal for 8 hours (B). Cells were lysed and prepared for immunoblotting using antibodies against SREBP-2 (IgG-1C6), and phosphorylated eIF2α (Ser51).

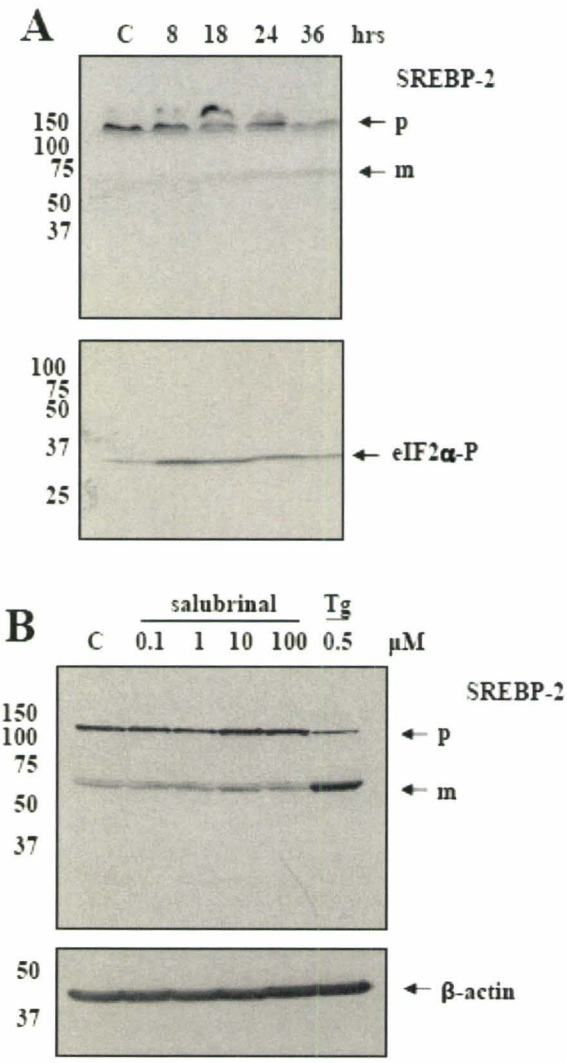
A
C 8 18 24 36 hrs
SREBP-2
150
100
75
50
37
p
m
100
75
50
37
25
eIF2α-P
B
salubrinal
Tg
C 0.1 1 10 100 0.5 μM
SREBP-2
150
100
75
50
37
p
m
50
37
β-actin

4.1.7 Intracellular Calcium and SREBP-2 Activation

A potential alternative mechanism to eIF2α-induced INSIG degradation and SREBP-2 activation could be a disruption in the INSIG-SCAP interaction under conditions that cause ER stress. It has previously been shown that ER membrane cholesterol depletion causes a dissociation of INSIG from SCAP leading to INSIG degradation and SREBP-2 activation (Gong *et al.*, 2006). Brown and Goldstein have shown that 25-hydroxycholesterol (25-HC) and cholesterol inhibit INSIG-SCAP dissociation by different mechanisms and that 25-HC treated cells do not respond to sterol starvation (Adams *et al.*, 2004). We used 25-HC to determine whether decreasing INSIG dissociation from SCAP, inhibits ER stress-mediated SREBP-2 cleavage. HeLa cells were pre-treated with 25-HC and then exposed to either U18666A or Tg for 18 hours. Lysates were collected and SREBP-2 cleavage was observed by immunoblotting. Immunoblotting for SREBP-2 revealed that 25-HC inhibits U18666A and Tg-induced SREBP-2 cleavage (Figure 12). This experiment provides evidence that ER stress-mediated SREBP-2 cleavage could be a result of disruption in the INSIG-SCAP interaction leading to a release of SCAP-SREBP-2 and subsequent SREBP-2 activation.

Through our studies, there has been a clear distinction between the effects of different ER stress agents on the ability to activate SREBP-2. Agents that acutely disrupt ER Ca^{2+} homeostasis such as Tg, induce SREBP-2 cleavage to a much greater extent than those agents (Tm, DTT, etc.) that cause ER stress by interfering with proper protein folding. Our goal was to examine SREBP-2 activation following treatment with agents that induce ER stress by disrupting intracellular Ca^{2+} homeostasis. HeLa cells were

Figure 12. 25-hydroxycholesterol (25-HC) inhibits Tg-induced SREBP cleavage

HeLa cells were pretreated with 25-HC and then treated with U18666A (2 μg/ml) or Tg (0.3 μM) for 18 hours. Lysates were collected and SREBP cleavage was observed by immunoblotting with an antibody against SREBP-2 (IgG-1C6). The U18666A and Tg-induced SREBP cleavage was inhibited by the addition of 25-HC.

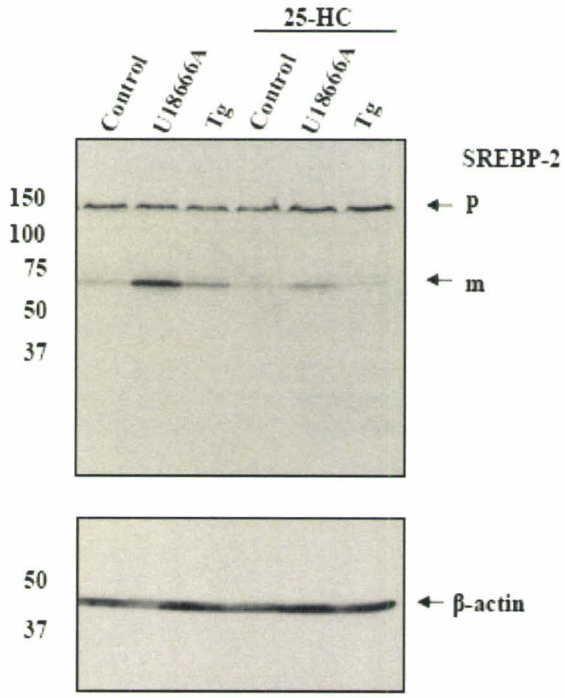
25-HC
Control
U18666A
Tg
Control
U18666A
Tg
SREBP-2
150
100
75
50
37
P
m
50
37
β-actin

Figure 13. SREBP cleavage occurs following treatment with ER stress-inducing agents that disrupt intracellular calcium stores

HeLa cells were treated with either 2 μg/ml U18666A (positive control), 0.1 μM Tg, 2 μM CPA, 1 μM A23187, or 5 mM Hcy for 4 hours. Cellular lysates were collected and SREBP cleavage was observed by immunoblotting using an antibody against SREBP-2 (IgG-1C6). All ER stress agents known to disrupt intracellular Ca^{2+} stores increased SREBP cleavage.

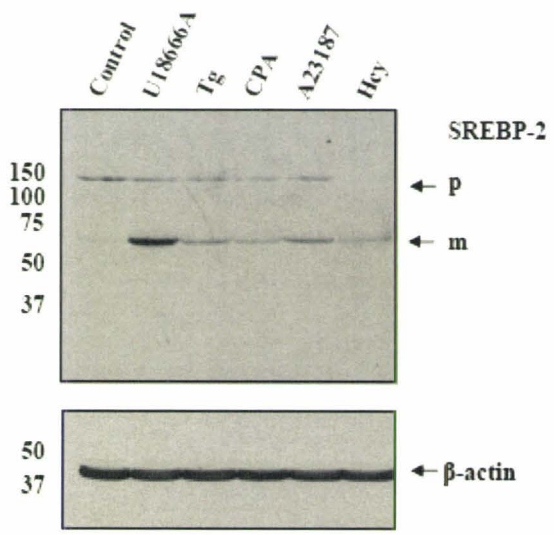
Control
U18666A
Tg
CPA
A23187
Hcy
SREBP-2
150
100
75
50
37
p
m
50
37
β-actin

treated for 4 hours with Tg, cyclopiazonic acid (CPA; specific inhibitor of SERCA), A23187, or Hcy. Lysates were collected and SREBP-2 cleavage was examined by immunoblotting (Figure 13). ER stress inducing agents such as Tm, DTT, Brefeldin A and 7-ketocholesterol were examined but did not enhance SREBP-2 cleavage in HeLa cells (data not shown). This experiment provides evidence that ER stress-induced SREBP-2 activation may be mediated by changes in ER Ca^{2+} homeostasis.

To further examine whether changes in intracellular Ca^{2+} induce SREBP-2 cleavage, we examined the Ca^{2+}chelating compound BAPTA-AM in the presence of Tg. These experiments were designed to determine whether SREBP-2 is activated upon a rise in intracellular Ca^{2+}. BAPTA was used to chelate Ca^{2+} entering the cytosol upon Tg treatment. HeLa cells were loaded with Fura-2 dye, which fluoresces upon binding with cytosolic free Ca^{2+}. Following pre-treatment with Fura-2, HeLa cells were treated with 100 μM BAPTA for 1 hour prior to the addition of 0.5 μM Tg for 1 hour. The addition of 0.5 μM Tg caused a sharp and sustained increase in cytosolic Ca^{2+} within minutes lasting for more than 1 hour (Figure 14). The addition of BAPTA inhibited the initial rise and sustained (1 hour) increase in cytosolic free Ca^{2+} and maintained the levels of cytosolic Ca^{2+} similar to that of control cells (Figure 14).

To examine whether BAPTA could inhibit the effect of Tg-induced SREBP-2 activation, HeLa cells were treated with 100 μM BAPTA for 1 hour prior to the addition of 0.5 μM Tg for 30 minutes or 1 hour (Figure 15). Cells treated with Tg alone characteristically increased SREBP-2 processing. The addition of BAPTA did not significantly decrease SREBP-2 cleavage following Tg treatment. Interestingly, BAPTA

Figure 14. BAPTA inhibits Tg-induced rise in cytosolic free calcium

HeLa cells were loaded with Fura-2 dye, which fluoresces upon binding with cytosolic free Ca^{2+}. Following pre-treatment with Fura-2 for 1 hour, HeLa cells were treated with 50 or 100 μM BAPTA for 1 hour prior to the addition of 0.5 μM Tg for 1 hour. The addition of 0.5 μM Tg caused a sharp and sustained increase in cytosolic Ca^{2+} within minutes lasting for more than one hour. The addition of BAPTA inhibited the initial rise and sustained (1 hour) increase in cytosolic free Ca^{2+} and maintained the levels of cytosolic Ca^{2+} similar to that of control.

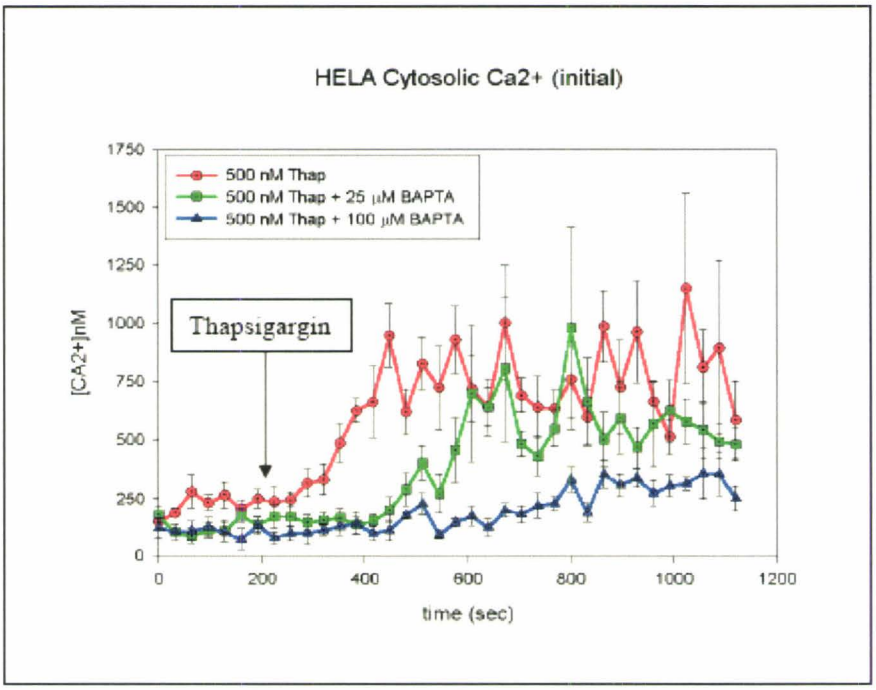
HELA Cytosolic Ca2+ (initial)
500 nM Thap
500 nM Thap + 25 µM BAPTA
500 nM Thap + 100 µM BAPTA
Thapsigargin
[CA2+]nM
time (sec)
0
250
500
750
1000
1250
1500
1750
0
200
400
600
800
1000
1200

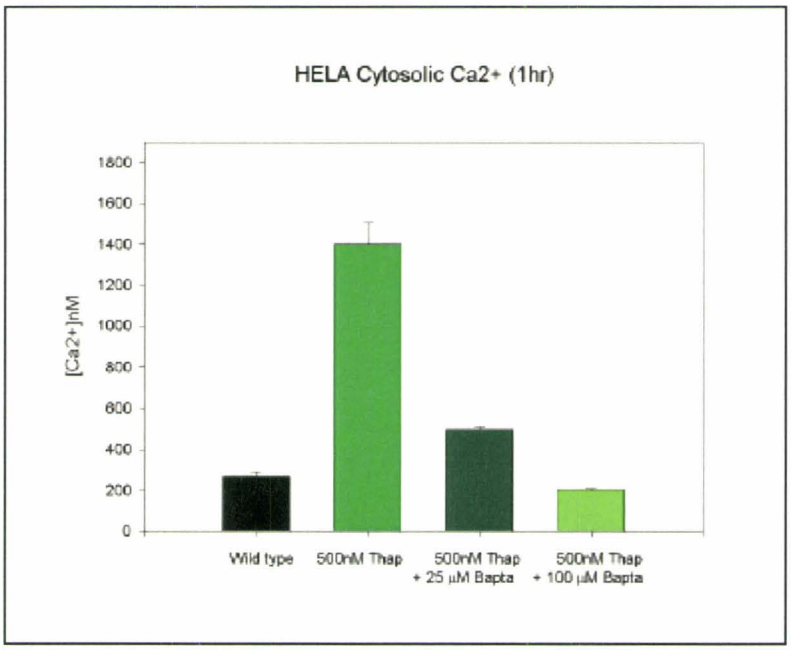
HELA Cytosolic Ca2+ (1hr)
[Ca2+]nM
0
200
400
600
800
1000
1200
1400
1600
1800
Wild type
500nM Thap
500nM Thap + 25 µM Bapta
500nM Thap + 100 µM Bapta

Figure 15. BAPTA does not inhibit Tg-induced SREBP-2 cleavage

HeLa cells were treated with 100 μM BAPTA for 1 hour prior to the addition of 0.5 μM Tg for 30 minutes or 1 hour. Cell lysates were prepared and SREBP and eIF2α phosphorylation was examined by immunoblotting with antibodies against SREBP-2 (IgG-1C6) and phosphorylated eIF2α (Ser51). The addition of BAPTA to Tg did not significantly decrease SREBP-2 cleavage compared to Tg alone. Interestingly BAPTA alone strongly induced eIF2α phosphorylation.

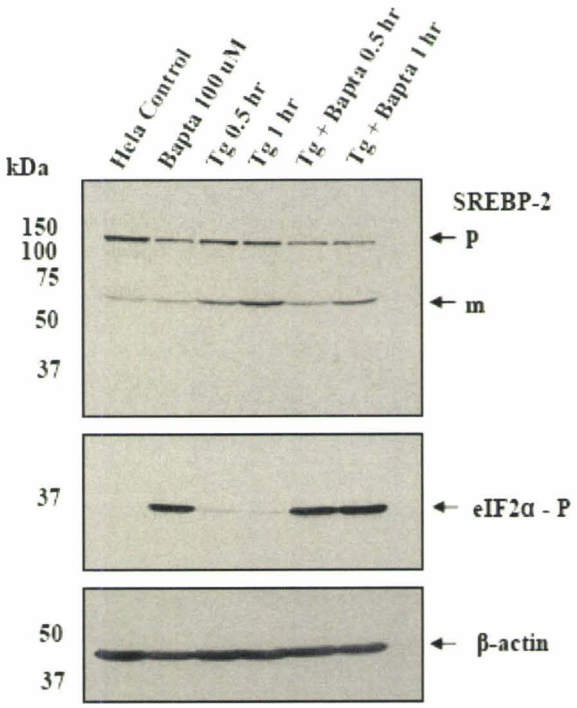
Hela Control
Bapta 100 uM
Tg 0.5 hr
Tg 1 hr
Tg + Bapta 0.5 hr
Tg + Bapta 1 hr
kDa
150
100
75
50
37
SREBP-2
P
m
37
eIF2α - P
50
37
β-actin

alone strongly induced eIF2α phosphorylation which suggests that at this concentration it was inducing ER stress. Since we observed that BAPTA causes eIF2α phosphorylation (Figure 15), we wanted to determine whether it could act as an ER stress agent and induce SREBP-2 activation. HeLa cells were treated with different concentrations of BAPTA over different time periods to examine its effect on SREBP-2 activation. HeLa cells were treated with either 100 μM BAPTA for 15 to 120 minutes (Figure 16A) or 10-100 μM of BAPTA for 120 minutes (Figure 16A and B). Interestingly, although BAPTA (100 μM) induced eIF2α phosphorylation at 120 minutes which correlated with SREBP-2 cleavage (Figure 16A), 25 μM BAPTA caused SREBP-2 cleavage at 120 minutes independent of eIF2α phosphorylation (Figure 16A and B). These results provide strong evidence that the disruption of ER Ca^{2+} caused by BAPTA leads to SREBP-2 activation prior to the induction of ER stress and eIF2α phosphorylation.

4.2 *IN VIVO* MODEL OF ER STRESS-INDUCED SREBP ACTIVATION

4.2.1 Tunicamycin-Induced Proximal Tubule Toxicity Causes Lipid Accumulation

To examine the physiological relevance of ER stress-induced SREBP activation and lipid accumulation we used an *in vivo* model of Tm-induced ER stress that causes renal proximal tubule cell damage. Histological examination of 3 days post-intraperitoneal injection (i.p.) sections revealed damage to some of the proximal tubules in the kidney cortex. This damage consisted of swollen cells filled with vacuoles. At 24 hours following i.p. injection, little or no damage was visible at the light microscopic level in H&E sections. These findings are in agreement with Zinszner *et al.* (1998), who

Figure 16. BAPTA causes SREBP-2 cleavage independent of eIF2α phosphorylation

HeLa cells were treated with 100 μM BAPTA for 15-120 minutes (A) or 10-100 μM for 120 minutes (A and B). Protein lysates were subjected to immunoblot analysis using antibodies against SREBP-2 (IgG-1C6) and phosphorylated eIF2α (Ser51). BAPTA (100 μM) induced eIF2α phosphorylation at 120 minutes which correlated with SREBP-2 cleavage (A). BAPTA (25 μM) caused SREBP-2 cleavage at 120 minutes without inducing eIF2α phosphorylation (A and B)

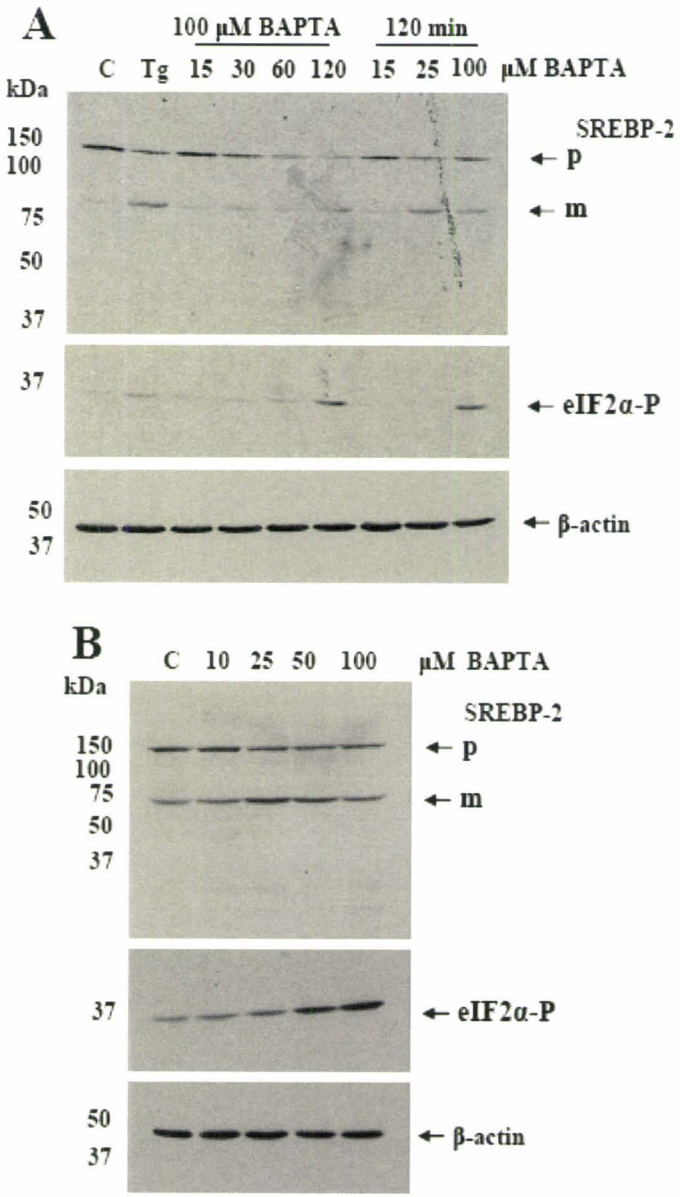
A
100 µM BAPTA
120 min
C Tg 15 30 60 120 15 25 100 µM BAPTA
kDa
150
100
75
50
37
SREBP-2
p
m
37
eIF2α-P
50
37
β-actin
B
C 10 25 50 100 µM BAPTA
kDa
150
100
75
50
37
SREBP-2
p
m
37
eIF2α-P
50
37
β-actin

described the time course of ultrastructural changes after Tm injection noting that 3-5 days post i.p. injection, epithelial cells in proximal tubules exhibit vacuolization, apoptosis and regeneration. Following 7-8 days post i.p. injection the kidney histology and function was fully restored. Zinszner *et al.* (1998), found that the expression of GADD153 and ER chaperones in the proximal tubules was dramatically increased within 24 hours following Tm treatment. This model is useful to study acute renal toxicity and ER stress-related pathways *in vivo*.

Mice injected with Tm were sacrificed at 24 hours or 3 days post i.p. injection. At 3 days post i.p. injection the injury to epithelial cells in proximal tubules was observed in H&E stained sections. Cells appeared swollen with large vacuoles (Figure 17A). ORO staining of kidney cryosections revealed that these vacuoles were indeed lipid droplets (Figure 17B). No histological changes or presence of lipid were observed in glomeruli or distal tubules in Tm treated mice. In control PBS injected mice, no changes to proximal tubular cells and/or no lipid accumulation were observed (Figure 17C, D).

4.2.2 Lipid and ER Stress Markers in Proximal Tubule Cells.

We performed double immunofluorescence for GRP78 and GADD153 on paraffin sections from mice sacrificed 24 hours after Tm injection. These two markers of ER stress co-localized to the same proximal tubules (Figure 18A); KDEL staining was cytoplasmic, whereas GADD153 was strongly labelled in the nuclei of the proximal tubule epithelial cells. Low, basal levels of GRP78 were apparent in distal tubules;

Figure 17. Tunicamycin-induced vacuolization and lipid deposition in proximal tubules in kidneys of C57BL/6J mice

Three days after i.p. injection with Tm, vacuoles were observed in proximal tubular cells (arrows; H&E; A). ORO staining of cryosections revealed lipid deposition in these cells (arrows; B). PBS injected mice did not exhibit vacuolization (C) or lipid deposition (D). Original magnification X20. G; glomerulus.

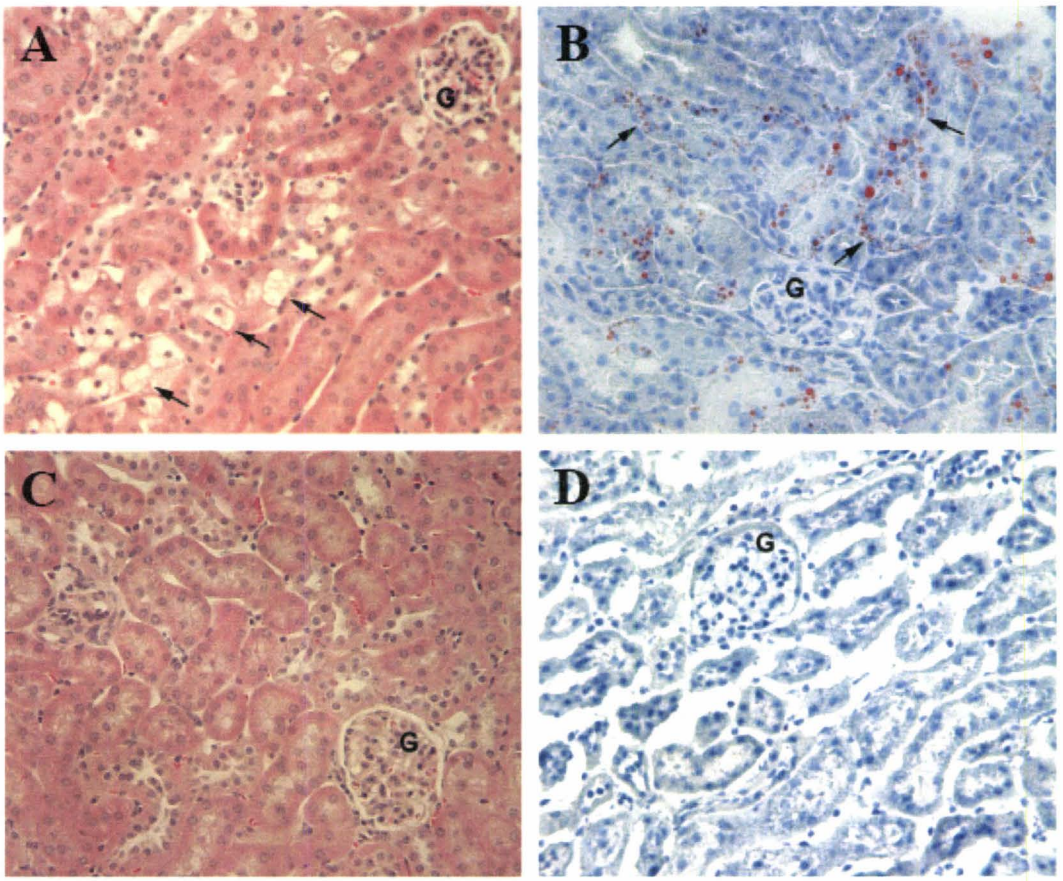
A
G
B
G
C
G
D
G

Figure 18. Correlation between ER stress and lipid deposition in proximal tubules in C57BL/6J mouse kidneys, 24 hours after Tm injection

GRP78 (KDEL antibody; green) and GADD153 (red) co-localized to the same proximal tubules (arrows by double immunofluorescence). Distal tubules expressed GRP78 at low level, and were negative for GADD153 (arrowheads; A). In PBS-injected mice no increased levels of GRP78 and GADD153 were observed in proximal tubules (B). Cryosections from Tm-treated mouse kidneys wee double stained with ORO and with an antibody to either GRP78 (KDEL) or GADD153, followed by a fluorescent Alexa 488 secondary antibody. ORO was visualized in brightfield microscopy (C,E), the immunostaining, using a fluorescence microscope with 520nm longpass filter (D,F). ORO staining revealed small lipid droplets in proximal tubules (arrows; C, E; larger droplets are also visible in D, F). High expression of GRP78 (D) or GADD153 (F) was observed in the same proximal tubules, co-localizing with ORO. Glomeruli and distal tubules were devoid of lipid droplets and GRP78 or GADD153 staining (arrowheads; C-F). Original magnification x20. G; glomerulus.

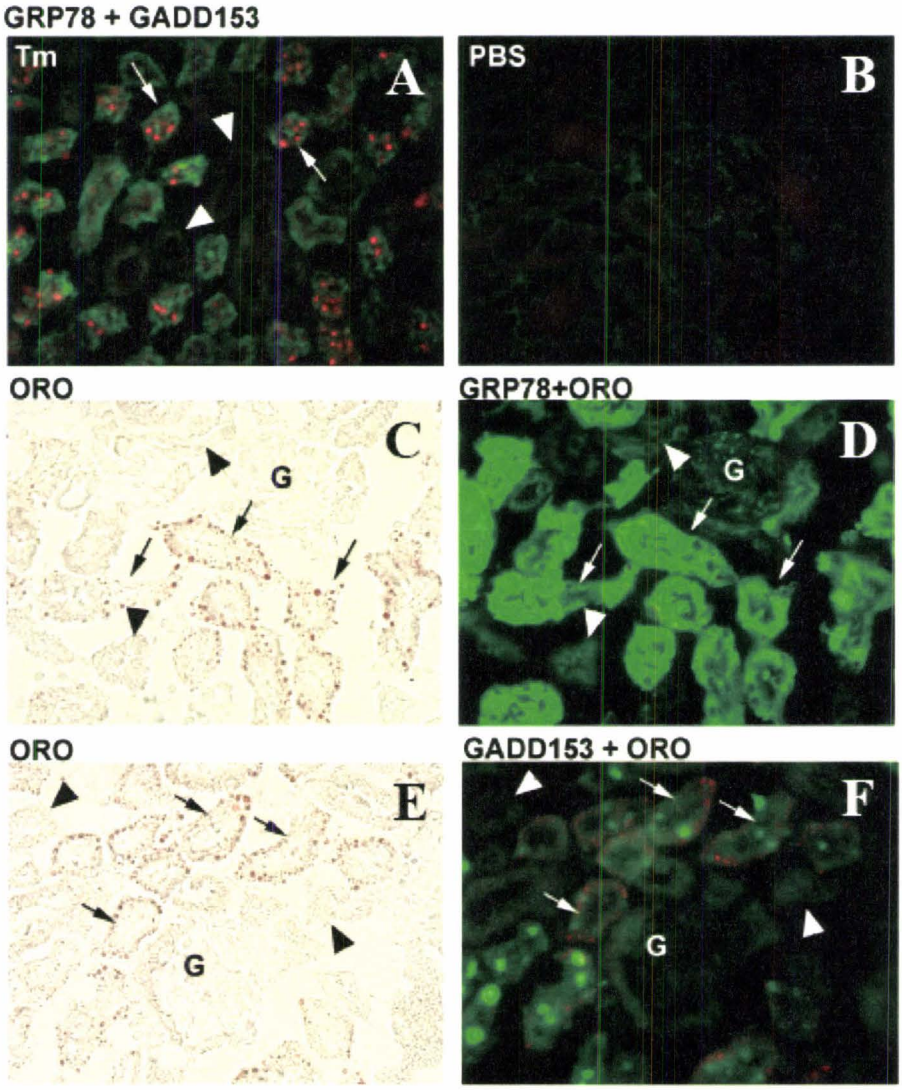
GRP78 + GADD153
Tm
A
PBS
B
ORO
C
G
GRP78+ORO
D
G
ORO
E
G
GADD153 + ORO
F
G

GADD153 staining was not seen in those structures. In PBS injected mice, only basal level of GRP78 was observed and no staining of GADD153 in proximal tubules or other structures in the kidney. Double staining of cryosections with ORO and GRP78 or GADD153 antibodies revealed that small lipid droplets were present in the proximal tubules as early as 24 hours after injection (Figure 18C, E). Moreover, the tubules that contained lipid droplets also displayed high expression of GRP78 (Figure 18D) and GADD153 (Figure 18F), suggesting a functional relationship between ER stress and the accumulation of lipid.

4.2.3 SREBP-2 Expression in Proximal Tubule Cells Undergoing ER Stress

Adjacent paraffin sections of kidneys from mice 24 hours after Tm injection were immunostained for SREBP-2 and GADD153, respectively. Comparing images from the same cortical area we observed increased SREBP-2 staining (Figure 19A) in the same proximal tubules that exhibited strong nuclear staining of GADD153 (Figure 19B). We conclude therefore that in the cells undergoing ER stress, SREBP-2 is activated, leading to the increased synthesis of genes in the lipid synthesis and uptake pathways.

4.2.4 ER Stress-Induced SREBP-2 Activation and Lipid Dysregulation in Cultured MDCK Renal Epithelial Cells

To confirm the above results that show proximal tubule cells undergoing ER stress correlate with increased SREBP-2 expression and ORO staining we examined ER

Figure 19. SREBP-2 was strongly expressed in the proximal tubules that were undergoing ER stress

Adjacent paraffin sections of kidneys from C57BL/6J mouse 24 hours after Tm injection were immunostained for (A) SREBP-2 (IgG-1C6) and (B) GADD153, respectively. High expression of SREBP-2 co-localized to the same proximal tubules which expressed GADD153 in the nuclei of the tubular cells (arrows; A,B). Original magnification x20. G; glomerulus.

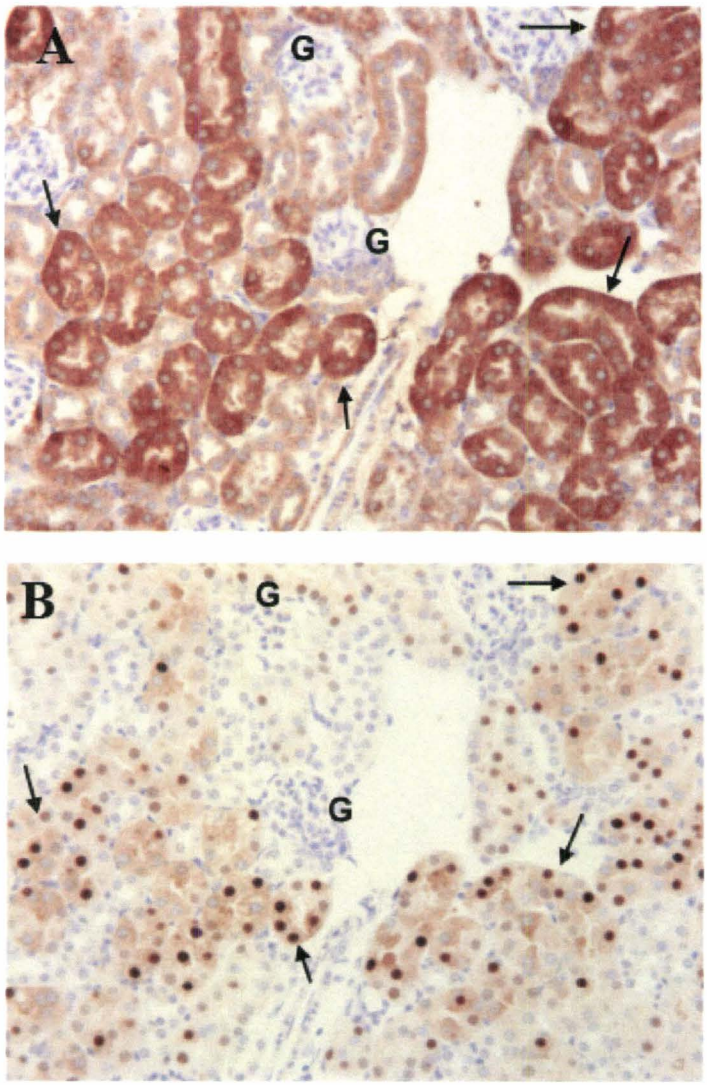
A
G
G
B
G
G

stress-induced SREBP-2 activation and lipid accumulation *in vitro* using a canine renal tubule epithelial cell line, MDCK (kindly provided by Dr. Damu Tang). Firstly, we examined whether the MDCK tubule epithelial cell line produced a normal UPR following Tm and Tg induced ER stress. MDCK cells were transfected with an XBP1 expression vector containing the cDNA for XBP1 and a venus (GFP) tag. Upon ER stress and the subsequent splicing of the 26-bp intron from the XBP1-venus mRNA, an XBP1-venus fusion protein is generated that can be assayed by fluorescent microscopy or immunoblotting with an anti-GFP antibody. MDCK cells transfected with pXBP1-ΔDBD-venus were treated with either 1 μg/ml Tm or 0.1 μM Tg for 24 hours. MDCK cells increased expression of GFP following treatment with Tm or Tg (Figure 20C and D), which provides evidence that MDCK cells respond to ER stress with a normal UPR. Treatment of MDCK cells with U18666A (2 μg/ml), an activator of SREBP-2, caused SREBP-2 cleavage without inducing ER stress or activating the UPR (Figure 20B). To confirm the result with markers for ER stress that were observed in the *in vivo* renal toxicity model, antibodies against KDEL (GRP78), GADD153, and GFP (XBP1-venus expression) were used. Both of these characteristic ER stress markers along with the expression of the XBP1-venus fusion protein were upregulated following Tm and Tg treatment (Figure 20E).

Given that Tm and Tg induced a normal UPR in MDCK cells, experiments were designed to examine whether this led to SREBP-2 activation and lipid accumulation. MDCK cells were transfected with the pSRE-GFP reporter plasmid. Following transfection, MDCK cells were treated with either 2 μg/ml U18666A, 1 μg/ml Tm, or 0.1

Figure 20. ER stress agents induce a typical ER stress response in MDCK renal tubule epithelial cells

MDCK cells were transfected with an XBP1 expression vector (A). This vector produces XBP1 mRNA with a venus (GFP) tag. Upon ER stress and the subsequent XBP1 mRNA splicing, the XBP1-venus protein is translated and can be assayed by fluorescent microscopy or immunoblotting with anti-GFP antibody. MDCK cells transfected with pXBP1-ΔDBD-venus were treated with either 1 mg/ml Tm (C) or 0.1 mM Tg (D) for 24 hours. As a negative control, MDCK cells were incubated with the SREBP activating agent, U18666A (2 mg/ml) (B). Antibodies against KDEL (GRP78), GADD153, and GFP (XBP1-venus expression) were used during immunoblotting (E).

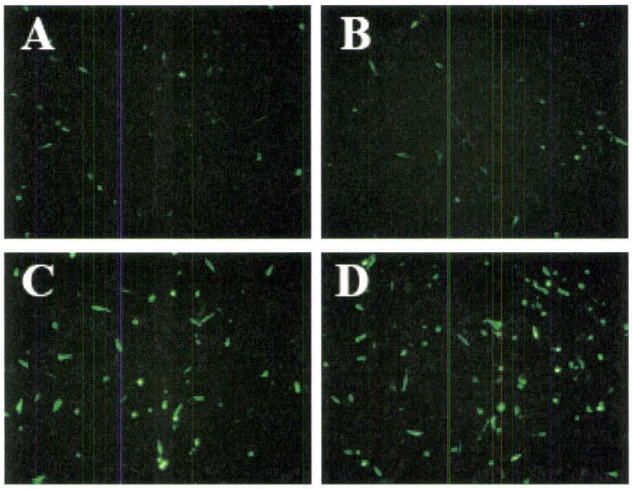
A
B
C
D

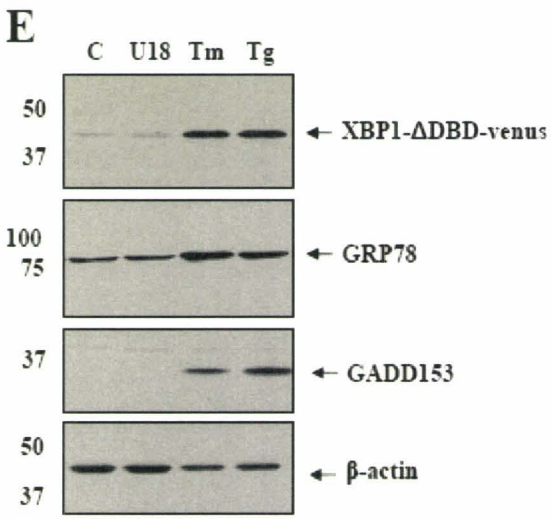
E
C
U18
Tm
Tg
50
37
XBP1-ΔDBD-venus
100
75
GRP78
37
GADD153
50
37
β-actin

μM Tg for 24 hours. Following treatment, MDCK cells were examined by fluorescent microscopy and immunoblotted for GFP expression. Consistent with our findings in HeLa cells, Tm and Tg induced GFP expression and therefore SREBP-2 activation similarly to U18666A in MDCK cells (Figure 21C and D). This is evident by the increased expression of GFP (Figure 21E), which occurs following the binding of activated SREBP-2 to the SRE element in the promoter of the SRE-GFP construct. MDCK epithelial cells were also examined for alterations in their lipid content following ER stress. MDCK cells were treated with U18666A, Tm or Tg for 24 hours prior to ORO staining. Examination of MDCK ORO staining by microscopy and 2-propanol lipid extraction revealed that ER stress agents induce lipid accumulation in proximal tubule cells *in vitro* (Figure 21F-I). Together these *in vitro* findings confirm the *in vivo* observations that ER stress-induced renal tubule lipid accumulation is associated with SREBP-2 activation.

4.3 ER STRESS-INDUCED SREBP ACTIVTION AND THE MACROPHAGE FOAM CELL

4.3.1 Examination of an *In Vivo* Mouse Model of Atherosclerosis for Macrophage SREBP Expression

Our current results suggest that ER stress-induced renal toxicity involves SREBP-2 activation and lipid accumulation. Another classic pathology that is characterized by elevated intracellular lipid accumulation is atherosclerosis. Events that are important during the progression of atherosclerotic lesion development include: macrophage

Figure 21. ER Stress Agents Induce SRE Element-Controlled Gene Expression, and Increase Free Cholesterol Accumulation in MDCK Renal Tubule Epithelial Cells

Following transfection with the pSRE-GFP reporter plasmid, MDCK cells were treated with either 2 μg/ml U18666A, 1 μg/ml Tm, or 0.1 μM Tg for 24 hours. Following treatment, MDCK cells were examined by fluorescent microscopy and assayed by immunoblotting for GFP expression (A-E). MDCK tubule epithelial cells were also examined for alterations in their lipid content following ER stress (F-J). MDCK cells were treated with U18666A, Tm or Tg for 24 hours prior to ORO staining. Examination of MDCK ORO staining by microscopy and 2-propanol lipid extraction (read at 510 nM) revealed that ER stress agents induce lipid accumulation in cultured proximal tubule cells. (* $p<0.05$, treatment compared to control, n=3)

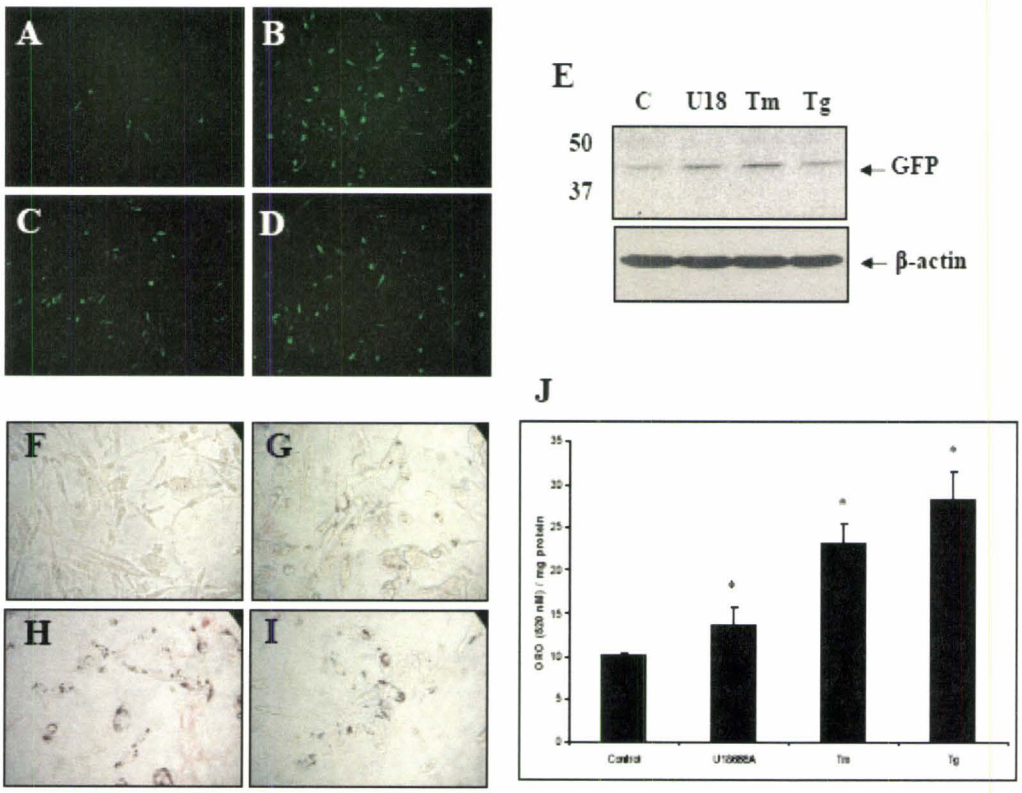
A
B
C
D
E
C U18 Tm Tg
50
37
GFP
β-actin
F
G
H
I
J
Control
Tm
Tg

differentiation, migration and lipid accumulation. Although it is well accepted that atherosclerotic lesion resident macrophages express scavenger receptors that promote the internalization of modified lipoproteins (Moore and Freeman, 2006), it is unknown whether macrophages undergoing ER stress show SREBP-2 activation and lipid accumulation, which could offer an alternative mechanism for macrophage foam cell formation.

To examine whether SREBP-2 activation occurs in lesion-resident macrophages, we examined early atherosclerotic lesions from apolipoprotein E knockout (ApoE-/-) mice. ApoE-/- mice were sacrificed and aortic tissue was harvested following 12 weeks on a normal chow diet. Following tissue processing, sections from the base of the aorta were examined by immunohistochemistry for SREBP expression. Interestingly, anti-SREBP-1 showed intense nuclear staining of lesion resident macrophages, which was confirmed by nuclear staining in adipose tissue (Figure 22A and B). SREBP-2 showed cytoplasmic and nuclear staining associated with macrophage foam cells and staining was confirmed in adipose tissue (Figure 22D and E). The immunohistochemistry results suggest that SREBP is upregulated in macrophages during atherosclerotic lesion development. It is tempting to suggest that ER stress-induced SREBP activation is driving macrophage lipid accumulation and foam cell formation.

4.3.2 Effect of SREBP Activation on Lipid Accumulation in Macrophages

In order to determine whether SREBP-2 activation promotes macrophage lipid accumulation, successful transfection of a suitable macrophage cell line was required.

Figure 22. Expression of the SREBPs in macrophage foam cells from early ApoE$^{-/-}$ atherosclerotic lesions

Panel A, macrophage foams cells in fatty streaks immunostained for SREBP-1. Majority of macrophage foam cells show intense nuclear staining for the N-terminal active form of SREBP-1 (H-160) (arrows). *Panel C*, expression of SREBP-1 in adipose tissue showing intense nuclear staining (arrows) (positive control). *Panel E*, non-specific immunostaining using nonimmune rabbit IgG as the primary antibody in the adventitia adjacent to a lesion. Adventitia contains various cells but mainly adipocytes, fibroblasts and macrophages. *Panel B*, macrophage foam cells in fatty streaks immunostained for SREBP-2 (N-19). Majority of macrophage foam cells show cytoplasmic staining for SREBP-2 (arrows). *Panel D*, expression of SREBP-2 in adipose tissue showing cytoplasmic staining (arrows) (positive control). *Panel F*, non-specific immunostaining using nonimmune goat IgG as the primary antibody in the adventitia adjacent to a lesion.

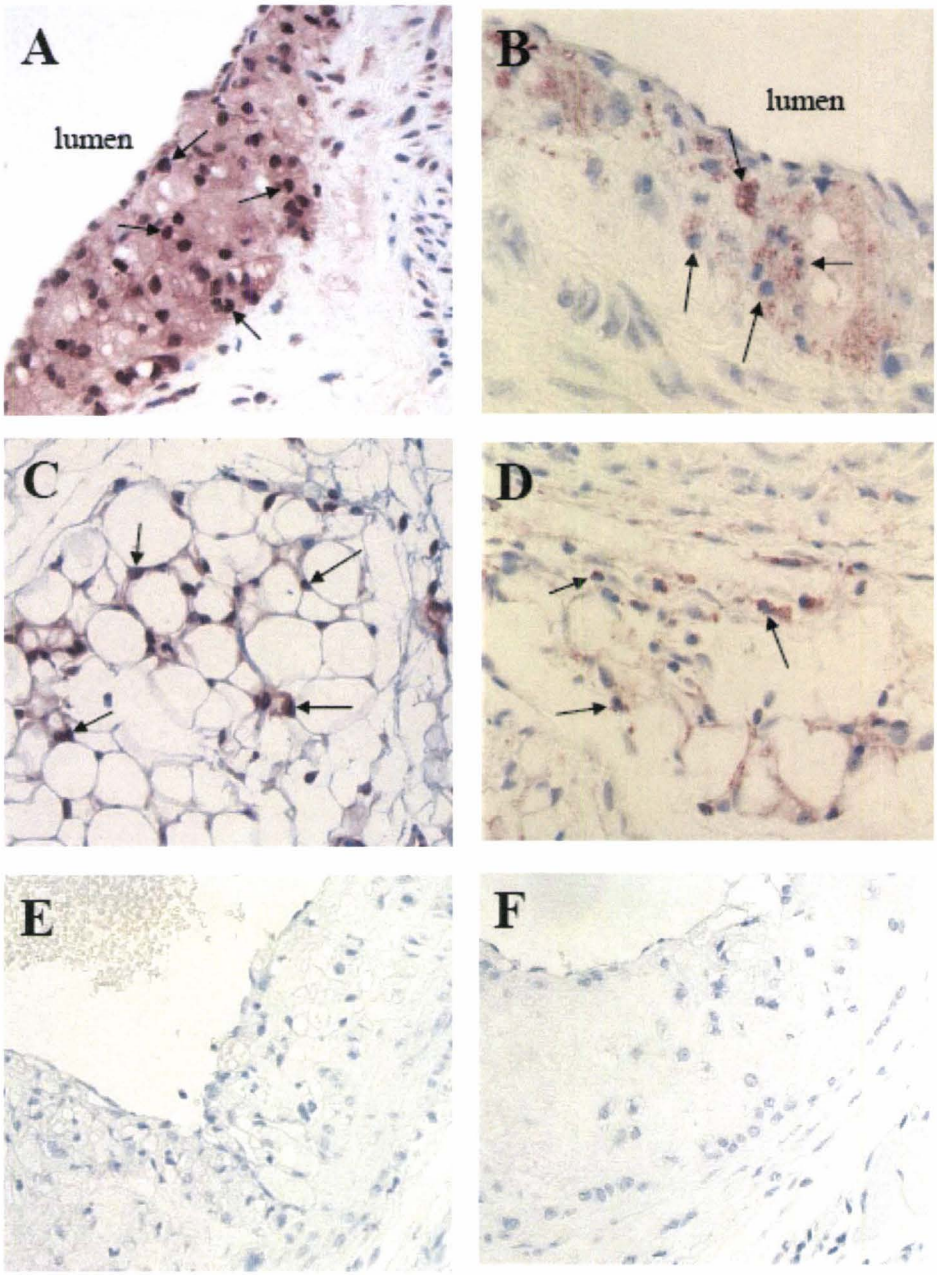
A
lumen
B
lumen
C
D
E
F

The transfection efficiency of THP-1 cells was determined through the use of various transfection reagents (data not shown). To determine whether active SREBP-2 promotes lipid accumulation in macrophages we examined whether active SREBP-2 upregulated SRE-GFP reporter expression. The reporter plasmid pSRE-GFP was co-transfected with pCMV-SREBP2-468 to determine whether the active SREBP2-468 was functional in THP-1 macrophages. Following 24 hour co-transfection with pSRE-GFP and pCMV-SREBP2-468, THP-1 cells were examined by fluorescent microscopy for GFP expression (Figure 23). The results from this experiment suggest that active SREBP-2 promotes increased SRE-controlled gene expression and lipid accumulation in THP-1 macrophages.

4.3.3 Effect of ER Stress-Induced SREBP Activation on Macrophage Lipid Accumulation

Although we have previously shown that SREBP activation occurs in response to ER stress in hepatocytes (Werstuck *et al.,* 2001), HeLa (Colgan *et al.,* 2007) and MDCK [unpublished results] cells, we do not know what role, if any, it plays in macrophage lipid accumulation. Following THP-1 macrophage differentiation, cells were treated with the ER stress-inducing agent Tg, to determine whether the above described mechanism of ER stress-induced SREBP activation occurs in macrophages. Following macrophage treatment with Tg, protein lysates were prepared and examined by immunoblotting for markers of ER stress and UPR activation (eIF2α-phosphorylation, GRP78) and SREBP-2 activation. THP-1 macrophages showed increased SREBP-2 activation in a dose (Figure

Figure 23. The active form of SREBP-2 promotes SRE-gene expression

THP-1 macrophages were cotransfected with the pSRE-GFP reporter plasmid and pCMV-SREBP2-468 for 24 hours. GFP expression was examined by fluorescence indicating SRE element activation.

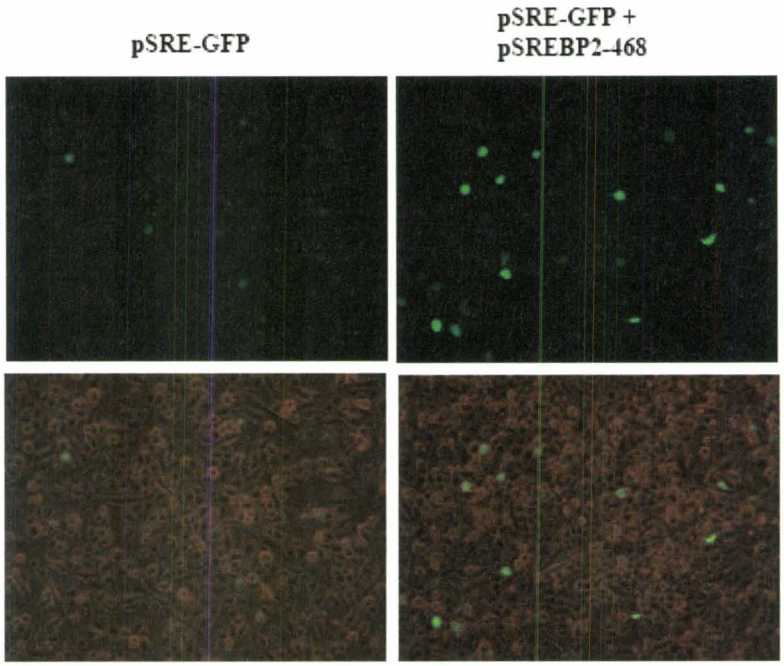
pSRE-GFP
pSRE-GFP +
pSREBP2-468

24A) and time (Figure 24B) dependent manner, which correlated with eIF2α-phosphorylation. Unlike Tg, Tm upregulated KDEL expression but did not induce SREBP-2 activation (Figure 24C).

In order to examine whether ER stress-induced SREBP-2 activation causes an upregulation of genes involved in the UPR and lipid metabolism, THP-1 macrophages were treated with 2 μg/ml U18666A, 0.1 μM Tg or 2 μg/ml Tm for 8 hours. Following incubation, total RNA was extracted from cell lysates and prepared for real-time PCR analysis of GRP78, SREBP-2 and HMGCR (Figure 25). GRP78 gene expression increased following treatment with the ER stress-inducing agents Tg and Tm. In support of the immunoblot data, U18666A and Tg induced SREBP-2 and HMGCR gene expression. In contrast to the immunoblot data, Tm was found to increase the steady-state mRNA levels of SREBP-2 and HMGCR (Figure 25B and C) which is most likely the result of a translational blocked caused by Tm. To examine whether macrophages treated with ER stress-inducing agents accumulate lipid in response to SREBP-2 activation, THP-1 cells were treated with U18666A, Tg or Tm for 24 hours and examined by ORO staining. Following treatment, macrophages were washed, fixed and stained with ORO to examine intracellular lipid content. ORO was de-stained in the presence of 2-propanol and the concentration of ORO in solution was determined. In contrast to our previous findings (Colgan *et al.*, 2007) both Tg and Tm produced a significant decrease in cellular lipid shown by ORO staining (Figure 26).

A more sensitive lipid quantification kit (Wako chemicals) was used to further examine whether any changes in macrophage lipid content occur following ER stress.

Figure 24. Thapsigargin causes SREBP cleavage in THP-1 macrophages

THP-1 macrophages were treated with 0.01-1 μM Tg for 4 hours (A), 0.3 μM Tg for 15-30 minutes (B), or 2 μg/ml U18666A, 0.1 μM Tg and 2 μg/ml Tm for 18 hours (C). Protein lysates were collected and SREBP cleavage, eIF2α phosphorylation, and KDEL expression was examined by immunoblotting. Tg (0.3 μM) induced SREBP-2 cleavage following 4 hour incubation (A) and cleavage occurred as early as 30 minutes (B). Cleavage of SREBP-2 correlated with phosphorylation of eIF2α (A,B). Unlike Tg, Tm upregulated KDEL expression but did not induce SREBP-2 activation (C).

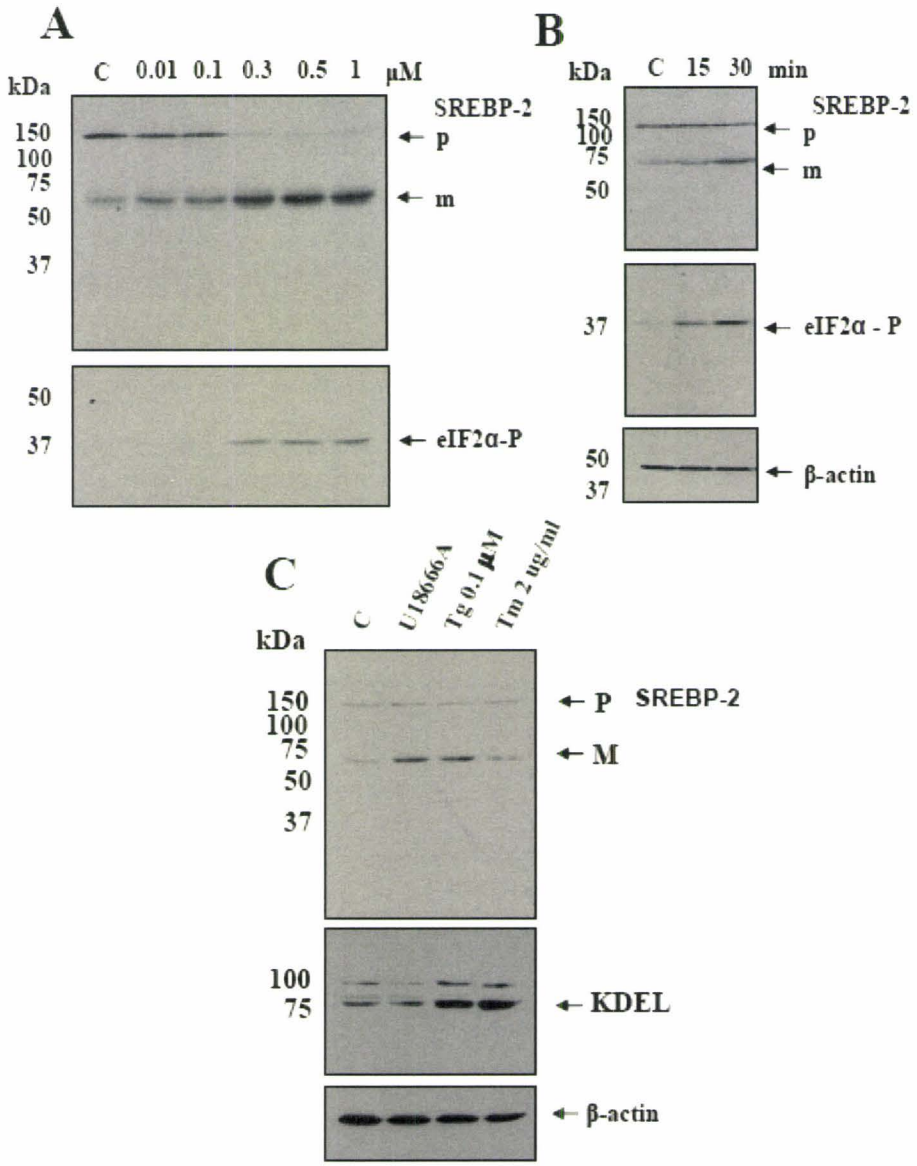
A
C 0.01 0.1 0.3 0.5 1 µM
kDa
150
100
75
50
37
SREBP-2
p
m
50
37
eIF2α-P
B
kDa
C 15 30 min
150
100
75
50
SREBP-2
p
m
37
eIF2α - P
50
37
β-actin
C
C
U18666A
Tg 0.1 µM
Tm 2 ug/ml
kDa
150
100
75
50
37
P SREBP-2
M
100
75
KDEL
β-actin

Figure 25. ER stress agents cause upregulation of genes involved in the UPR and lipid metabolism

THP-1 macrophages were treated with 2 μg/ml U18666A, 0.1 μM Tg or 2 μg/ml Tm for 8 hours. Following incubation, total RNA was extracted from cells and cDNA was prepared for real-time PCR analysis of GRP78, SREBP-2, HMGCR, CEH, ACAT1 and FAS. GRP78 gene expression increased following treatment with the ER stress-inducing agents Tg and Tm. U18666A and Tg induced SREBP-2 and HMGCR gene expression. Tm was found to increase the expression of all of the genes that were examined. (* $p<0.05$, treatment compared to control, n=3)

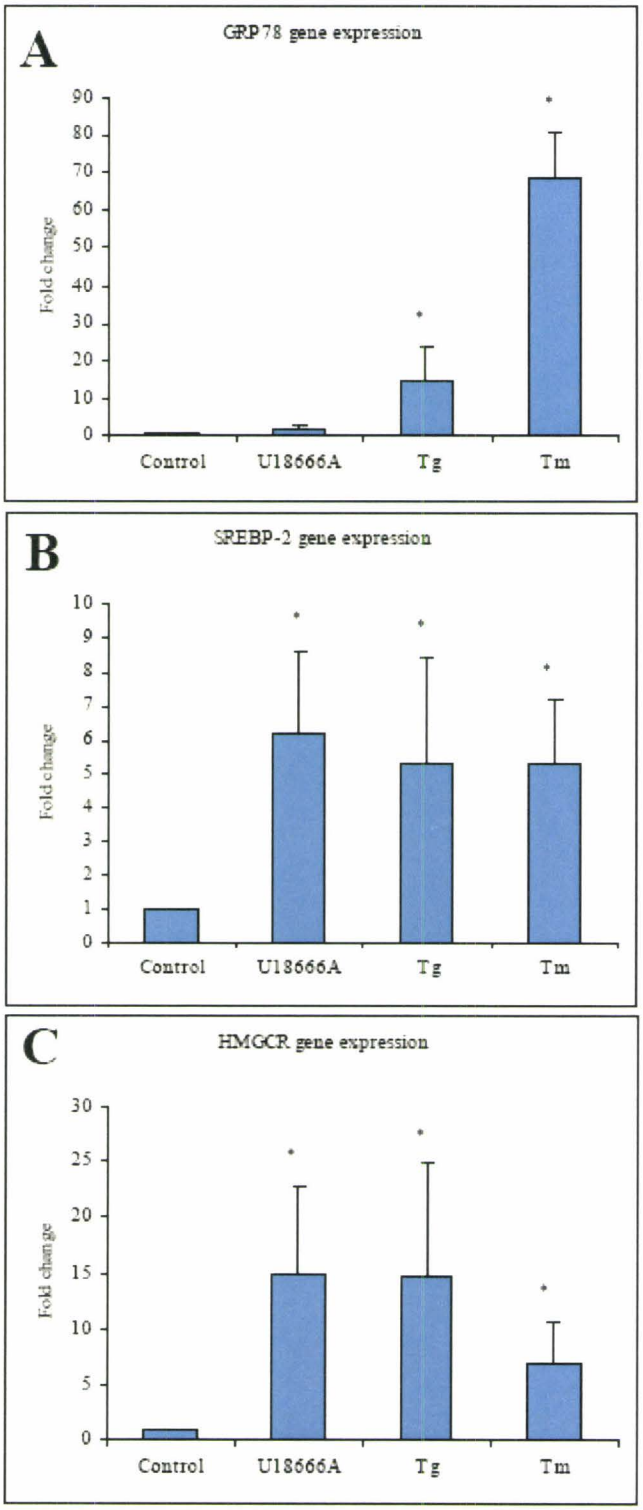
A
GRP78 gene expression
Fold change
90
80
70
60
50
40
30
20
10
0
Control
U18666A
Tg
Tm
B
SREBP-2 gene expression
Fold change
10
9
8
7
6
5
4
3
2
1
0
Control
U18666A
Tg
Tm
C
HMGCR gene expression
Fold change
30
25
20
15
10
5
0
Control
U18666A
Tg
Tm

U18666A produced a characteristic rise in THP-1 macrophage total and free cholesterol content (Figure 27A and B). The ER stress agents Tg and Tm did not produce a significant change in the total or free cholesterol content of THP-1 macrophages (Figure 27A and B). Consistent with the results obtained with ORO staining (Figure 26), ER stress-induced by Tg and Tm significantly decreased intracellular levels of triglyceride (Figure 27C).

To confirm the results from THP-1 macrophages that ER stress-induced SREBP-2 activation does not cause macrophage lipid accumulation, other well-established sources of macrophages were used. Peripheral blood monocyte derived macrophages (PBMC) (Figure 28), mouse (RAW264.7) macrophages, U937 macrophages and mouse peritoneal macrophages (data not shown) were examined by ORO and Filipin staining for changes in cellular lipid content following ER stress. Similarly to the results from THP-1 macrophages, treatment of PBMC (Figure 28), RAW264.7, U937 and peritoneal macrophages (data not shown) with Tg or Tm for 24 hours significantly decreased intracellular neutral lipid (ORO) content and had no observed change in levels of free cholesterol (Filipin).

Although Tg causes SREBP-2 activation in THP-1 macrophages, lipid accumulation does not occur. A possible explanation comes from an experiment in which THP-1 macrophages were transfected with the pSRE-GFP reporter plasmid and treated with the ER stress agents Tg and Tm for 24 hours. Cell lysates were prepared and markers for ER stress (KDEL) and SREBP-2 activation (SREBP-2 and GFP) were assayed by immunoblotting. Figure 29 reveals that although Tg causes SREBP-2

Figure 26. ER stress-induced changes in THP1 macrophage lipid content

THP-1 cells were treated with U18666A, Tg or Tm for 24 hours and examined by ORO staining. Following treatment, macrophages were washed, fixed and stained with ORO. ORO was destained in the presence of 2-propanol and the concentration of ORO in solution was determined at 510nM. Tg or Tm were found to significantly decrease ORO staining in THP-1 macrophages. (* $p<0.05$, treatment compared to control, n=3)

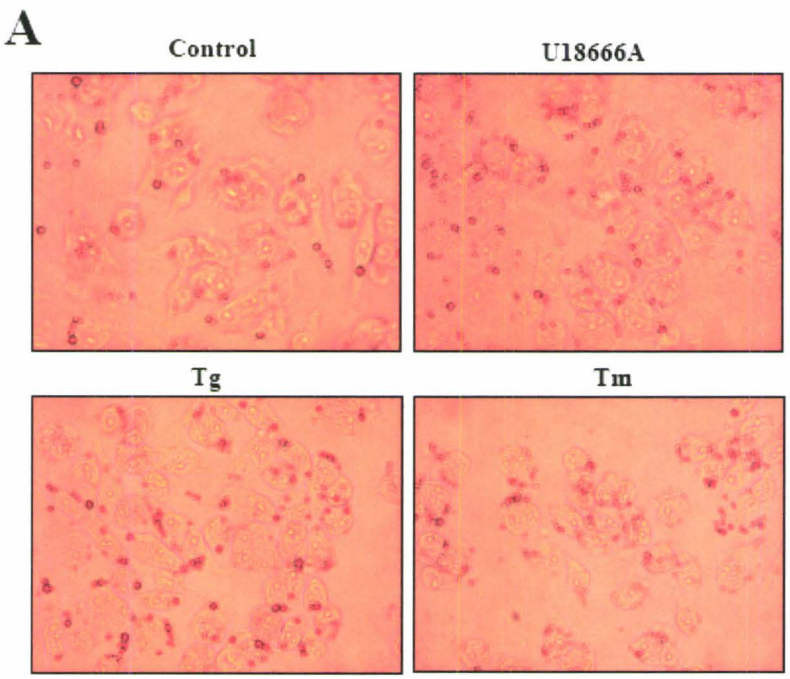
A
Control
U18666A
Tg
Tm

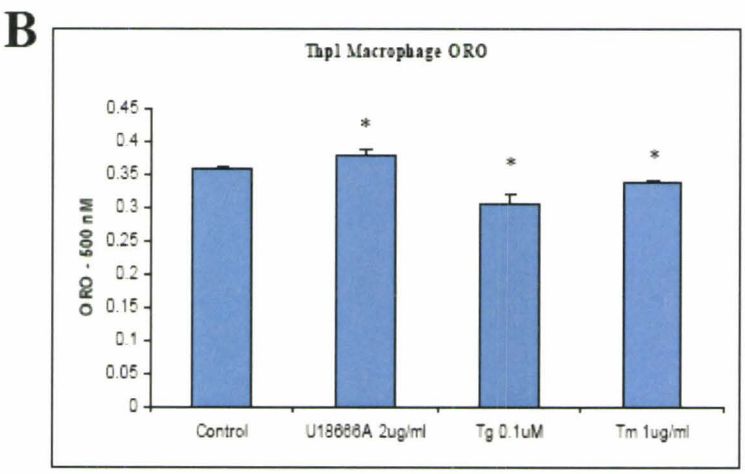
B
Thp1 Macrophage ORO
ORO - 500 nM
0.45
0.4
0.35
0.3
0.25
0.2
0.15
0.1
0.05
0
*
*
*
Control
U18666A 2ug/ml
Tg 0.1uM
Tm 1ug/ml

Figure 27. ER stress does not change total or free cholesterol and decreases triglycerides in THP-1 macrophages

THP-1 macrophages were treated with 2 μg/ml U18666A, 0.1 μM Tg or 2 μg/ml Tm for 24 hours. Cell lysates were prepared for intracellular lipid analysis. U18666A significantly increased THP-1 total and free cholesterol but not total triglycerides. Tg and Tm did not change total or free cholesterol but significantly decreased intracellular triglycerides. (* $p<0.05$, treatment compared to control, n=3)

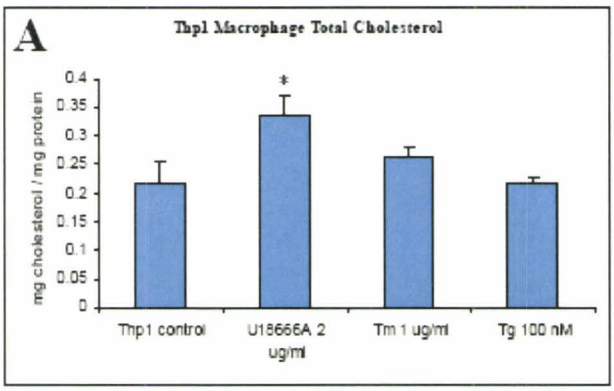
A
Thp1 Macrophage Total Cholesterol
mg cholesterol / mg protein
0.4
0.35
0.3
0.25
0.2
0.15
0.1
0.05
0
*
Thp1 control
U18666A 2 ug/ml
Tm 1 ug/ml
Tg 100 nM

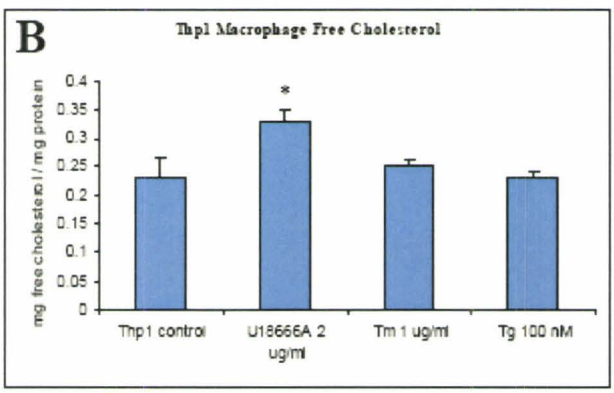
B
Thp1 Macrophage Free Cholesterol
mg free cholesterol / mg protein
0.4
0.35
0.3
0.25
0.2
0.15
0.1
0.05
0
*
Thp1 control
U18666A 2 ug/ml
Tm 1 ug/ml
Tg 100 nM

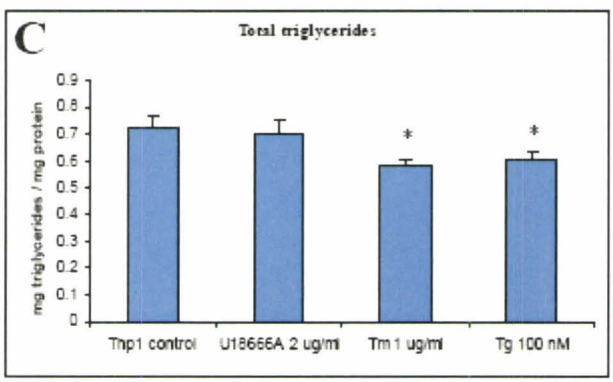
C
Total triglycerides
mg triglycerides / mg protein
0.9
0.8
0.7
0.6
0.5
0.4
0.3
0.2
0.1
0
*
*
Thp1 control
U18666A 2 ug/ml
Tm 1 ug/ml
Tg 100 nM

Figure 28. ER stress-induced changes in PBMC macrophage lipid content

Peripheral blood mononuclear cells were isolated from a healthy donor by magnetic bead separation. Cells were allowed to differentiate for 7 days before treated with 0.1μM Tg or 1μg/ml Tm. Following 24 hour incubation, PBMCs were stained with ORO and Filipin and examined for changes in intracellular lipid content. (* $p<0.05$, treatment compared to control, n=3)

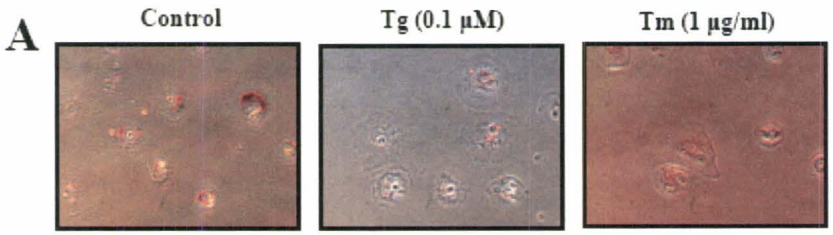
A
Control
Tg (0.1 µM)
Tm (1 µg/ml)

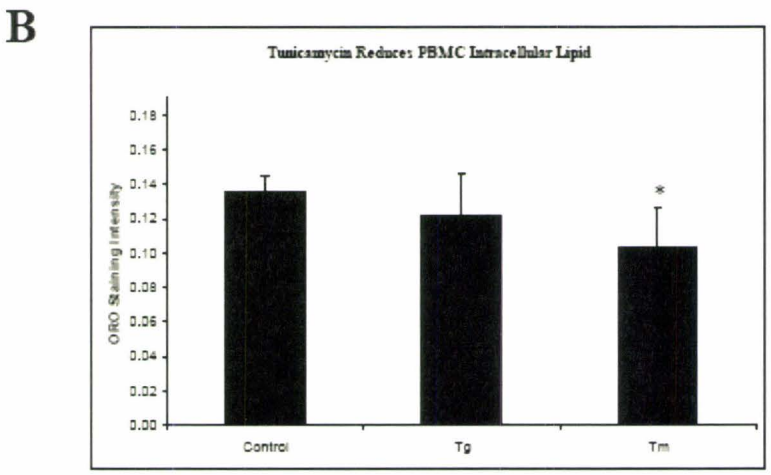
B
Tunicamycin Reduces PBMC Intracellular Lipid
ORO Staining Intensity
0.18
0.16
0.14
0.12
0.10
0.08
0.06
0.04
0.02
0.00
*
Control
Tg
Tm

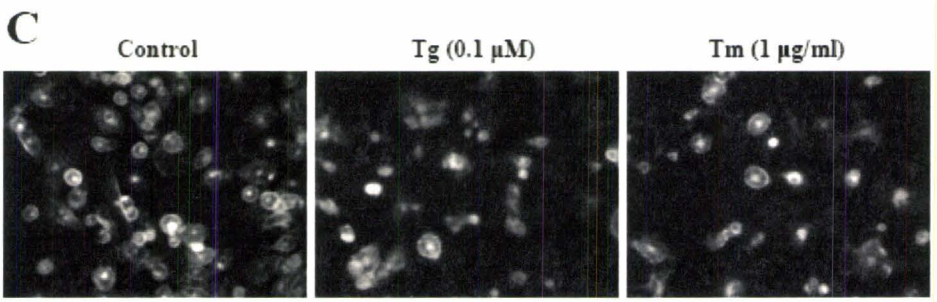
C
Control
Tg (0.1 µM)
Tm (1 µg/ml)

cleavage and increased KDEL expression it does not increase GFP expression beyond basal levels. Although Tm induces KDEL expression it does not induce SREBP-2 cleavage and decreases GFP expression below the basal level.

4.3.4 Alternative Hypothesis for Potential Involvement of SREBP in Atherosclerosis

Although our *in vitro* findings suggest that ER stress-induced SREBP-2 activation may not play a significant role in macrophage lipid accumulation, we cannot reject the immunohistological evidence of increased SREBP-1 and SREBP-2 expression in early atherosclerotic lesions from ApoE-/- mice (Figure 22). Recently, we determined that UPR response genes are upregulated during monocyte to macrophage differentiation (Dickout J, Colgan SM and Austin RC, unpublished). Since SREBP was originally identified as the adipocyte differentiation factor (Tontonoz *et al.,* 1993) and recent reports have described a role for SREBP-1 and -2 activation during membrane biosynthesis and migration (Yao *et al.,*2006; Menendez *et al.,* 2005; Zhou *et al.,* 2004), it would be interesting to determine whether SREBP activation is important during macrophage differentiation. To provide evidence that SREBP-2 is involved in monocyte to macrophage differentiation, THP-1 monocytes were treated with 100 nM PMA to induce the differentiation process. Cells were collected at various time points ranging from 15 minutes to 8 hours, and examined by immunoblotting for SREBP-2 activation and eIF2α phosphorylation (Figure 30A). Results show that PMA-induced differentiation corresponds with SREBP-2 activation over the 8 hour time course. Figure 30A shows

Figure 29. Tg does not induce GFP expression in THP-1 cells.

THP-1 macrophages were transfected with the pSRE-GFP reporter plasmid and treated with the ER stress agents Tg and Tm for 24 hours. Cell lysates were prepared and markers for ER stress (KDEL) and SREBP activation (SREBP and GFP) were assayed by immunoblotting.

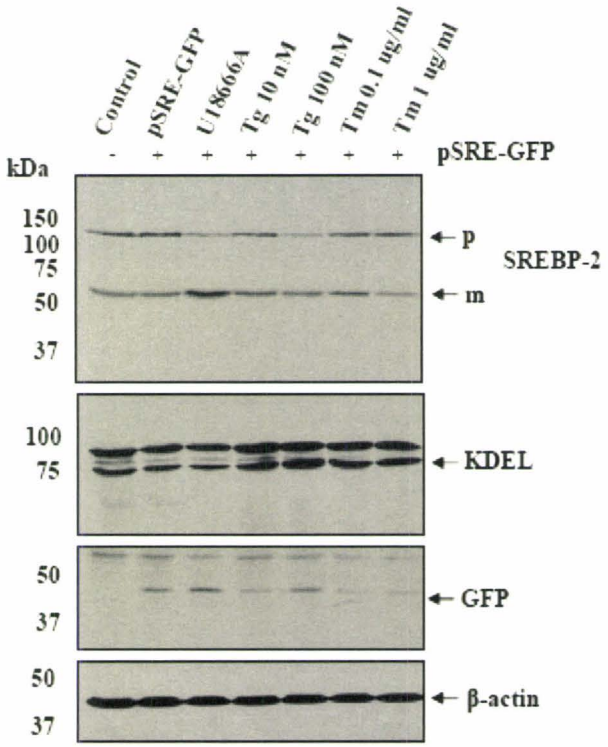
Control
pSRE-GFP
U18666A
Tg 10 nM
Tg 100 nM
Tm 0.1 ug/ml
Tm 1 ug/ml
- + + + + + +
pSRE-GFP
kDa
150
100
75
50
37
p
m
SREBP-2
100
75
KDEL
50
37
GFP
50
37
β-actin

that SREBP-2 is activated at an early time point and results in an increase in expression of the precursor (p) form following 4 and 8 hours of incubation with PMA. This result supports the hypothesis that SREBP may be an important mediator of the macrophage differentiation process.

To further examine the importance of SREBP activation during macrophage differentiation, THP-1 monocytes were pre-treated with or without AEBSF (to inhibit S1P-mediated SREBP activation) followed by PMA to induce differentiation. Monocytes grown in suspension (Figure 30B) that are stimulated to undergo differentiation with PMA characteristically adhere and spread to the tissue culture plate (Figure 30C). Results examining the morphologic changes during monocyte-macrophage differentiation suggest that AEBSF inhibits PMA-induced macrophage differentiation (Figure 30D). Pre-treatment with AEBSF inhibited the characteristic adhesion and spreading that is observed with PMA differentiated macrophages.

The results from the experiments examining ER stress and lipid content suggest that the mechanism of sterol-independent SREBP activation following ER stress, may not contribute to macrophage lipid accumulation. The findings may be the result of SREBP activation following macrophage differentiation and may explain why intracellular lipid levels are elevated prior to treating with ER stress agents. Further clarification of these results required the examination of lipoprotein uptake in the presence or absence of ER stress-inducing agents since the decrease in triglycerides following ER stress could be caused by a decrease in lipoprotein uptake. THP-1 macrophages were incubated in the presence of fluorescent-labelled LDL. Following exposure to Tg and Tm, cells were

Figure 30. SREBP is activated by PMA during THP-1 macrophage differentiation.

Panel A, THP-1 monocytes were treated with PMA (100 ηM) for 15 minutes to 4 hours to induce monocyte to macrophage differentiation. Total cell lysates were subjected to immunoblot analysis using antibodies against SREBP-2 (to assess SREBP activation) or eIF2α (to assess ER stress). *Panel B,* THP-1 monocytes were pretreated with AEBSF to inhibit S1P-mediated SREBP activation. Morphologic changes during monocyte-macrophage differentiation were examined and suggest that AEBSF inhibits PMA induced macrophage differentiation due to the monocytes inability to adhere and spread when treated with AEBSF.

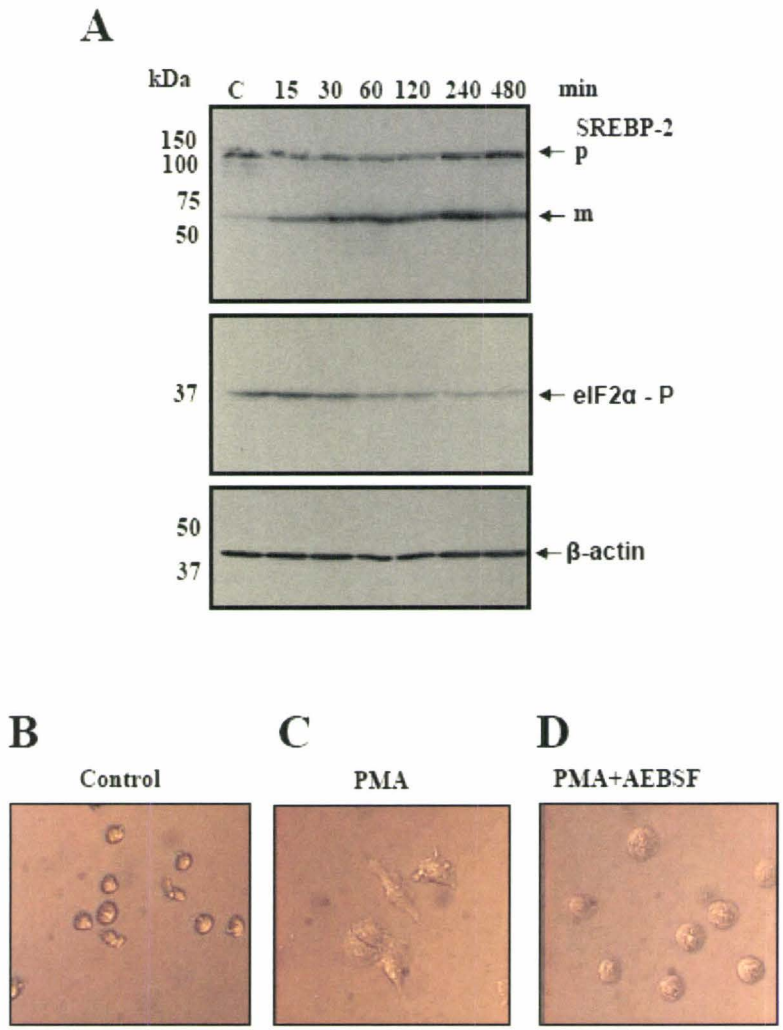
A
kDa
C 15 30 60 120 240 480 min
SREBP-2
150
100
75
50
p
m
37
eIF2α - P
50
37
β-actin
B
Control
C
PMA
D
PMA+AEBSF

examined by fluorescent microscopy for any changes in fluorescent-LDL incorporation (Figure 31). THP-1 macrophages characteristically increased the binding and/or internalization of fluorescent-LDL following treatment with U18666A. Consistent with our previous findings that Tg and Tm decrease intracellular macrophage lipid, binding and/or internalization of fluorescent-LDL in THP-1 macrophages decreased following Tg and Tm treatment. These results provide further evidence that although ER stress causes SREBP-2 cleavage and increased SRE-gene transcription, cells do not respond by increasing intracellular lipid due to a possible defect in LDL uptake during ER stress.

Previous work by Yeh *et al.* (2004) observed that SREBP-1 and -2 was upregulated in atherosclerotic lesions and that it increases the expression and secretion of IL-8 from endothelial cells. Since macrophages are a well established source of the pro-inflammatory molecule IL-8, we examined whether ER stress-induced SREBP-2 activation increased IL-8 secretion from THP-1 macrophages (Figure 32). Following treatment with U18666A, Tg or Tm for 24 hours, cell culture media was removed from THP-1 macrophages and analyzed for IL-8 secretion by ELISA.

Figure 31. ER stress agents decrease macrophage LDL binding and uptake.

THP-1 macrophages (Panel A, E) were treated with either U18666A (2 μg/ml), Tg (0.1 μM) or Tm (2 μg/ml) for 24 hours. Following incubation with U18666A (Panel B, F), Tg (Panel C, G) or Tm (Panel D, H), cells were washed and incubated with serum free medium and DiI-LDL for 1 hour. Following incubation with the fluorescent labelled LDL, cells were washed, fixed and examined for the binding/internalization of fluorescent DiI-LDL (E-H). U18666A increased the binding and uptake of DiI-LDL (F) whereas Tg and Tm decreased DiI-LDL binding (G, H) compared to untreated control (E). Uptake of AcLDL was not effected (data not shown).

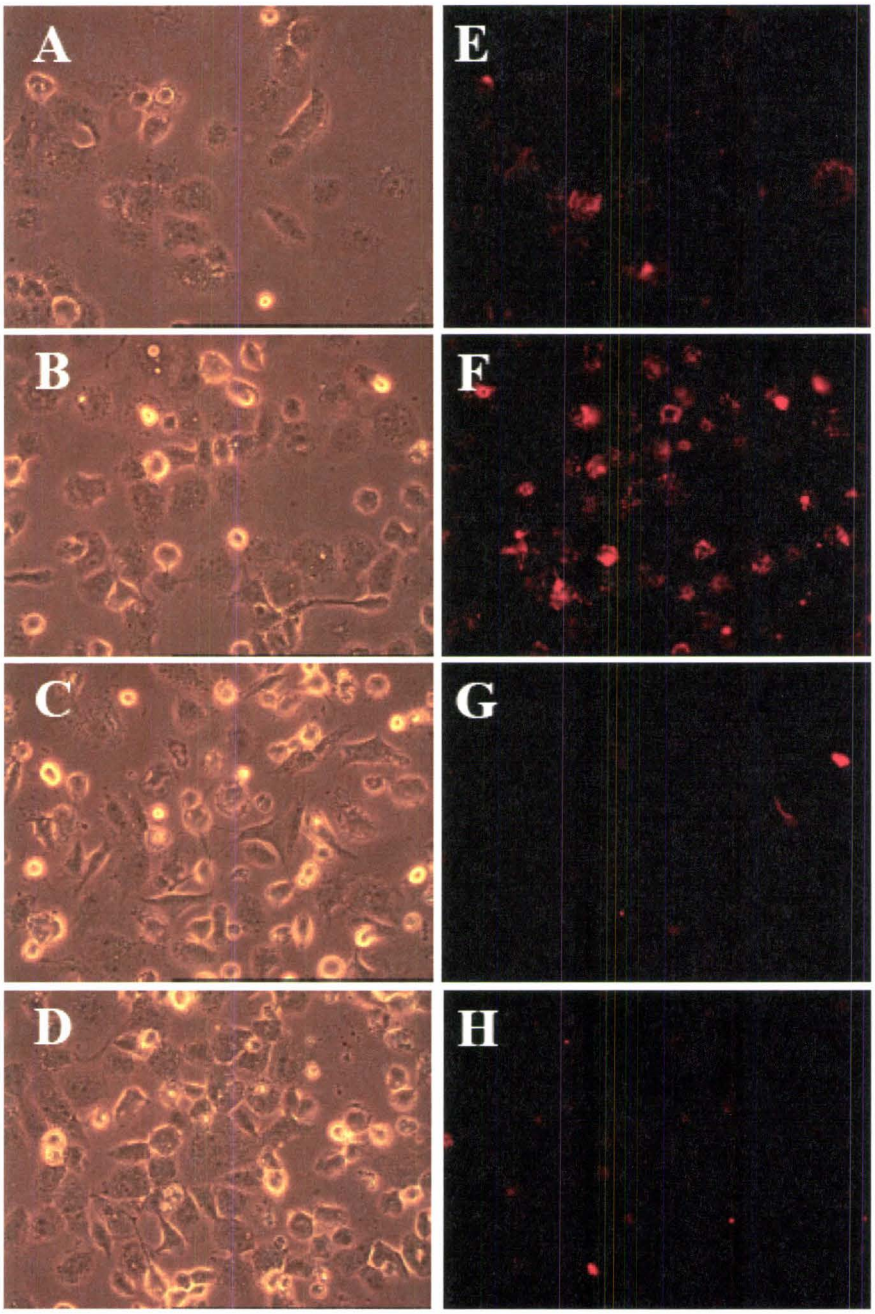
A
E
B
F
C
G
D
H

Figure 32. Thapsigargin increases IL-8 secretion from THP-1 macrophages.

THP-1 macrophages were treated with U18666A (2μg/ml), Tg (0.1 μM), and Tm (2 μg/ml for 24 hours. Cell medium was collected and analyzed by ELISA for IL-8 secretion. Thapsigargin significantly increased IL-8 secretion from THP-1 macrophages. (* $p<0.05$, treatment compared to control, n=3)

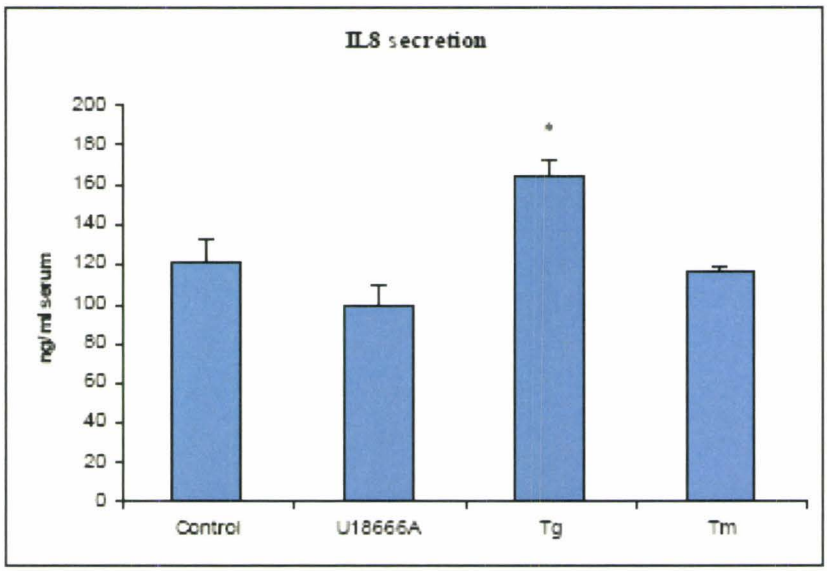
IL8 secretion
ng/ml serum
200
180
160
140
120
100
80
60
40
20
0
*
Control
U18666A
Tg
Tm

5 DISCUSSION

We and others have shown that SREBP activation and lipid dysregulation is associated with conditions that cause ER stress and the activation of the UPR (Kim *et al.*, 2005; Esfandiari *et al.*, 2005; Ji and Kaplowitz, 2003; Werstuck *et al.*, 2001; Colgan *et al.*, 2007). ER stress-induced lipid dysregulation was observed when Outinen and colleagues showed by cDNA microarray analysis that elevated Hcy levels upregulate ER stress response genes and SREBP expression in human umbilical vein endothelial cells (Outinen *et al.*, 1998; Outinen *et al.*, 1999). Werstuck *et al.* (2001) subsequently reported that ER stress led to SREBP-1 activation and increased gene expression essential for the biosynthesis and uptake of cholesterol and triglycerides. Furthermore, ER stress-induced SREBP-1 activation caused the accumulation of cholesterol *in vitro* and led to hepatic steatosis *in vivo* (Werstuck *et al.*, 2001). Werstuck and colleagues (2001) determined that *in vitro* overexpression of GRP78, which relieves ER stress, could inhibit ER stress-induced SREBP associated gene expression. Since the report by Werstuck *et al* (2001), subsequent publications have confirmed the findings that ER stress is associated with the activation of SREBP and hepatic lipid accumulation (Esfandiari *et al.*, 2005; Ji and Kaplowitz, 2003; Woo *et al.*, 2005; Kammoun *et al.*, 2009).

During this research project, I examined the mechanism by which ER stress activates SREBP-2 in various cell lines, including MCF7, HeLa and MDCK epithelial cells and THP-1 macrophage cells. While examining the mechanism of ER stress-induced SREBP-2 activation, I discovered that (1) ER stress activates SREBP-2 by the

conventional sterol-mediated proteolytic pathway (Colgan *et al.*, 2007); (2) there is a strong relationship between changes in ER Ca^{2+} and SREBP-2 activation; (3) ER stress is associated with SREBP-2 activation and lipid dysregulation in a model of renal injury; and (4) ER stress-induced SREBP activation is not associated with lipid accumulation in macrophage foam cells *in vitro*. Since previous experiments have determined that SREBP-1 is active during ER stress and is associated with lipid accumulation (discussed above), we cannot rule out the involvement of SREBP-1-induced lipid accumulation in our experiments. Although SREBP-1 may play a role in the accumulation of lipid in our experimental conditions, there are three explanations that suggest SREBP-2 is additionally involved. Firstly, our experiments show that following ER stress, SREBP-2 is activated and observed by immunoblotting with an antibody specific for SREBP-2. Secondly, cholesterol accumulation has been observed following treatment with ER stress causing conditions and SREBP-2 is the predominant isoform that induces cholesterol accumulation. Finally, downstream markers of SREBP-2 activation such as increased HMG-CoA reductase expression were observed. Together, although we cannot rule out the possibility that SREBP-1 activation is involved in our experiments, we are confident that SREBP-2 activation significantly contributes to the observed changes in cellular cholesterol content.

5.1 ER STRESS ACTIVATES SREBP-2 BY THE CONVENTIONAL PATHWAY

The Austin laboratory has demonstrated that agents or conditions known to cause ER stress are associated with enhanced SREBP gene expression, activation, and lipid

accumulation (Outinen *et al.*, 1998; Outinen *et al.*, 1999; Werstuck *et al.*, 2001; Colgan *et al.*, 2007). Werstuck *et al.* (2001) examined the mechanism by which Hcy-induced ER stress promotes hepatic steatosis. Incubation of cultured human hepatocytes, vascular endothelial cells, and aortic smooth muscle cells with Hcy caused the activation of the UPR and the SREBP pathway. Consistent with the findings that Hcy causes ER stress in human umbilical vein endothelial cells (HUVEC) (Outinen *et al.*, 1998; Outinen *et al.*, 1999), cultured human hepatocytes (HepG2) responded to Hcy by increasing the expression of UPR responsive genes GRP78 and GADD153 (Werstuck *et al.*, 2001). In association with increased GRP78 and GADD153 gene expression, Werstuck *et al* (2001), found that Hcy-induced ER stress caused the activation of SREBP-1 and SREBP-2 and the upregulation of their associated target genes responsible for lipid biosynthesis and uptake. To confirm the findings, Werstuck *et al* (2001) overexpressed GRP78 *in vitro* and inhibited ER stress-induced SREBP activation. To verify the pathological mechanism *in vivo*, diet-induced hyperhomocysteinemia caused hepatic accumulation of cholesterol and triglycerides in wild type C57 mice. The observed hepatic steatosis was associated with ER stress and the activation of the UPR and SREBP pathways since mRNA isolated from the liver showed an upregulation of GADD153, SREBP-1 and the LDL receptor (Werstuck *et al.*, 2001).

A group led by Drs. Michael Brown and Joseph Goldstein demonstrated that SREBP was cleaved under conditions that cause apoptosis and this regulation was independent of cellular cholesterol content (Wang *et al.*, 1995; Pai *et al.*, 1996). These studies revealed that in the presence of cholesterol, caspase-3 and -7 directly cleave

SREBP-2 following apoptotic stimuli. Subsequent to these findings, Higgins and Ioannou (2001) revealed that SREBP-2 was not simply a random substrate of caspases during apoptosis, but when cleaved it had the potential to increase gene expression associated with cholesterol accumulation that preceded the apoptotic process. Wang and colleagues suggested that SREBP-2 activation and cholesterol synthesis at initiation of apoptosis may be required to maintain plasma membrane integrity (Wang *et al.*, 1996). Higgins and Ioannou (2001) confirmed and extended these studies by showing that an increase in SREBP-2 activation and subsequent lipid accumulation may be required for the successful completion of the apoptotic program since cholesterol biosynthesis is critical for normal cellular functioning.

Given that ER stress (Kim *et al.*, 2005; Esfandiari *et al.*, 2005; Ji and Kaplowitz, 2003; Outinen *et al.*, 1998; Werstuck *et al.*, 2001; Lee and Ye, 2004; Colgan *et al.*, 2007; Kammoun *et al.*, 2009) and apoptotic stimuli (Wang *et al.*, 1995; Pai *et al.*, 1996; Wang *et al.*, 1996; Higgins and Ioannou, 2001) have been associated with SREBP activation and that prolonged ER stress causes caspase activation and apoptosis (Shiraishi *et al.*, 2006; Rao *et al.*, 2002), it was our goal to determine whether ER stress-induced SREBP activation was dependant on caspase activation. The MCF7 cell line, which contains a mutation in the caspase-3 gene causing a complete loss of caspase-3 expression (Janicke *et al.*, 1998), was stably transfected with functional caspase-3 and used to examine the effects of caspase-3 on ER stress-induced SREBP-2 cleavage (Figure 4). To determine whether ER stress-induced SREBP cleavage is dependant on caspase-3, MCF7 cells were treated with Tg and examined for SREBP-2 cleavage. Interestingly, both wild type and

caspase-3 overexpressing MCF7 cells increased SREBP-2 cleavage following treatment with Tg. Therefore, the absence of caspase-3 in wild type MCF7 cells had no effect on Tg-induced SREBP-2 cleavage (Figure 4C).

Although SREBP-2 cleavage was observed following apoptotic stimuli, the above experiments provide evidence that ER stress-induced SREBP-2 activation does not require the expression or activation of caspase-3. Although these experiments determined that caspase-3 is not required for ER stress-induced SREBP-2 activation, caspase-7 is an additional caspase that was identified to cleave SREBP-2 similarly to caspase-3 (Wang *et al.*, 1995; Pai *et al.*, 1996) and could potentially be activated during ER stress and lead to SREBP-2 cleavage. To determine whether caspase-7 or additional caspases are involved in SREBP-2 activation during ER stress, HeLa cells were exposed to either STS or Tg in the presence of the pan-caspase inhibitor ZVAD-fmk and examined for SREBP-2 cleavage (Figure 5). Although consistent with previous findings (Wang *et al.*, 1995; Pai *et al.*, 1996) showing that ZVAD-fmk inhibited STS-induced caspase-3 activation and SREBP-2 cleavage, it had no effect on Tg-induced SREBP-2 cleavage (Figure 5). In addition to ZVAD-fmk, inhibitors of caspase-1, caspase-7 or calpain did not decrease Tg-induced SREBP-2 cleavage (data not shown).

The results from the above experiments challenged our original hypothesis that the cleavage of SREBP-2 following Tg-induced ER stress is caused by the activation of caspases and subsequent sterol-independent cleavage of SREBP-2. These experiments provide evidence that the effect of ER stress on SREBP-2 cleavage occurs independently of caspase activation. In order to determine whether ER stress-induced SREBP-2

cleavage occurs through the conventional sterol-mediated pathway, the serine protease inhibitor AEBSF was used to inhibit the cleavage of SREBP-2 by S1P. Okada *et al.* (2003) previously determined that AEBSF could inhibit ER stress-induced ATF6 cleavage and SREBP-2 activation following lipid deprivation. The inhibition of both ATF6 and SREBP-2 activation was mediated by the inhibitory effect of AEBSF on S1P (Okada *et al.,* 2003). Incubation of MCF7 cells with Tg in the presence or absence of AEBSF determined that Tg-induced SREBP-2 cleavage occurred via the conventional sterol-mediated pathway (Figure 6). AEBSF inhibited both sterol-mediated (U18666A) and Tg-induced SREBP-2 cleavage but had no effect on STS-induced (caspase-mediated) SREBP activation in HeLa cells (Figure 6). Based on these findings, our hypothesis is that ER stress-induced SREBP-2 activation occurs through the conventional sterol-mediated pathway and does not require caspase activation, but likely involves the expression and/or activity of the proteins that regulate SREBP-2 activation. Our hypothesis is consistent with recent findings that *in vitro* overexpression of GRP78 inhibits ER stress-induced SREBP activation through interaction with the SREBP regulatory complex (Kammoun *et al.,* 2009). This mechanism is comparable to the conventional role of INSIG binding to SCAP and anchoring SREBP in the ER. GRP78 may sequester SREBP in the ER through interaction with its regulatory complex in a similar manner to its regulation of other ER membrane proteins such as ATF6 (Kammoun *et al.,* 2009).

To provide further evidence that ER stress causes SREBP-2 activation through the conventional S1P/S2P proteolytic pathway, AEBSF inhibited free cholesterol

accumulation in HeLa cells observed following incubation with ER stress-inducing or lipid-depleting agents (Figure 7). This experiment provides additional evidence that ER stress-induced SREBP-2 activation and cholesterol accumulation occurs through the conventional S1P/S2P proteolytic pathway.

5.2 INTRACELLULAR CALCIUM AND SREBP ACTIVATION

It has been demonstrated during the course of this project that the ER stress-inducing agent Tg, causes SREBP-2 activation independent of changes in cellular lipid content. Although ER stress-induced SREBP-2 activation occurs in the presence of sterols, it is not mediated by caspases during apoptosis but rather occurs through the conventional sterol mediated activation pathway normally reserved for SREBP activation following intracellular cholesterol depletion. It was reported by Lee and Ye (2004) that translational inhibition following Tg-induced eIF2α phosphorylation causes SREBP-2 activation. Evidence for this hypothesis was the correlation of Tg-induced SREBP-2 cleavage with INSIG-1 degradation (Lee and Ye, 2004). The proposed mechanism of ER stress-induced SREBP-2 activation was suggested to involve the degradation of INSIG-1. Since INSIG-1 is the molecular "anchor" that binds and retains the SCAP/SREBP complex in the ER, it was suggested that ER stress-induced inhibition of protein synthesis caused INSIG-1 degradation and subsequent SREBP-2 activation (Lee and Ye, 2004). It was the goal of my research project to determine whether our observation that Tg-mediated SREBP-2 activation and lipid accumulation involved eIF2α phosphorylation as

previously suggested (Lee and Ye, 2004), or to provide evidence for an alternative mechanism that would explain Tg-induced SREBP-2 cleavage.

Lee and Ye (2004) as well as Gong *et al* (2006) reported that INSIG-1 has a short half life when dissociated from SCAP. This could explain how ER-stress induced translation inhibition depletes INSIG-1 levels, allowing SREBP activation. We wanted to examine whether the cleavage of SREBP-2 following Tg correlated with phosphorylation of eIF2α. Following Tg treatment, a time-dependant increase of eIF2α phosphorylation was observed and was accompanied by the activation of SREBP-2 (Figure 9). This experiment helped determine the earliest time point for SREBP-2 cleavage and whether it was relevant to the hypothesis that a decrease in INSIG protein levels caused by inhibition of translation resulted in SREBP-2 activation. Although Lee and Ye (2004) measured the half-life of exogenous INSIG-1 to be approximately 2 hours, Gong *et al*. (2006) reported the half-life of endogenous INSIG-1 to be approximately 20 minutes. The proposed half-life of endogenous INSIG-1 correlates with our results that Tg-induces eIF2α phosphorylation and SREBP-2 cleavage following incubation for 15 and 25 minutes, respectively. These results support the hypothesis proposed by Lee and Ye (2004) and Gong *et al* (2006) that ER stress-induced translation inhibition may cause SREBP-2 activation due to INSIG-1 degradation. Unfortunately, we were unable to demonstrate INSIG-1 degradation following Tg-induced ER stress. Although eIF2α phosphorylation and SREBP-2 cleavage occurred, the degradation of exogenous INSIG-1 was not observed following treatment with Tg (data not shown).

To further examine whether eIF2α phosphorylation causes SREBP-2 activation, 293 cells were transfected with a plasmid that expresses wild type (eIF2α-WT) or mutant form of eIF2α (eIF2α-S51D). Although the eIF2α-S51D mutant caused the loss of the SREBP-2 precursor protein, overexpression of eIF2α-WT also induced SREBP-2 cleavage to the same extent seen with the eIF2α-S51D mutant (Figure 10). A potential explanation for the observed loss of SREBP-2 precursor protein following overexpression of eIF2-S51D is that SREBP-2 is being activated or de novo protein synthesis is inhibited due to inhibition of translation. The observed increase in SREBP-2 cleavage/loss of precursor protein following overexpression of eIF2α-WT may be explained by the over expression of a functional eIF2α protein, which under these conditions may be phosphorylated, causing SREBP-2 cleavage.

It is not known whether the observed SREBP-2 cleavage (loss of the SREBP-2 precursor) in our experiments (Figure 10) is due to eIF2α-induced SREBP-2 activation or a result of an inhibition in protein synthesis, thereby leading to the depletion of full length SREBP-2. Thus, to further examine the role of eIF2α phosphorylation-induced SREBP-2 activation, HeLa cells were treated with the GADD34 inhibitor, salubrinal (Boyce *et al.*, 2005), to examine whether inhibition of GADD34 mediated eIF2α dephosphorylation causes SREBP-2 cleavage (Figure 11). Although salubrinal induced and sustained eIF2α phosphorylation, there was no observed increase in SREBP-2 cleavage over time (Figure 11A) or various concentrations (Figure 11B). Since salubrinal-induced inhibition of

eIF2α phosphorylation did not increase SREBP-2 cleavage, the results provide evidence that eIF2α phosphorylation alone may not be required for SREBP-2 activation.

Alternatively to eIF2α-induced INSIG degradation causing SREBP-2 activation, disruption of the INSIG-SCAP interaction under conditions that cause ER stress, could be an alternative mechanism that explains the findings. It has previously been shown that depletion of ER membrane cholesterol causes a dissociation of INSIG from SCAP leading to INSIG degradation and SREBP-2 activation (Gong *et al.,* 2006). In addition, Brown and Goldstein have shown that cholesterol and 25-hydroxycholesterol (25-HC) inhibit INSIG-SCAP dissociation through interaction with INSIG-1 at alternate sites (Adams *et al.,* 2004). As a result, cells treated with 25-HC do not respond to cholesterol depletion by activating SREBP (Adams *et al.,* 2004). We used 25-HC to demonstrate that inhibiting the potential for INSIG dissociation from SCAP, caused a decrease in Tg-induced SREBP-2 cleavage (Figure 12). Since 25-HC has been shown to inhibit INSIG dissociation from SCAP under conditions of cholesterol depletion, our experiment suggests that Tg-induced SREBP-2 cleavage mimics the mechanism of SREBP activation following cholesterol-induced INSIG-SCAP dissociation. 25-HC would have no effect if the primary mechanism of Tg-induced SREBP-2 cleavage was INSIG degradation caused by eIF2α phosphorylation and translation inhibition unless 25-HC stabilized INSIG-1 and inhibited its degradation, which has not been shown. This experiment provides evidence that ER stress-mediated SREBP-2 cleavage may be a result of disrupting the INSIG-SCAP complex, thereby leading to a release of SCAP-SREBP-2 from the ER and subsequent SREBP-2 activation within the Golgi.

Throughout our studies, there has been a distinction between the effects of ER stress agents, with different mechanisms of action, on the ability to activate SREBP-2. SREBP-2 cleavage responds to agents/conditions that disrupt ER Ca^{2+} homeostasis such as Tg, more robustly than compounds that cause ER stress by interfering with protein folding, such as Tm or DTT. Our goal was to examine SREBP-2 activation following treatment with agents that cause ER stress by disrupting intracellular Ca^{2+} homeostasis. We found that all of the agents that affect ER Ca^{2+} homeostasis induced SREBP-2 cleavage to a similar extent compared to U18666A (Figure 13). ER stress inducing agents such as Tm and DTT were examined but did not enhance SREBP-2 cleavage in HeLa cells (data not shown). This experiment provides evidence that the effect of some ER stress inducing agents on SREBP-2 cleavage in HeLa cells is mediated by changes in ER Ca^{2+} homeostasis rather then ER stress and the UPR.

To further examine whether changes in intracellular Ca^{2+} induce SREBP-2 cleavage, we examined the Ca^{2+}-chelating compound BAPTA-AM in the presence of Tg. These experiments were designed to determine whether SREBP-2 is activated upon a rise in intracellular Ca^{2+}. BAPTA was used to chelate Ca^{2+} entering the cytosol upon Tg treatment. The addition of BAPTA did not significantly decrease Tg-induced SREBP cleavage and interestingly, BAPTA alone strongly induced eIF2α phosphorylation and therefore may be inducing ER stress. In addition to PERK, eIF2α protein kinases include dsRNA-activated protein kinase (PKR) (Meurs *et al.,* 1990), general control of nitrogen metabolism kinase-2 (GCN2) (Dever *et al.,* 1992), and heme-regulated inhibitor kinase (HRI) (Levin *et al.,* 1976; Farrell *et al.,* 1977) that normally induce eIF2α

phosphorylation in response to viral infection, amino acid and heme deprivation, heat shock, and oxidative stress, but theoretically could be activated by BAPTA under our experimental conditions.

Together, these experiments provide evidence that Tg-induced SREBP-2 activation correlates with but may not be a result of eIF2α phosphorylation. Lee and Ye (2004) suggest that Tg causes eIF2α phosphorylation-induced translation inhibition, INSIG-1 degradation, and release of the SCAP-SREBP-2 complex from the ER. Our results suggest that although Tg may induce eIF2α phosphorylation and translation inhibition, SREBP-2 cleavage may be a result of the dissociation of INSIG from SCAP caused by alterations in ER Ca^{2+} homeostasis. The observation that BAPTA does not significantly decrease SREBP-2 cleavage following Tg, provides evidence that changes in ER Ca^{2+} may not be important in ER stress-mediated SREBP-2 activation. Previous experiments that overexpressed the Ca^{2+} binding chaperone GRP78, observed a decrease in ER stress-induced SREBP activation (Werstuck *et al.*, 2001; Kammoun *et al.*, 2009) and suggest a possible link between ER Ca^{2+} and the mechanism of SREBP activation. Future experiments should be designed to examine whether overexpression of GRP78 causes an increased concentration of ER Ca^{2+} that correlates with an inhibition of ER stress-induced SREBP activation. Experiments have been performed to examine the possible involvement of cytosolic proteases and signalling molecules that may be involved in Ca^{2+} mediated SREBP-2 activation. Agents that inhibit calpains and the PI3K/AKT pathway were unable to inhibit Tg-induced SREBP-2 activity (data not shown). Future experiments should examine the movement of the SCAP-SREBP-2

complex during disruption of ER Ca^{2+} homeostasis. An increase in cytosolic Ca^{2+} may increase the rate of vesicle turnover between the ER and Golgi, which may account for enhanced SREBP-2 activation upon ER stress.

Since it has been shown that BAPTA disrupts cellular Ca^{2+} homeostasis, inducing eIF2α phosphorylation and the UPR (Paschen *et al.,* 2003) (Figure 15), we wanted to determine whether the effect of BAPTA on SREBP-2 activation was dependent on ER stress. Interestingly, although 100 μM BAPTA induced eIF2α phosphorylation, which correlated with SREBP-2 cleavage, 25 μM BAPTA caused SREBP-2 cleavage independently of eIF2α phosphorylation (Figure 16A and B). These results provide the first evidence that agents known to disrupt ER Ca^{2+} cause SREBP-2 cleavage independent of ER stress and eIF2α phosphorylation. Based on these findings, future experiments should explore whether other conditions that induce ER stress (Tm), disrupt ER Ca^{2+} homeostasis, and determine the mechanism of how alterations in ER Ca^{2+} leads to SREBP-2 activation and lipid accumulation.

5.3 ER STRESS AND SREBP-2 ACTIVATION IN RENAL TOXICITY

The pathology associated with acute renal toxicity is the accumulation of lipid, mainly cholesterol, within the proximal tubules. Zager and colleagues have extensively studied lipid accumulation in proximal tubules in response to ischemia and cytotoxic compounds both *in vivo* and *in vitro* (Zager and Johnson, 2001; Zager *et al.,* 2001; Zager *et al.,* 2002; Zager *et al.,* 2003; Johnson *et al.,* 2005).

Interestingly, a commonality of the studies is the increase in the expression of enzymes and receptors responsible for the uptake and biosynthesis of cholesterol and triglycerides (Zager and Johnson, 2001; Zager *et al.*, 2001; Zager *et al.*, 2003; Johnson *et al.*, 2005; Zager *et al.*, 2005). An *in vivo* model of ER stress was used to examine the physiological relevance of ER stress-induced SREBP activation and lipid accumulation. Intraperitoneal injection of Tm into mice causes injury to proximal tubules in the kidneys resembling the acute tubular necrosis induced in humans by ischemia, infection or toxins (Zinszner *et al.*, 1998). Zinszner *et al.* (1998) found that the expression of GADD153 and ER chaperones in the proximal tubules was dramatically increased within 24 hours following Tm treatment. This model is useful to study acute renal toxicity and ER stress-related pathways *in vivo*. Renal proximal tubule cells appeared swollen with large vacuoles containing lipid droplets (Figure 17A,B). Increased expression and the co-localization of GRP78 and GADD153 with lipid droplets (ORO) suggests a functional relationship between ER stress and the accumulation of lipid in this model (Figure 18D,F). Increased expression of SREBP-2 was correlated to the same proximal tubules that exhibited strong nuclear staining of GADD153 (Figure 19A, B). These *in vivo* findings provide evidence that SREBP-2 activation is associated with proximal tubule cells undergoing ER stress, leading to lipid accumulation.

Our previously described *in vitro* findings using HeLa and MCF7 cells led us to believe that agents known to disrupt ER Ca^{2+}, such as Tg, preferentially activate SREBP-2 over those that cause ER stress by disrupting protein folding, such as Tm. In the above *in vivo* experiments, Tm is used to induce ER stress and increase lipid accumulation in

correlation with increased SREBP-2 expression. Our goal was to confirm these observations *in vitro* in a cell line relevant to the kidney. To support the *in vivo* findings that show proximal tubule cells undergoing ER stress correlated with SREBP-2 expression and ORO staining, we examined ER stress induced SREBP-2 activation and lipid accumulation using a canine renal tubule epithelial cell line, MDCK. Markers for ER stress that were observed in the *in vivo* renal toxicity model, GRP78 (KDEL) and GADD153, were used to show that MDCK cells produce a normal UPR in response to Tm and Tg (Figure 20E). Given that Tm and Tg induced a normal UPR in MDCK cells, experiments were designed to examine whether this led to SREBP-2 activation and lipid accumulation. Consistent with our findings in HeLa cells, MDCK cells transfected with pSRE-GFP showed increased GFP expression following treatment with Tm or Tg (Figure 21C and D). In addition, MDCK epithelial cells were examined for alterations in intracellular lipid and it was observed that MDCK cells increased lipid accumulation following treatment with Tg and Tm (Figure 21F-I). Together these *in vitro* findings confirm the *in vivo* observations that ER stress induced renal tubule lipid accumulation is associated with SREBP-2 activation.

Since SREBPs are responsible for regulating the expression of these lipid associated enzymes and receptors it is not surprising that our results show an association between ER stress-induced cytotoxicity, SREBP-2 expression, and lipid accumulation. Future experiments will determine whether SREBP inhibition decreases lipid accumulation following proximal tubule toxicity. Future experiments should also examine whether pathophysiologic agents/conditions such as cyclosporine A or

proteinuria known to cause human renal toxicity induce ER stress-induced SREBP-2 activation and lipid dysregulation. Since the accumulation of lipids following cytotoxic stress have been suggested to provide an advantage to the cell by protecting them from further injury (Zager *et al.,* 1999; Zager and Kalhorn, 2000; Zager, 2000), it will be important in future experiments to determine whether the activation of SREBP will protect renal tubule cells from subsequent cytotoxic injury. Although SREBP regulation is an essential component of cell growth and differentiation, these studies have demonstrated that disruption of this tightly controlled lipogenic pathway can lead to various lipid-associated pathologies.

5.4 ER STRESS AND SREBP-2 ACTIVATION IN MACROPHAGES

Our current findings suggest that ER stress-induced renal toxicity involves SREBP-2 activation and lipid accumulation. Atherosclerosis is another classic pathology that is characterized by elevated intracellular lipid accumulation in macrophages of the arterial vessel walls. Macrophages are important during the progression of atherosclerotic lesion development and the relevant steps in their maturation from circulating monocyte to lesion resident foam cell include binding and migration, differentiation, and lipid accumulation. Although it is well accepted that atherosclerotic lesion resident macrophages express scavenger receptors that promote the internalization of modified lipoproteins (Moore and Freeman, 2006), it has also been found that scavenger receptor knockout mouse models continue to develop atherosclerosis with pronounced foam cell formation (Manning-Tobin *et al.,* 2009). It is unknown whether

macrophages undergoing ER stress, activate SREBP-2 and promote lipid accumulation, which could offer an additional mechanism to explain macrophage foam cell formation.

To determine whether SREBP activation occurs in lesion-resident macrophages, we examined early atherosclerotic lesions from apolipoprotein E knockout ($ApoE^{-/-}$) mice. Nuclear staining of SREBP-1 and cytoplasmic and nuclear staining of SREBP-2 was associated with lesion resident macrophages (Figure 22A and D). The immunohistochemistry results suggest that SREBP-1 and -2 are upregulated in macrophages during atherosclerotic lesion development. It is tempting to suggest that ER stress-induced SREBP activation contributes to macrophage lipid accumulation and foam cell formation.

To determine whether active SREBP-2 promotes lipid accumulation in macrophages *in vitro,* we examined whether active SREBP-2 upregulated genes involved in lipid biosynthesis promoted lipid accumulation. Following co-transfection with pSRE-GFP and pCMV-SREBP2-468, THP-1 cells had increased GFP expression which correlated with lipid accumulation (Figure 23A and B). These results suggest that active SREBP-2 affects SRE-controlled gene expression promotes lipid accumulation in THP-1 macrophages. Although we have previously shown that SREBP activation occurs in response to ER stress in hepatocytes (Werstuck *et al.,* 2001), HeLa (Colgan *et al.,* 2007) and MDCK [unpublished results] cells, we do not know what role, if any, it plays in macrophage lipid accumulation. Following treatment with Tg, THP-1 macrophages showed increased SREBP-2 activation in a dose (Figure 24A) and time (Figure 24B) dependent manner, which correlated with eIF2α-phosphorylation. Unlike Tg, Tm

upregulated KDEL expression but did not induce SREBP-2 activation (Figure 24C). To examine whether ER stress-induced SREBP-2 activation causes upregulated gene expression involved in the UPR and lipid metabolism, THP-1 macrophages were treated with U18666A, Tg or Tm for 8 hours. GRP78 gene expression increased following treatment with the ER stress-inducing agents Tg and Tm (Figure 25). In support of the immunoblot data, U18666A and Tg induced SREBP-2 and HMGCR gene expression. In contrast to the immunoblot data, Tm was found to increase the steady-state mRNA levels of SREBP-2 and HMGCR (Figure 25B and C) which is most likely the result of the translational inhibition induced by Tm. Together, these findings show that ER stress causes SREBP activation in THP-1 macrophages similarly to the previously examined cell lines, HeLa, MCF7, and MDCK.

In contrast to our results in HeLa, MCF7, and MDCK cells, both Tg and Tm produced a significant decrease in cellular lipid as measured by ORO staining (Figure 26). Using a lipid quantification kit that measures total and free cholesterol and total triglycerides revealed that under conditions that caused ER stress and SREBP-2 activation shown by immunoblotting and RT-PCR, Tg and Tm did not produce a significant change in the total or free cholesterol content of THP-1 macrophages (Figure 27A and B). Consistent with the results obtained with ORO staining (Figure 26), ER stress induced by Tg and Tm significantly decreased intracellular levels of triglycerides (Figure 27C). To confirm these findings, human peripheral blood monocyte derived macrophages (PBMC) (Figure 28), mouse derived macrophages (RAW264.7), human lymphoma derived macrophages (U937) and mouse peritoneal macrophages were

examined by ORO and Filipin staining for changes in cellular lipid content following ER stress. Interestingly, incubation of PBMC (Figure 28), RAW264.7, U937 and peritoneal macrophages (data not shown) with Tg or Tm for 24 hours significantly decreased intracellular lipid (ORO) and had no observed change in levels of free cholesterol (Filipin). These results support the findings from THP-1 macrophages and suggest that ER stress-induced activation of SREBP-2 and upregulation of lipid biosynthetic genes is not adequate to produce macrophage lipid accumulation *in vitro*.

Further examination of ER stress-induced SREBP-2 cleavage in THP-1 macrophages revealed that Tg causes SREBP-2 activation but some inhibition at the transcriptional or translational level is blocking lipid accumulation. Evidence for this comes from an experiment in which THP-1 macrophages were transfected with the pSRE-GFP reporter plasmid and treated with the ER stress agents Tg and Tm for 24 hours. Although Tg causes SREBP-2 cleavage and increased GRP78 (KDEL) expression, it does not increase GFP expression beyond basal levels (Figure 29). Although Tm induces KDEL expression it does not induce SREBP-2 cleavage and decreases GFP expression below the basal level. We conclude that although ER stress causes SREBP-2 activation and increased gene expression in macrophages, it does not translate into increased protein expression, therefore disrupting the lipid biosynthesis and uptake pathway. There is precedence for a cell specific effect of ER stress-induced SREBP-2 activation and lipid accumulation in the literature. Although our lab has shown the mechanism to be present in hepatocytes (Werstuck *et al.*, 2001), renal (MDCK) [unpublished] and cervical (HeLa) (Colgan *et al.*, 2007) epithelial cells, other reports

using Chinese hamster ovary cells (CHO) have suggested that either ER stress does not induce SREBP-2 activation (Harding *et al.,* 2005) or it does with no subsequent increases in lipid accumulation (Lee and Ye, 2004).

Although our *in vitro* findings suggest that ER stress-induced SREBP activation may not play a significant role in macrophage lipid accumulation, we cannot reject the immunohistological evidence of increased SREBP expression in early atherosclerotic lesions from $ApoE^{-/-}$ mice (Figure 22). Recently, we determined that UPR response genes are upregulated during monocyte to macrophage differentiation (Dickout J, Colgan SM and Austin RC, unpublished). Since SREBP was originally identified as the adipocyte differentiation factor (Tontonoz *et al.,* 1993) and recent reports have described a role for SREBP activation during membrane biosynthesis and migration (Yao *et al.,* 2006; Menendez *et al.,* 2005; Zhou *et al.,* 2004), it would be interesting to determine whether SREBP activation is important during macrophage differentiation. THP-1 monocytes stimulated to undergo differentiation showed that SREBP-2 activation occurs early and throughout the differentiation process (Figure 30A). SREBP-2 was activated at an early time point and results in an increase in expression of the precursor (P) form following 4 and 8 hours of incubation with PMA (indicating a transcriptionally active SREBP-2). This experiment and the results of an experiment examining the morphologic changes during monocyte to macrophage differentiation (Figure 30) suggest that SREBP-2 may be an important mediator of the macrophage differentiation process.

The results from the experiments examining ER stress, SREBP-2 activation, and lipid accumulation in macrophages *in vitro* are interesting but unexpected. The results

suggest that although active SREBP-2 increases lipid accumulation in macrophages, the mechanism of sterol-independent SREBP activation following ER stress, does not contribute to macrophage lipid accumulation. These findings are of interest because not only does ER stress-induced SREBP activation and increased gene expression in macrophages not increase cholesterol levels, it significantly decreases intracellular triglycerides. Further clarification of these results required the examination of lipoprotein uptake in the presence or absence of ER stress-inducing agents. THP-1 macrophages were incubated in the presence of fluorescent-labelled LDL. THP-1 macrophages characteristically increased the binding and/or internalization of fluorescent-LDL following treatment with U18666A (Figure 31). Consistent with our previous findings that Tg and Tm decrease intracellular macrophage lipid, binding and/or internalization of fluorescent-LDL in THP-1 macrophages decreased following Tg and Tm treatment. This experiment provides evidence that although ER stress causes SREBP-2 cleavage and increased SRE-gene transcription, cells do not respond by increasing intracellular lipid due to a possible defect in LDL internalization during ER stress. Two potential explanations can be proposed that may affect LDLR expression at the cell surface: 1) although SREBP-2 is activated during ER stress, the expression, proper folding and maturation of the LDLR may not be taking place under ER stress causing conditions and 2) it has recently been described that SREBP-2 activation induces the expression of PCSK9 that negatively regulates the expression of the LDLR (Jeong *et al.*, 2008). Taken together, the potential decrease in LDLR expression under conditions causing ER stress and the upregulation of PCSK9 following SREBP-2 activation may lead to a decrease in

plasma membrane LDLR and decrease LDL binding and internalization. Along with experimentation pertaining to the expression of the LDLR, future experiments should employ biochemical assays to determine the effect of ER stress on the rate of cholesterol synthesis.

Another explanation for the observation of SREBP upregulation in atherosclerotic lesions (Figure 22) and its activation during ER stress (Figure 24) could be that ER stress-induced SREBP activation promotes inflammation through IL-8 upregulation and secretion from lesion resident macrophages. Previous work by Yeh *et al.* (2004) observed that SREBP-1 and -2 was upregulated in atherosclerotic lesions and that it increases the expression and secretion of IL-8 from endothelial cells. Since macrophages are a well established source of the pro-inflammatory molecule IL-8, we examined whether ER stress-induced SREBP-2 activation increased IL-8 secretion from THP-1 macrophages (Figure 32). Interestingly, although U18666A did not have an effect, Tg caused an increase in THP-1 macrophage IL-8 secretion. Tm had no effect on THP-1 macrophage IL-8 secretion which is consistent with the findings that Tm does not increase SREBP-2 cleavage in THP-1 macrophages (Figure 24). Although ER stress-induced sterol-independent SREBP activation does not contribute to macrophage lipid accumulation, the results examining IL-8 secretion provide a potential explanation for the physiologic role of SREBP activation following ER stress in macrophages.

5.5 OVERALL MODEL

Our findings demonstrate that (1) ER stress activates SREBP-2 by the conventional sterol-mediated proteolytic pathway; (2) there is a strong relationship between changes in ER Ca^{2+} and SREBP-2 activation; (3) ER stress is associated with SREBP-2 activation and lipid dysregulation in a model of renal injury; (4) ER stress-induced SREBP-2 activation is not associated with lipid accumulation in macrophage foam cells.

Previous studies have shown that under ER stress conditions, SREBP is activated causing upregulation of genes responsible for lipid biosynthesis and uptake, and resulting in intracellular lipid accumulation. Our studies provide evidence that ER stress-induced SREBP-2 activation is not mediated by caspase activation and is associated with the conventional sterol regulated pathway. In comparison to agents that cause ER stress by interrupting ER protein folding (Tm, DTT), molecules that specifically disrupt ER Ca^{2+} homeostasis, preferentially increase SREBP-2 cleavage and induce lipid accumulation in various cultured cell lines. A potential explanation for our observations is that disruption of ER Ca^{2+} may alter the INSIG-SCAP-SREBP-2 complex, where Ca^{2+} mediated dissociation of SCAP-SREBP-2 from INSIG would permit SREBP-2 cleavage, upregulation of lipid biosynthetic genes, and subsequent lipid accumulation.

Although Ca^{2+}-induced ER stress and SREBP-2 activation was not observed *in vivo*, the overall mechanism of ER stress-induced SREBP-2 activation and lipid accumulation was described in an *in vivo* model of renal toxicity. Although the above mechanism of ER stress-induced SREBP-2 cleavage was replicated in macrophages, there was no concomitant intracellular lipid accumulation and therefore could not provide

an explanation of *in vivo* lipid accumulation in atherosclerotic lesion resident macrophages. The *in vivo* expression of SREBP in lesion resident macrophages may be related to other mechanisms that induce SREBP activation independent of ER stress. We determined that *in vitro* monocyte to macrophage differentiation was associated with SREBP activation but it has also been described that vascular endothelial cells *in vitro*, respond to shear stress by activating SREBP through a signalling pathway independent of ER stress or cholesterol (Liu *et al.*, 2002; Lin *et al.*, 2003). In addition, SREBP has been implicated in vascular endothelial growth factor (VEGF)-induced angiogenesis (Zhou *et al.*, 2004). Zhou and colleagues (2004) provided evidence that endothelial cells require SREBP activation for efficient proliferation and migration and similarly to our experiment with macrophage differentiation, inhibition SREBP activation decreased endothelial pseudopodia extension and migration (Zhou *et al.*, 2004). Together, these findings represent mechanisms of SREBP activation that are independent of ER stress and may provide an explanation for the observed *in vivo* upregulation of SREBP in atherosclerotic lesion resident macrophages but not in our *in vitro* studies.

5.6 FUTURE DIRECTIONS

Important questions still remain to be answered pertaining to the mechanism of ER stress-induced SREBP activation and its role in lipid accumulation in renal pathology and atherosclerosis. These questions include: (1) What is the mechanism by which changes in ER Ca^{2+} causes SREBP-2 activation? (2) What is the physiological relevance of SREBP-2 activation and lipid accumulation following renal toxicity? (3) What is the

role of ER stress-induced SREBP-2 activation in macrophage foam cell formation and atherosclerosis?

Although our findings demonstrate that ER stress activates SREBP-2, it is unknown how ER stress mimics cholesterol depletion and activates SREBP-2 through the conventional pathway. Interestingly, our *in vitro* results demonstrated that there is a strong relationship between agents that disrupt ER Ca^{2+} homeostasis, and rapid activation of SREBP-2 (Figures 1, 7, 13). Lee and Ye (2004) reported a relationship between Tg-induced eIF2α phosphorylation and INSIG-1 degradation. Although our research confirms that Tg causes a rapid activation of SREBP-2 that correlates with eIF2α phosphorylation, we provide evidence that INSIG-1 degradation may not explain the mechanism of SREBP-2 activation. Firstly, although Tg-induced SREBP-2 cleavage occurred rapidly and correlated with eIF2α phosphorylation (Figure 9), eIF2α phosphorylation alone was not sufficient to cause SREBP-2 cleavage (Figure 12). Secondly, the Ca^{2+} chelating agent BAPTA caused SREBP-2 activation at a concentration that did not effect eIF2α phosphorylation (Figure 18). Thirdly, overexpression of INSIG-1 did not inhibit SREBP-2 cleavage and contrary to Lee and Ye (2004), exogenous INSIG-1 was not degraded in correlation with Tg-induced SREBP-2 cleavage (data not shown). Together, these findings suggest that although there is a correlation between Tg-induced eIF2α phosphorylation and SREBP-2 cleavage, eIF2α phosphorylation and INSIG-1 degradation is not required.

Kammoun and colleagues (2009) confirmed previous work by Werstuck *et al.* (2001) who showed that conditions that caused ER stress led to hepatic lipid

accumulation. Kammoun *et al.* (2009) used adenovirus to overexpress GRP78 in the liver of genetically-induced obese and insulin resistant mice. Liver expression of GRP78 decreased markers of ER stress and lipid accumulation. In addition, Kammoun *et al* (2009) performed co-immunoprecipitation experiments with GRP78 and SREBP and found that GRP78 binds to the SREBP complex (SREBP-SCAP-INSIG) but could not identify a specific binding partner. The authors presented a hypothesis in which GRP78 regulates SREBP in a similar manner as ATF6 (Figure 33). It was suggested that under ER stress conditions, GRP78 may dissociated from SREBP or its regulatory molecules SCAP/INSIG and allow the SCAP-SREBP complex to transport to the Golgi for S1P and S2P processing. Our findings that ER Ca^{2+} disruption causes SREBP-2 cleavage is supported by the evidence that overexpression of GRP78 inhibits ER stress-induced SREBP activation (Werstuck *et al.*, 2001; Kammoun *et al.*, 2009). The hypothesis presented by Kammoun and colleagues (2009) supports our results since ER stress caused by ER Ca^{2+} depletion would lead to a GRP78 dissociation GRP78 from the SREBP complex, allowing SREBP activation. This exciting new data provides further evidence of ER stress-induced SREBP activation but additional research is required to determine the precise mechanism by which ER stress and more specifically, changes in ER Ca^{2+}, causes SREBP-2 activation. In addition, we determined that 25-HC inhibits Tg-induced SREBP-2 cleavage (Figure 13), and suggests that although INSIG-1 degradation may not be required, its dissociation from SCAP-SREBP-2 may be important.

Experiments should be designed to examine the physical interaction between SREBP-2 and its regulatory proteins, INSIG and SCAP. To further investigate this

Figure 33. ER Stress and SREBP Activation

UPR activation occurs in response to ER stress and the dissociation of GRP78 from its sensors PERK, ATF6, and IRE-1. In addition, GRP78 has been shown to interact with the SREBP regulatory complex (INSIG, SCAP or SREBP) and inhibit its activation. In the presence of ER stress, GRP78 may dissociated from the SREBP complex and allow for its proteolytic activation. In addition, ER stress-induced SREBP activation has been suggested to involve eIF2α phosphorylation and the subsequent decrease in INSIG-1 protein levels that may induce SREBP activation. The induction of the UPR could potentially result in the feedback control of SREBP activation through de-phosphorylation of eIF2α and the subsequent return of INSIG-1 expression along with the upregulation of GRP78 that may bind and stabilize the INSIG-SCAP-SREBP complex.

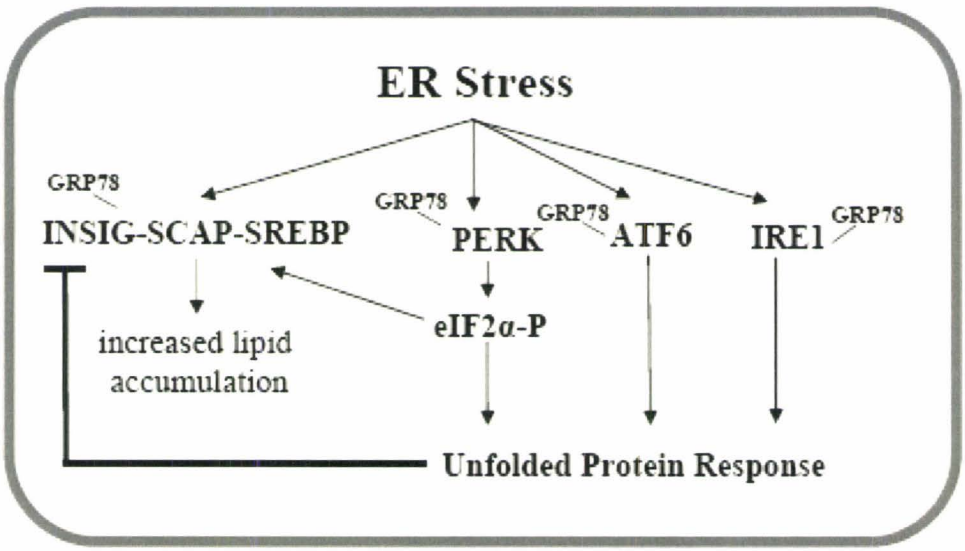
ER Stress
GRP78
INSIG-SCAP-SREBP
GRP78
PERK
GRP78
ATF6
IRE1
GRP78
increased lipid accumulation
eIF2α-P
Unfolded Protein Response

hypothesis, INSIG binding to SCAP following Tg treatment could be examined using the blue-native PAGE gel technique previously described (Yang *et al.*, 2002). If the results from this experiment revealed that INSIG dissociated from SCAP at a time point not correlated with eIF2α phosphorylation or INSIG degradation, than this would provide evidence that Tg-induced changes in ER Ca^{2+} were having a direct effect on the INSIG-SCAP interaction. In addition to the interaction between INSIG-1 and SCAP, other proteins may potentially be involved in the regulation of SREBP activation. Oxysterol-binding protein-1 (OSBP) was the first member of a family of OSBP-related proteins that was shown to bind 25-HC (Dawson *et al.*, 1989a; Dawson *et al.*, 1989b). Following examination of the relationship of OSBP-1 and SREBP, Adams *et al.* (2004) suggested that although OSBP-1 overexpression had no effect on SREBP activation, one of the additional OSBP-related proteins could potentially interact with 25-HC and influence SREBP activation.

Additional research will be required to determine the physiological relevance of ER stress-induced SREBP-2 activation and lipid accumulation following renal toxicity. Our examination of an *in vivo* model of acute renal toxicity and ER stress determined that vacuoles associated with renal proximal tubule cells following toxic insult, contained lipid droplets and were correlated with increased expression of ER stress responsive genes and SREBP-2. These *in vivo* findings provide evidence that SREBP-2 activation is associated with proximal tubule cells undergoing ER stress, leading to lipid accumulation. Future experiments should examine whether pathophysiological agents known to cause human renal toxicity, modulate ER stress-induced SREBP-2 activation

and lipid dysregulation. It will also be interesting to determine whether the observed acute toxicity-induced SREBP-2 activation and lipid accumulation is a pathology associated with cellular toxicity or a potential protective mechanism against the cytotoxic agents.

Experiments should be designed to examine the effect of kidney specific knockout of SREBP-2. Since previous studies have demonstrated that SCAP is required for SREBP processing (Matsuda *et al.,* 2001), a transgenic mouse model with a tissue specific deletion in SCAP could attenuate proximal tubule cell lipid accumulation and have an effect on the survival outcome of the experimental animal. Kidney proximal tubule cell specific deletion of SCAP can be achieved using mice homozygous for the floxed SCAP allele (Matsuda *et al.,* 2001), bred with the kidney androgen regulated protein (KAP) promoter, KAP-Cre transgenic mice (Li *et al.,* 2008). Generation of these transgenic mice, lacking proximal tubule cell SCAP and the subsequent decrease in SREBP-2 activation, would provide strong evidence for the role of SREBP-2 activation and lipid accumulation following renal toxic injury. Results from this experiment would help to explain whether SREBP-2 activation and lipid accumulation following renal toxic injury was protective or contributed to the observed pathology.

In contrast to our *in vitro* research describing ER stress-induced SREBP-2 activation and lipid accumulation in various cell lines such as HeLa, MCF7, and MDCK cells, our findings from macrophages suggest that ER stress-induced SREBP activation does not cause a significant increase in lipid accumulation. A possible explanation for this is that macrophages *in vitro* have elevated baseline intracellular lipids that are not

significantly changed under our experimental conditions. Alternatively, Tg-induced ER stress may alter the amount or function of macrophage LDL receptor, which may inhibit the binding and internalization of lipoproteins. Future experiments should be designed to examine the *in vivo* relevance of SREBP-2 activation on macrophage foam cell formation.

Similarly to the above described kidney specific disruption in SCAP expression, macrophage SREBP activation could be inhibited using a monocyte specific Cre-transgenic mouse bred to mice homozygous for the floxed SCAP allele. Cre recombinase driven by the lysozyme promoter is active in myeloid cell lineages which include monocytes and granulocytes (Clausen *et al.*, 1999). The consequence of monocyte/macrophage specific deletion of SCAP and subsequent inhibition of SREBP-2 activation could be examined for its direct influence on macrophage foam cell formation and atherogenesis. In addition, peritoneal macrophages could be isolated from these transgenic mice and examined for SREBP activation and lipid accumulation in response to ER stress-inducing agents.

Taken together, these future experiments would help to determine the cellular mechanism by which SREBPs are activated by ER stress, specifically, how changes in ER Ca^{2+} induce SREBP activation. In addition, these experiments will help determine the physiological relevance of SREBP activation in renal proximal tubule cells following toxic injury and help determine whether ER stress-induced SREBP activation enhances macrophage foam cell formation and contributes to atherosclerotic lesion development. Overall, our results and future research will (1) better explain the cellular pathways that

mediate SREBP activation and lipid biosynthesis, and (2) lead to the development of novel therapeutic strategies that will help attenuate pathologies associated with intracellular lipid accumulation by preventing excessive ER stress and SREBP activation.

6 REFERENCES

Adams, C.M., Goldstein, J.L., and Brown, M.S. (2003) Cholesterol-induced conformational change in SCAP enhanced by Insig proteins and mimicked by cationic amphiphiles. Proc Natl Acad Sci U S A. 100: 10647-10652.

Adams, C.M., Reitz, J., De Brabander, J.K., Feramisco, J.D., Li, L., Brown, M.S., Goldstein, J.L. (2004) Cholesterol and 25-hydroxycholesterol inhibit activation of SREBPs by different mechanisms, both involving SCAP and Insigs. J Biol Chem. 279: 52772-52780.

Austin, R.C., Lentz, S.R., and Werstuck, G.H. (2004) Role of hyperhomocysteinemia in endothelial dysfunction and atherothrombotic disease. Cell Death Differ. Suppl 1:S56-64.

Bloch, K. (1982) The structure of cholesterol and of the bile acids. Trends Biochem Sci. 7: 334-336.

Boyce, M., Bryant, K.F., Jousse, C., Long, K., Harding, H.P., Scheuner, D., Kaufman, R.J., Ma, D., Coen, D.M., Ron, D., Yuan, J. (2005) A selective inhibitor of eIF2alpha dephosphorylation protects cells from ER stress. Science. 307: 935-939.

Brown, M.S., and Goldstein, J.L. (1974) Expression of the familial hypercholesterolemia gene in heterozygotes: mechanism for a dominant disorder in man. Science. 185: 61-63.

Brown, M.S., and Goldstein, J.L. (1999) A proteolytic pathway that controls the cholesterol content of membranes, cells, and blood. Proc Natl Acad Sci U S A. 96: 11041-11048.

Brown, A.J., Sun, L., Feramisco, J.D., Brown, M.S., and Goldstein, J.L. (2002) Cholesterol addition to ER membranes alters conformation of SCAP, the SREBP escort protein that regulates cholesterol metabolism. Mol Cell. 10: 237-245.

Briggs, M.R., Yokoyama, C., Wang, X., Brown, M.S., and Goldstein, J.L. (1993) Nuclear protein that binds sterol regulatory element of low density lipoprotein receptor promoter. I. Identification of the protein and delineation of its target nucleotide sequence. J Biol Chem. 268: 14490-14496.

Chang, C.C., Chen, J., Thomas, M.A., Cheng, D., Del Priore, V.A., Newton, R.S., Pape, M.E., and Chang, T.Y. (1995) Regulation and immunolocalization of acyl-coenzyme A: cholesterol acyltransferase in mammalian cells as studied with specific antibodies. J Biol Chem. 270: 29532-29540.

Chang, T.Y., Chang, C.C., Ohgami, N., and Yamauchi, Y. (2006) Cholesterol sensing trafficking, and esterification. Annu Rev Cell Dev Biol. 22: 129-157.

Chang, T.Y., Reid, P.C., Sugii, S., Ohgami, N., Cruz, J.C., and Chang, C.C.Y. (2005) The Niemann-Pick type C disease and intracellular cholesterol trafficking. J Biol Chem. 280:20917-20920.

Chen, X., Shen, J., and Prywes, R. (2002) The luminal domain of ATF6 senses endoplasmic reticulum (ER) stress and causes translocation of ATF6 from the ER to the Golgi. J Biol Chem. 277: 13045-13052.

Chung, K.T., Shen, Y., and Hendershot, L.M. (2002) BAP, a mammalian BiP-associated protein, is a nucleotide exchange factor that regulates the ATPase activity of BiP. J Biol Chem. 277: 47557-47563.

Clausen, B.E., Burkhardt, C., Reith, W., Renkawitz, R., and Forster, I. (1999) Conditional gene targeting in macrophages and granulocytes using LysMcre mice. Transgenic Res. 8: 265-277.

Colgan, S.M., Tang, D., Werstuck, G.H., and Austin, R.C. (2007) Endoplasmic reticulum stress causes the activation of sterol regulatory element binding protein-2. Int J Biochem Cell Biol. 39: 1843-1851.

Corbett, E.F., and Michalak, M. (2000) Calcium, a signaling molecule in the endoplasmic reticulum? Trends Biochem Sci. 25: 307-311.

Dawson, P.A., Van der Westhuyzen, D.R., Goldstein, J.L., and Brown, M.S. (1989)(a) Purification of oxysterol binding protein from hamster liver cytosol. J Biol Chem. 264: 9046-9052.

Dawson, P.A., Ridgway, N.D., Slaughter, C.A., Brown, M.S., and Goldstein, J.L. (1989)(b) cDNA cloning and expression of oxysterol-binding protein, an oligomer with a potential leucine zipper. J Biol Chem. 264: 16798-16803.

Denmeade, S.R., and Isaacs, J.T. (2005) The SERCA Pump as a Therapeutic Target Making a "Smart Bomb" for Prostate Cancer. Cancer Biol Ther 4: 14-22

Dever, T.E., Feng, L., Wek, R.C., Cigan, A.M., Donahue, T.F., and Hinnebusch, A.G. (1992) Phosphorylation of initiation factor 2 alpha by protein kinase GCN2 mediates gene-specific translational control of GCN4 in yeast. Cell. 68: 585-596.

Duncan, E.A., Brown, M.S., Goldstein, J.L., and Sakai, J. (1997) Cleavage site for sterol-regulated protease localized to a leu-Ser bond in the lumenal loop of sterol regulatory element-binding protein-2. J Biol Chem. 272: 12778-12785.

Duncan, E.A., Dave, U.P., Sakai, J., Goldtein, J.L., and Brown, M.S. (1998) Second-site cleavage in sterol regulatory element-binding protein occurs at transmembrane junction as determined by cysteine panning. J Biol Chem. 273: 17801-17809.

Ellgaard, L., and Helenius, A. (2003) Quality control in the endoplasmic reticulum. Nat Rev Mol Cell Biol. 4: 181-191.

Esfandiari, F., Villanueva, J.A., Wong, D.H., French, S.W., and Halsted, C.H. (2005) Chronic ethanol feeding and folate deficiency activate hepatic endoplasmic reticulum stress pathway in micropigs. Am J Physiol Gastrointest Liver Physiol. 289: G54-63.

Espenshade, P.J., and Hughes, A.L. (2007) Regulation of sterol synthesis in eukaryotes. Annu Rev Genet. 41: 401-427.

Espenshade, P.J., Li, W.P., and Yabe, D. (2002) Sterols block binding of COPII proteins to SCAP, thereby controlling SCAP sorting in ER. Proc Natl Acad Sci U S A. 99: 11694-11699.

Farrell, P.J., Balkow, K., Hunt, T., Jackson, R.J., and Trachsel, H. (1977) Phosphorylation of initiation factor eIF-2 and the control of reticulocyte protein synthesis. Cell. 11: 187-200.

Feng, B., Yao, P.M., Li, Y., Devlin, C.M., Zhang, D., Harding, H.P., Sweeney, M., Rong, J.X., Kuriakose, G., Fisher, E.A., Marks, A.R., Ron, D., Tabas, I. (2003) The endoplasmic reticulum is the site of cholesterol-induced cytotoxicity in macrophages. Nat Cell Biol. 5: 781-792.

Flynn, G.C., Pohl, J., Flocco, M.T., and Rothman, J.E. (1991) Peptide-binding specificity of the molecular chaperone BiP. Nature 353:726-730.
Gething, M.J. (1999) Role and regulation of the ER chaperone BiP. Semin Cell Dev Biol. 10: 465-472.

Goldstein, J.L., DeBose-Boyd, R.A., and Brown, M.S. (2006) Protein sensors for membrane sterols. Cell. 124: 35-46.

Goldstein, J.L., and Brown, M.S. (1990) Regulation of the mevalonate pathway. Nature. 343: 425-430.

Goldstein, J.L., and Brown, M.S., (2008) From fatty streak to fatty liver: 33 years of joint publications in the JCI. J Clin Invest. 118: 1220-1222.

Goldstein, J.L., Dana, S.E., Brunschede, G.Y., and Brown, M.S. (1975) Genetic heterogeneity in familial hypercholesterolemia: evidence for two different mutations

affecting functions of low-density lipoprotein receptor. Proc Natl Acad Sci USA. 72: 1092-1096.

Goldstein, J.L., Harrod, M.J., and Brown, M.S. (1974) Homozygous familial hypercholesterolemia: specificity of the biochemical defect in cultured cells and feasibility of prenatal detection. Am J Hum Genet. 26: 199-206.

Gong, Y., Lee, J.N., Lee, P.C., Goldstein, J.L., Brown, M.S., and Ye, J. (2006) Sterol-regulated ubiquitination and degradation of Insig-1 creates a convergent mechanism for feedback control of cholesterol synthesis and uptake. Cell Metab. 3:15-24.

Harding, H.P., Zhang, Y., and Ron, D. (1999) Protein translation and folding are coupled by an endoplasmic-reticulum-resident kinase. Nature. 397:271-274.

Harding, H.P., Zhang, Y., Khersonsky, S., Marciniak, S., Scheuner, D., Kaufman, R.J., Javitt, N., Chang, Y.T., and Ron, D. (2005) Bioactive small molecules reveal antagonism between the integrated stress response and sterol-regulated gene expression. Cell Metab. 2:361-371.

Haze, K., Yoshida, H., Yanagi, H., Yura, T., and Mori, K. (1999) Mammalian transcription factor ATF6 is synthesized as a transmembrane protein and activated by proteolysis in response to endoplasmic reticulum stress. Mol Biol Cell. 10:3787-3799.

Hebert, D.N., Foellmer, B., and Helenius, A. (1995) Glucose trimming and reglucosylation determine glycoprotein association with calnexin in the endoplasmic reticulum. Cell. 81:425-433.

Hegarty, B.D., Bobard, A., Hainault, I., Ferre, P., Bossard, P., and Foufelle, F. (2005) Distinct roles of insulin and liver X receptor in the induction and cleavage of sterol regulatory element-binding protein-1c. Proc Natl Acad Sci U S A. 102: 791-796.

Hendershot, L., Wei, J., Gaut, J., Melnick, J., Aviel, S., and Argon, Y. (1996) Inhibition of immunoglubulin folding and secretion by dominant negative BiP ATPase mutants. Proc Natl Acad Sci U S A. 93:5269-5274.

Hengartner, M.O. (2000) The biochemistry of apoptosis. Nature. 407:770-776.

Higgins, M.E., and Ioannou, Y.A., (2001) Apoptosis-induced release of mature sterol regulatory element-binding proteins activates sterol-responsive genes. J Lipid Res. 42: 1939-1946.

Horton, J.D., Goldstein, J.L., and Brown, M.S. (2002) SREBPs: activators of the complete program of cholesterol and fatty acid synthesis in the liver. J Clin Invest. 109:1125-1131.

Horton, J.D., Shimomura, I., Ikemoto, S., Bashmakov, Y., Hammer, R.E. (2003) Overexpression of sterol regulatory element-binding protein-1a in mouse adipose tissue produces adipocyte hypertrophy, increased fatty acid secretion, and fatty liver. J Biol Chem. 278:36652-36660.

Horton, J.D., Shimomura, I., Brown, M.S., Hammer, R.E., Goldstein, J.L., and Shimano, H. (1998) Activation of cholesterol synthesis in preference to fatty acid synthesis in liver and adipose tissue of transgenic mice overproducing sterol regulatory element-binding protein-2. J Clin Invest. 101: 2331-2339.

Hossain, G.S., van Thienen, J.V., Werstuck, G.H., Zhou, J., Sood, S.K., Dickhout. J.G., de Koning, A.B., Tang, D., Wu, D., Falk, E., Poddar, R., Jacobsen, D.W., Zhang, K., Kaufman, R.J., Austin, R.C. (2003) TDAG51 is induced by homocysteine, promotes detachment-mediated programmed cell death, and contributes to the cevelopment of atherosclerosis in hyperhomocysteinemia. J Biol Chem. 278: 30317-30327.

Hua, X., Yokoyama, C., Wu, J., Briggs, M.R., Brown, M.S., Goldstein, J.L., and Wang, X. (1993) SREBP-2, a second basic-helix-loop-helix-leucine zipper protein that stimulates transcription by binding to a sterol regulatory element. Proc Natl Acad Sci U S A. 90: 11603-11607.

Hua, X., Wu, J., Goldstein, J.L., Brown, M.S., and Hobbs, H.H. (1995) Structure of the human gene encoding sterol regulatory element binding protein-1 (SREBF1) and localization of SREBF1 and SREBF2 to chromosomes 17p11.2 and 22q13. Genomics. 25: 667-673.

Hua, X., Nohturfft, A., Goldstein, J.L., and Brown, M.S. (1996)(a) Sterol resistance in CHO cells traced to point mutation in SREBP cleavage-activating protein. Cell. 87: 415-426.

Hua, X., Sakai, J., Brown, M.S., and Goldstein, J.L. (1996)(b) Regulated cleavage of sterol regulatory element binding proteins requires sequences on both sides of the endoplasmic reticulum membrane. J Biol Chem. 271:10379-10384.

Janicke, R.U., Sprengart, M.L., Wati, M.R., and Porter, A.G. (1998) Caspase-3 is required for DNA fragmentation and morphological changes associated with apoptosis. J Biol Chem. 273:9357-9360.

Jacobson, M.D., Weil, M. Raff, M.C. (1997) Programmed cell death in animal development. Cell. 88:347-354.

Jeong, H.J., Lee, H.S., Kim, K.S., Kim, Y.K., Yoon, D., and Park, S.W. (2008) Sterol-dependent regulation of proprotein convertase subtilisin/kexin type 9 expression by sterol-regulatory element binding protein-2. J Lipid Res. 49: 399-409.

Ji, C., and Kaplowitz, N. (2003) Betaine decreases hyperhomocysteinemia, endoplasmic reticulum stress, and liver injury in alcohol-fed mice. Gastroenterology. 124: 1488-1499.

Johnson, A.E., and van Waes, M.A. (1999) The translocon: a dynamic gateway at the ER membrane. Annu Rev Cell Dev Biol. 15:799-842.

Johnson, A.C., Stahl, A., Zager, R.A. (2005) Triglyceride accumulation in injured renal tubular cells: alterations in both synthetic and catabolic pathways. Kidney Int. 67:2196-2209.

Kammoun, H.L., Chabanon, H., Hainault, I., Luquet, S., Magnan, C., Koike, T., Ferre, P., and Foufelle, F. (2009) GRP78 expression inhibits insulin and ER stress-induced SREBP-1c activation and reduces hepatic steatosis in mice. J Clin Invest. 119:1201–1215.

Kasturi, R., and Joshi, V.C. (1982) Hormonal regulation of stearoyl coenzyme A desaturase activity and lipogenesis during adipose conversion of 3T3-L1 cells. J Biol Chem. 257:12224-12230

Kaufman, R.J. (2002) Orchestrating the unfolded protein response in health and disease. J Clin Invest. 110:1389-1398.

Kim, A.J., Shi, Y., Austin, R.C., and Werstuck, G.H. (2005) Valproate protects cells from ER stress-induced lipid accumulation and apoptosis by inhibiting glycogen synthase kinase-3. J Cell Sci. 118: 89-99.

Kim, J.B., Spotts, G.D., Halvorsen, Y.D., Shih, H.M., Ellenberger, T., Towle, H.C., and Spiegleman, B.M. (1995) Dual DNA binding specificity of ADD1/SREBP1 controlled by a single amino acid in the basic helix-loop-helix domain. Mol Cell Biol. 15:2582-2588.

Kimura, K., Jin, H., Ogawa, M., Aoe, T. (2008) Dysfunction of the ER chaperone BiP accelerates the renal tubular injury. Biochem Biophys Res Commun. 366:1048-1053.

Kuri-Harcuch, W., and Green, H. (1978) Adipose conversion of 3T3 cells depends on a serum factor. Proc Natl Acad Sci U S A. 75:6107-6109.

Lawrence de Koning, A.B., Werstuck, G.H., Zhou, J., and Austin, R.C. (2003) Hyperhomocysteinemia and its role in the development of atherosclerosis. Clin Biochem. 36: 431-441.

Lee, A.S., (2001) The glucose-regulated proteins: stress induction and clinical applications. Trends Biochem Sci. 26: 504-510.

Lee, J.N. and Ye, J. (2004) Proteolytic activation of sterol regulatory element-binding protein induced by cellular stress through depletion of Insig-1. J Biol Chem. 279: 45257-45265.

Lee, K., Tirasophon, W., Shen, X., Michalak, M., Prywes, R., Okada, T., Yoshida, H., Mori, K., and Kaufman, R.J. (2002) IRE1-mediated unconventional mRNA splicing and S2P-mediated ATF6 cleavage merge to regulate XBP1 in signaling the unfolded protein response. Genes Dev. 16:452-466.

Levin, D., Ranu, R.S., Ernst, V., and London, I.M. (1976) Regulation of protein synthesis in reticulocyte lysates: phosphorylation of methionyl-tRNAf binding factor by protein kinase activity of translational inhibitor isolated from hemedeficient lysates. Proc Natl Acad Sci U S A. 73: 3112-3116.

Li, H., Zhou, X., Davis, D.R., Xu, D. and Sigmund, C.D. (2008) An androgen-inducible proximal tubule-specific Cre recombinase transgenic model. Am J Physiol Renal Physiol. 294: F1481-F1486.

Liberek, K., Marszalek, J., Ang, D., Georgopoulos, C., and Zylicz, M. (1991) Escherichia coli DnaJ and GrpE heat shock proteins jointly stimulate ATPase activity of DnaK. Proc Natl Acad Sci U S A. 88: 2874-2878.

Lin, T., Zeng, L., Liu, Y., DeFea, K., Schwartz, M.A., Chien, S., and Shyy, J.Y. (2003) Rho-ROCK-LIMK-cofilin pathway regulates shear stress activation of sterol regulatory element binding proteins. Circ Res. 92: 1296-1304.

Liscum, L., and Faust, J.R. (1989) The intracellular transport of low density lipoprotein-derived cholesterol is inhibited in Chinese hamster ovary cells cultured with 3-beta-[2-(diethylamino)ethoxy]androst-5-en-17-one. J Biol Chem. 264: 11796-11806.

Liu, Y., Chen, B.P., Lu, M., Zhu, Y., Stemerman, M.B., Chien, S., and Shyy, J.Y. (2002) Shear Stress activation of SREBP1 in endothelial cells is mediated by integrins. Arterioscler Thromb Vasc Biol. 22: 76-81.

Ma, Y., and Hendershot, L.M. (2004) ER chaperone functions during normal and stress conditions. J Chem Neuroanatomy. 28: 51-65.

Manning-Tobin, J.J., Moore, K.J., Seimon, T.A., Bell, S.A., Sharuk, M., Alvarez-Leite, J.I., de Winther, M.P., Tabas, I., Freeman, M.W. (2009) Loss of SR-A and CD36 activity reduces atherosclerotic lesion complexity without abrogating foam cell formation in hyperlipidemic mice. Arterioscler Thromb Vasc Biol. 29: 19-26.

Matsuda, M., Korn, B.S., Hammer, R.E., Moon, Y.A., Komuro, R., Horton, J.D., Goldstein, J.L., Brown, M.S., and Shimomura, I. (2001) SREBP cleavage-activating protein (SCAP) is required for increased lipid synthesis in liver induced by cholesterol deprivation and insulin elevation. Genes Dev. 15: 1206-1216.

Maxfield, F.R., and Tabas, I. (2005) Role of cholesterol and lipid organization in disease. Nature. 438: 612-21.

Maxfield, F.R., and Wustner, D. (2002) Intracellular cholesterol transport. J Clin Invest. 110: 891-898.

Menendez, J.A., Colomer, R., and Lupu, R. (2005) Why does tumor-associated fatty acid synthase (oncogenic antigen-519) ignore dietary fatty acids? Med Hypotheses. 64: 342-349.

Meunier, L., Usherwood, Y.K., Chung, K.T., and Hendershot, L.M. (2002) A subset of chaperones and folding enzymes from multiprotein complexes in endoplasmic reticulum to bind nascent proteins. Mol Biol Cell. 13: 4456-4469.

Meurs, E., Chong, K., Galabru, J., Thomas, N.S., Kerr, I.M., Williams, B.R., Hovanessian, A.G. (1990) Molecular cloning and characterization of the human double-stranded RNA-activated protein kinase induced by interferon. Cell. 62: 379-390.

Miserez, A.R., Cao, G., Probst, L.C., and Hobbs, H.H. (1997) Structure of the human gene encoding sterol regulatory element binding protein 2 (SREBF2). Genomics. 40: 31-40.

Moore, K.J., and Freeman, M.W. (2006) Scavenger receptors in atherosclerosis: beyond lipid uptake. Arterioscler Thromb Vasc Biol. 26: 1702-1711.

Morishima, N., Nakanishi, K., Takenouchi, H., Shibata, T., and Yasuhiko, Y. (2002) An endoplasmic reticulum stress-specific caspase cascade in apoptosis. Cytochrome c-independent activation of caspase-9 by caspase-12. J Biol Chem. 277: 34287-34294.

Munro, S., and Pelham, H.R. (1986) An Hsp70-like protein in the ER: identity with the 78 kd glucose-regulated protein and immunoglobulin heavy chain binding protein. Cell. 46:291-300.

Nakagawa, T., Zhu, H., Morishima, N., Li, E., Xu, J., Yankner, B.A., and Yuan, J. (2000) Caspase-12 mediates endoplasmic-reticulum-specific apoptosis and cytotoxicity by amyloid-beta. Nature. 403: 98-103.

Nakamura, K., Zuppini, A., Arnaudeau, S., Lynch, J., Ahsan, I., Krause, R., Papp, S., De Smedt, H., Parys, J.B., Muller-Esterl, W., Lew, D.P., Krause, K.H., Demaurex, N., Opas, M., Michalak, M. (2001) Functional specialization of calreticulin domains. J Cell Biol. 154:961-972.

Neer, E.J., Schmidt, C.J., Nambudripad, R., and Smith, T.F. (1994) The ancient regulatory-protein family of WD-repeat proteins. Nature. 371:297-300.

Nhan, T.Q., Liles, W.C., Chait, A., Fallon, J.T., and Schwartz, S.M. (2003) The p17 cleaved form of caspase-3 is present within viable macrophages *in vitro* and in atherosclerotic plaque. Arterioscler Thromb Vasc Biol. 23:1276-1282.

Nohturfft, A., Hua, X., Brown, M.S., and Goldstein, J.L. (1996) Recurrent G-to-A substitution in a single codon of SREBP cleavage-activating protein causes sterol resistance in three mutant Chinese hamster ovary cell lines. Proc Natl Acad Sci U S A. 93: 13709-13714.

Nohturfft, A., Brown, M.S., and Goldstein, J.L. (1998)(a) Topology of SREBP cleavage-activating protein, a polytopic membrane protein with a sterol-sensing domain. J Biol Chem. 273: 17243-17250.

Nohturfft, A., Brown, M.S., and Goldstein, J.L. (1998)(b) Sterols regulate processing of carbohydrate chains of wild-type SREBP cleavage-activating protein (SCAP), but not sterol-resistant mutants Y298C or D443N. Proc Natl Acad Sci U S A. 95:12848-12853.

Nohturfft, A., DeBose-Boyd, R.A., Scheek, S., Goldstein, J.L., and Brown, M.S. (1999) Sterols regulate cycling of SREBP cleavage-activating protein (SCAP) between endoplasmic reticulum and Golgi. Proc Natl Acad Sci U S A. 96:11235-11240.

Nohturfft, A., Yabe, D., Goldstein, J.L., Brown, M.S., and Espenshade, P.J. (2000) Regulated step in cholesterol feedback localized to budding of SCAP from ER membranes. Cell. 102: 315-323.

Okada, T., Haze, K., Nadanaka, S., Yoshida, H., Seidah, N.G., Hirano, Y., Sato, R., Negishi, M., Mori, K. (2003) A serine protease inhibitor prevents endoplasmic reticulum stress-induced cleavage but not transport of the membrane-bound transcription factor ATF6. J Biol Chem. 278: 31024-31032.

Olson, R.E. (1998) Discovery of the lipoproteins, their role in fat transport and their significance as risk factors. J Nutr. 128: 439S-443S.

Oram, J.F. (2002) Molecular basis of cholesterol homeostasis: lessons from Tangier disease and ABCA1. Trends Mol Med. 8: 168-173

Outinen, P.A., Sood, S.K., Liaw, P.C., Sarge, K.D., Maeda, N., Hirsh, J., Ribau, J., Podor, T.J., Weitz, J.I., and Austin, R.C. (1998) Characterization of the stress-inducing effects of homocysteine. Biochem J. 332: 213-221.

Outinen, P.A., Sood, S.K., Pfeifer, S.I., Pamidi, S., Podor, T.J., Li, J., Weitz, J.I., and Austin, R.C. (1999) Homocysteine-induced endoplasmic reticulum stress and growth arrest leads to specific changes in gene expression in human vascular endothelial cells. Blood. 94: 959-967.

Paschen, W., Hotop, S., and Aufenberg, C. (2003) Loading neurons with BAPTA-AM activates xbp1 processing indicative of induction of endoplasmic reticulum stress. Cell Calcium. 33: 83-89.

Pai, J.T., Brown, M.S., and Goldstein, J.L. (1996) Purification and cDNA cloning of a second apoptosis-related cysteine protease that cleaves and activates sterol regulatory element binding proteins. Proc Natl Acad Sci U S A. 93: 5437-5442.

Peyrou, M., Cribb, A.E. (2007) Effect of endoplasmic reticulum stress preconditioning on cytotoxicity of clinically relevant nephrotoxins in renal cell lines. Toxicol In Vitro 21:878-886.

Porter, A.G., and Janicke, R.U. (1999) Emerging roles of caspase-3 in apoptosis. Cell Death Differ. 6:99-104.

Rao, R.V., Castro-Obregon, S., Frankowski, H., Schuler, M., Stoka, V., del Rio, G., Bredesen, D.E., Ellerby, H.M. (2002) Coupling endoplasmic reticulum stress to the cell death program. An Apaf-1-independent intrinsic pathway. J Biol Chem. 277:21836-21842.

Rawson, R.B,, Zelenski, N.G,, Nijhawan, D,, Ye, J,, Sakai, J,, Hasan, M.T,, Chang, T.Y,, Brown, M.S,, and Goldstein, J.L. (1997) Complementation cloning of S2P, a gene encoding a putative metalloprotease required for intramembrane cleavage of SREBPs. Mol Cell. 1:47-57.

Rawson, R.B. (2003) The SREBP pathway-insights from insigs and insects. Nat Rev Mol Cell Biol. 4:631-640.

Rawson, R.B., DeBose-Boyd, R., Goldstein, J.L., and Brown, M.S. (1999) Failure to cleave sterol regulatory element-binding proteins (SREBPs) causes cholesterol auxotrophy in Chinese hamster ovary cells with genetic absence of SREBP cleavage-activating protein. J Biol Chem. 274: 28549-28556.

Ron, D. (2002) Translational control in the endoplasmic reticulum stress response. J Clin Invest. 110:1383-1388.

Ron, D., and Hubbard, S.R. (2008) How IRE1 reacts to ER stress. Cell. 132:24-26

Rutkowski, D.T., and Kaufman, R.J. (2004) A trip to the ER: coping with stress. Trends Cell Biol. 14: 20-28.

Sakai, J,, Duncan, E.A,, Rawson, R.B., Hua, X., Brown, M.S., and Goldstein, J.L. (1996) Sterol-regulated release of SREBP-2 from cell membranes requires two sequential cleavages, one within a transmembrane segment. Cell. 85:1037-1046.

Sakai, J., Nohturfft, A., Goldstein, J.L., and Brown, M.S. (1998) Cleavage of sterol regulatory element-binding proteins (SREBPs) at site-1 requires interaction with SREBP cleavage-activating protein. Evidence from *in vivo* competition studies. J Biol Chem. 273: 5785-5793.

Sakai, J., Rawson, R.B., Espenshade, P.J., Cheng, D., Seegmiller, A.C., Goldstein, J.L., and Brown, M.S. (1998) Molecular identification of the sterol-regulated luminal protease that cleaves SREBPs and controls lipid composition of animal cells. Mol Cell. 2:505-514.

Sakai, J., Nohturfft, A., Cheng, D., Ho, Y.K., Brown, M.S., and Goldstein, J.L. (1997) Identification of complexes between the COOH-terminal domains of sterol regulatory element-binding proteins (SREBPs) and SREBP cleavage-activating protein. J Biol Chem. 272: 20213-20221.

Sakashita, N., Miyazaki, A., Takeya M., Horiuchi, S., Chang, C.C., Chang, T.Y., and Takahashi, K. (2000) Localization of human acyl-coenzyme A: cholesterol acyltransferase-1 (ACAT-1) in macrophages and in various tissues. 156: 227-236.

Schagger, H., Cramer, W.A., von Jagow, G. (1994) Analysis of molecular masses and oligomeric states of protein complexes by blue native electrophoresis and isolation of membrane protein complexes by two-dimensional native electrophoresis. Anal Biochem. 217:220-230.

Seidah, N.G., Khatib, A.M., and Prat, A. (2006) The proprotein convertases and their implication in sterol and/or lipid metabolism. Biol Chem. 387: 871-877.

Shen, J., Chen, X., Hendershot, L., and Prywes, R. (2002) ER stress regulation of ATF6 localization by dissociation of BiP/GRP78 binding and unmasking of Golgi localization signals. Dev Cell. 3:99-111.

Sheng, Z., Otani, H., Brown, M.S., and Goldstein, J.L. (1995) Independent regulation of sterol regulatory element-binding proteins 1 and 2 in hamster liver. Proc Natl Acad Sci U S A. 92: 935-938.

Shimano, H., Horton, J.D., Hammer R.E., Shimomura, I., Brown, M.S., and Goldstein, J.L. (1996) Overproduction of cholesterol and fatty acids causes massive liver enlargement in transgenic mice expressing truncated SREBP-1a. J Clin Invest. 98: 1575-1584.

Shimano, H., Horton, J.D., Shimomura, I., Hammer, R.E., Brown, M.S., and Goldstein, J.L. (1997) Isoform 1c of sterol regulatory element binding protein is less active than isoform 1a in livers of transgenic mice and in cultured cells. J Clin Invest. 99: 846-854.

Shimomura, I., Shimano, H., Horton, J.D., Goldstein, J.L., and Brown, M.S. (1997) Differential expression of exons 1a and 1c in mRNAs for sterol regulatory element binding protein-1 in human and mouse organs and cultured cells. J Clin Invest. 99: 838-845.

Shimomura, I., Hammer, R.E., Richardson, J.A., Ikemoto, S., Bashmakov, Y., Goldstein, J.L., Brown, M.S. (1998) Insulin resistance and diabetes mellitus in transgenic mice expressing nuclear SREBP-1c in adipose tissue: model for congenital generalized lipodystrophy. Genes Dev. 12:3182-3194.

Shiraishi, H., Okamoto, H., Yoshimura, A., and Yoshida, H. (2006) ER stress-induced apoptosis and caspase-12 activation occurs downstream of mitochondrial apoptosis involving Apaf-1. J Cell Sci. 119:3958-3966.

Shiu, R.P., Pouyssequr, J., and Pastan, I. (1977) Glucose depletion accounts for the induction of two transformation-sensitive membrane proteinsin Rous sarcoma virus-transformed chick embryo fibroblasts. Proc Natl Acad Sci U S A. 74:3840-3844.

Sitia, R., and Braakman, I. (2003) Quality control in the endoplasmic reticulum protein factory. Nature. 426:891-894.

Smith, J.R., Osborne, T.F., Goldstein, J.L., and Brown, M.S. (1990) Identification of nucleotides responsible for enhancer activity of sterol regulatory element in low density lipoprotein receptor gene. J Biol Chem. 265: 2306-2310.

Soccio, R.E., and Breslow, J.L. (2004) Intracellular cholesterol transport. Arterioscler Thromb Vasc Biol, 24: 1150-1160.

Sugii, S., Reid, P.C., Ohgami, N., Du, H., and Chang, T.Y. (2003) Distinct endosomal compartments in early trafficking of low density lipoprotein-derived cholesterol. J Biol Chem. 278: 27180-27189.

Sudhof, T.C., Russell, D.W., Brown, M.S., and Goldstein, J.L. (1987)(a) 42 bp element from LDL receptor gene confers end-product repression by sterols when inserted into viral TK promoter. Cell. 48: 1061-1069.

Sudhof, T.C., Van der Westhuyzen, D.R., Goldstein, J.L., Brown, M.S., and Russell, D.W. (1987)(b) Three direct repeats and a TATA-like sequence are required for regulated expression of the human low density lipoprotein receptor gene. J Biol Chem. 262: 10773-10779.

Sun, L.P., Li, L., Goldstein, J.L., and Brown, M.S. (2005) Insig required for sterol-mediated inhibition of Scap/SREBP binding to COPII proteins *in vitro*. J Biol Chem. 280: 26483-26490.
Sun, L.P., Seemann, J., Brown, M.S., and Goldstein, J.L. (2007) Sterol-regulated transport of SREBPs from endoplasmic reticulum to Golgi: Insig renders sorting signal in Scap inaccessible to COPII proteins. Proc Natl Acad Sci USA. 104: 6519–6526.

Thompson, C.B. (1995) Apoptosis in the pathogenesis and treatment of disease. Science. 267:1456-1462.

Tirasophon, W., Lee, K., Callaghan, B., Welihinda, A., and Kaufman, R.J. (2000) The endoribonuclease activity of mammalian IRE1 autoregulates its mRNA and is required for the unfolded protein response. Genes Dev. 14:2725-2736.

Tontonoz, P., Kim, J.B., Graves, R.A., Spigelman, B.M. (1993) ADD1: a novel helix-loop-helix transcription factor associated with adipocyte determination and differentiation. Mol Cell Biol. 13:4753-4759.

Vallett, S.M., Sanchez, H.B., Rosenfeld, J.M., and Osborne, T.F. (1996) A direct role for sterol regulatory element binding protein in activation of 3-hydroxy-3-methylglutaryl coenzyme A reductase gene. J Biol Chem. 271: 12247-12253.

Vance, D.E., and Van den Bosch, H. (2000) Cholesterol in the year 2000. Biochim Biophys Acta. 1529: 1-8.

Wang, X., Briggs, M.R., Hua, X., Yokoyama, C., Goldstein, J.L., and Brown, M.S. (1993) Nuclear protein that binds sterol regulatory element of low density lipoprotein receptor promoter. II. Purification and characterization. J Biol Chem. 268: 14497-14504.

Wang, X., Sato, R., Brown, M.S., Hua, X., and Goldstein, J.L. (1994) SREBP-1, a membrane-bound transcription factor released by sterol-regulated proteolysis. Cell. 77: 53-62.

Wang, X., Pai, J.T., Wiedenfeld, E.A., Medina, J.C., Slaughter, C.A., Goldstein, J.L., and Brown, M.S. (1995) Purification of an interleukin-1 beta converting enzyme-related cysteine protease that cleaves sterol regulatory element-binding proteins between the leucine zipper and transmembrane domains. J Biol Chem. 270: 18044-18050.

Wang, X., Zelenski, N.G., Yang, J., Sakai, J., Brown, M.S., and Goldstein, J.L. (1996) Cleavage of sterol regulatory element binding proteins (SREBPs) by CPP32 during apoptosis. EMBO J. 15:1012-1020.

Wang, H., Kouri, G., and Wollheim, C.B. (2005) ER stress and SREBP-1 activation are implicated in beta-cell glucolipotoxicity. J Cell Sci. 118:3905-3915.

Werstuck, G.H., Lentz, S.R., Dayal, S., Hossain, G.S., Sood, S.K., Shi, Y.Y., Zhou, J., Maeda, N., Krisans, S.K., Malinow, M.R., Austin, R.C. (2001) Homocysteine-induced endoplasmic reticulum stress causes dysregulation of the cholesterol and triglyceride biosynthetic pathways. J Clin Invest. 107: 1263-1273.

Woo, C.W., Siow, Y.L., Pierce, G.N., Choy, P.C., Minuk, G.Y., Mymin, D., O, K. (2005) Hyperhomocysteinemia induces hepatic cholesterol biosynthesis and lipid accumulation via activation of transcription factors. Am J Physiol Endocrinol Metab. 288: E1002-E1010.

Yabe, D., Brown, M.S., and Goldstein, J.L. (2002) Insig-2, a second endoplasmic reticulum protein that binds SCAP and blocks export of sterol regulatory element-binding proteins. Proc Natl Acad Sci U S A. 99: 12753-12758.

Yang, T., Goldstein, J.L., and Brown, M.S. (2000) Overexpression of membrane domain of SCAP prevents sterols from inhibiting SCAP.SREBP exit from endoplasmic reticulum. J Biol Chem. 275:29881-29886.

Yang, T., Espenshade, P.J., Wright, M.E., Yabe, D., Gong, Y., Aebersold, R., Goldstein, J.L., and Brown, M.S. (2002) Crucial step in cholesterol homeostasis: sterols promote binding of SCAP to INSIG-1, a membrane protein that facilitates retention of SREBPs in ER. Cell. 110:489-500.

Yao, M., Zhou, R.H., Petreaca, M., Zheng, L., Shyy, J., Martins-Green, M. (2006) Activation of sterol regulatory element-binding proteins (SREBPs) is critical in IL-8-induced angiogenesis. J Leukoc Biol. 80:608-620.

Ye, J., Rawson, R.B., Komuro, R., Chen, X., Dave, U.P., Prywes, R., Brown, M.S., and Goldstein, J.L. (2000) ER stress induces cleavage of membrane-bound ATF6 by the same proteases that process SREBPs. Mol Cell. 6:1355-1364.

Yeh, M., Cole, A.L., Choi, J., Liu, Y., Tulchinsky, D., Qiao, J.H., Fishbein, M.C., Dooley, A.N., Hovnanian, T., Mouilleseaux, K., Vora, D.K., Yang, W.P., Gargalovic, P., Kirchgessner, T., Shyy, J.Y., Berliner, J.A. (2004) Role for sterol regulatory element-binding protein in activation of endothelial cells by phospholipid oxidation products. Circ Res. 95:780-788.

Yellaturu, C.R., Deng, X., Park, E.A., Raghow, R., and Elam, M.B. (2009) Insulin enhances biogenesis of the nuclear SREBP-1c by posttranscriptional downregulation of Insig-2a and its dissociation from SCAP-SREBP-1c complex. J Biol Chem. (epub ahead of print).

Yokoyama, C., Wang, X., Briggs, M.R., Admon, A., Wu, J., Hua, X., Goldstein, J.L., and Brown, M.S. (1993) SREBP-1, a basic-helix-loop-helix-leucine zipper protein that controls transcription of the low density lipoprotein receptor gene. Cell. 75: 187-197.

Yoshida, H., Haze, K., Yanagi, H., Yura, T., and Mori, K. (1998) Identification of the cis-acting endoplasmic reticulum stress response element responsible for transcriptional induction of mammalian glucose-regulated proteins. Involvement of basic leucine zipper transcription factors. J Biol Chem. 273:33741-33749.

Yoshida, H., Matsui, T., Yamamoto, A., Okada, T., and Mori, K. (2001) XBP1 mRNA is induced by ATF6 and spliced by IRE1 in response to ER stress to produce a highly active transcription factor. Cell. 107:881-891.

Zager, R.A., Burkhart, K.M., Johnson, A.C., Sacks, B.M. (1999) Increased proximal tubular cholesterol content: implications for cell injury and "acquired cytoresistance". Kidney Int. 56:1788-1797.

Zager, R.A. (2000) Plasma membrane cholesterol: a critical determinant of cellular energetics and tubular resistance to attack. Kidney Int. 58:193-205

Zager, R.A., Kalhorn, T.F. (2000) Changes in free and esterified cholesterol: hallmarks of acute renal tubular injury and acquired cytoresistance. Am J Pathol. 157:1007-1016.

Zager, R.A., Johnson, A. (2001) Renal cortical cholesterol accumulation is an integral component of the systemic stress response. Kidney Int. 60:2299-2310.

Zager, R.A., Johnson, A., Anderson, K., Wright, S. (2001) Cholesterol ester accumulation: an immediate consequence of acute *in vivo* ischemic renal injury. Kidney Int. 59:1750-1761.

Zager, R.A., Shah, V.O., Shah, H.V., Zager, P.G., Johnson, A.C., Hanson, S. (2002) The mevalonate pathway during acute tubular injury: selected determinants and consequences. Am J Pathol. 161:681-692.

Zager, R.A., Johnson, A.C., Hanson, S.Y., Shah, V.O. (2003) Acute tubular injury causes dysregulation of cellular cholesterol transport proteins. Am J Pathol. 163:313-320.

Zager, R.A., Johnson, A.C., and Hanson, S.Y. (2005) Renal tubular triglyceride accumulation following endotoxic, toxic, and ischemic injury. Kidney Int. 67:111-121.

Zhou, R.H., Yao, M., Lee, T.S., Zhu, Y., Martins-Green, M., Shyy, J.Y. (2004) Vascular endothelial growth factor activation of sterol regulatory element binding protein: a potential role in angiogenesis. Circ Res. 95:471-478.

Zinszner, H., Kuroda, M., Wang, X., Batchvarova, N., Lightfoot, R.T., Remotti, H., Stevens, J.L., Ron, D. (1998) CHOP is implicated in programmed cell death in response to impaired function of the endoplasmic reticulum. Genes Dev. 12:982-995.